Università degli Studi di Palermo

AREA RICERCA E TRASFERIMENTO TECNOLOGICO
SETTORE DOTTORATI E CONTRATTI PER LA RICERCA
U. O. DOTTORATI DI RICERCA

PhD in Earth and Marine Sciences
Department of Earth and Marine Sciences (DiSTeM)
Scientific Sector GEOS/02

SISMOMED project: Study of the seismicity of the central Mediterranean for the definition of seismogenic structures and crustal-lithospheric models

PhD STUDENT
Simona Bongiovanni

COORDINATOR
Prof. Christian Conoscenti

TUTOR
Prof. Attilio Sulli

CO TUTOR
Prof. Raffaele Martorana
Dott. Antonino D'Alessandro

XXXVII CICLO
A.A. 2023/2024

A nonna Emma e mamma Alessandra,
che mi hanno permesso di perseguire
le mie passioni e i miei sogni, incoraggiandomi in ogni passo.
Senza di loro, non sarei la persona che sono oggi.

CONTENTS

ABSTRACT

The Central Mediterranean is a geodynamically very complex area and is the result of the interaction between the European and African plates. Despite numerous studies, current models that attempt to describe the detailed kinematics and dynamics of this interaction have insufficient resolution or do not cover the entire Central Mediterranean area.

The major challenge is to build high-resolution crustal-lithospheric models for understanding past and future geodynamic evolution of the region and for accurate assessment of seismic and tsunami hazards associated with tectonic structures. The main problems lie in poor and heterogeneous data coverage and the predominantly mono-disciplinary approach used in the literature.

This PhD thesis aims to improve current knowledge of the shallow and deep structures of the central Mediterranean and to contribute to knowledge of the complex geodynamics of the region.

The use of data from different disciplines has enabled the coverage areas that otherwise would have shown significant gaps.

Seismic reflection profiles, P-wave velocity models (Vp), S-wave velocity models (Vs) converted to Vp through appropriate Vp/Vs ratios, and density models, have enabled the construction of the most extensive and high-resolution map of the Central Mediterranean Moho currently available. This shows strong lateral variation and good correlation with tectonic structures in the region. Using the same data and with the inclusion of well data, a preliminary crustal 3D model was produced. Despite some holes, this model is consistent with the tectonic and morphobathymetric structures of the study area. In addition, it is an important tool to build velocity models useful for optimizing the location of the hypocenter of earthquakes.

Statistical analysis of seismic earthquakes, through the use of purpose-written scripts, allowed the identification and construction of two lithospheric seismogenetic volumes (LSVs) located in the west-central sector of the Sicily Channel and a first subduction ionic crustal seismogenetic volume (CSV). The LSVs were related to the tectonic structures, banks and volcanoes located in the area and compared with existing rheological models. The geometric features of the upper and lower surfaces constituting the CSV were analyzed, and the slab was compared with those proposed in the literature.

This thesis project is a valuable tool to advance understanding of the geodynamic framework of the central Mediterranean, as well as to delineate surface and subsurface structures and associated seismic and tsunami hazards.

The main data and methods used, and the main results obtained in this PhD thesis are summarized in Figure 1.

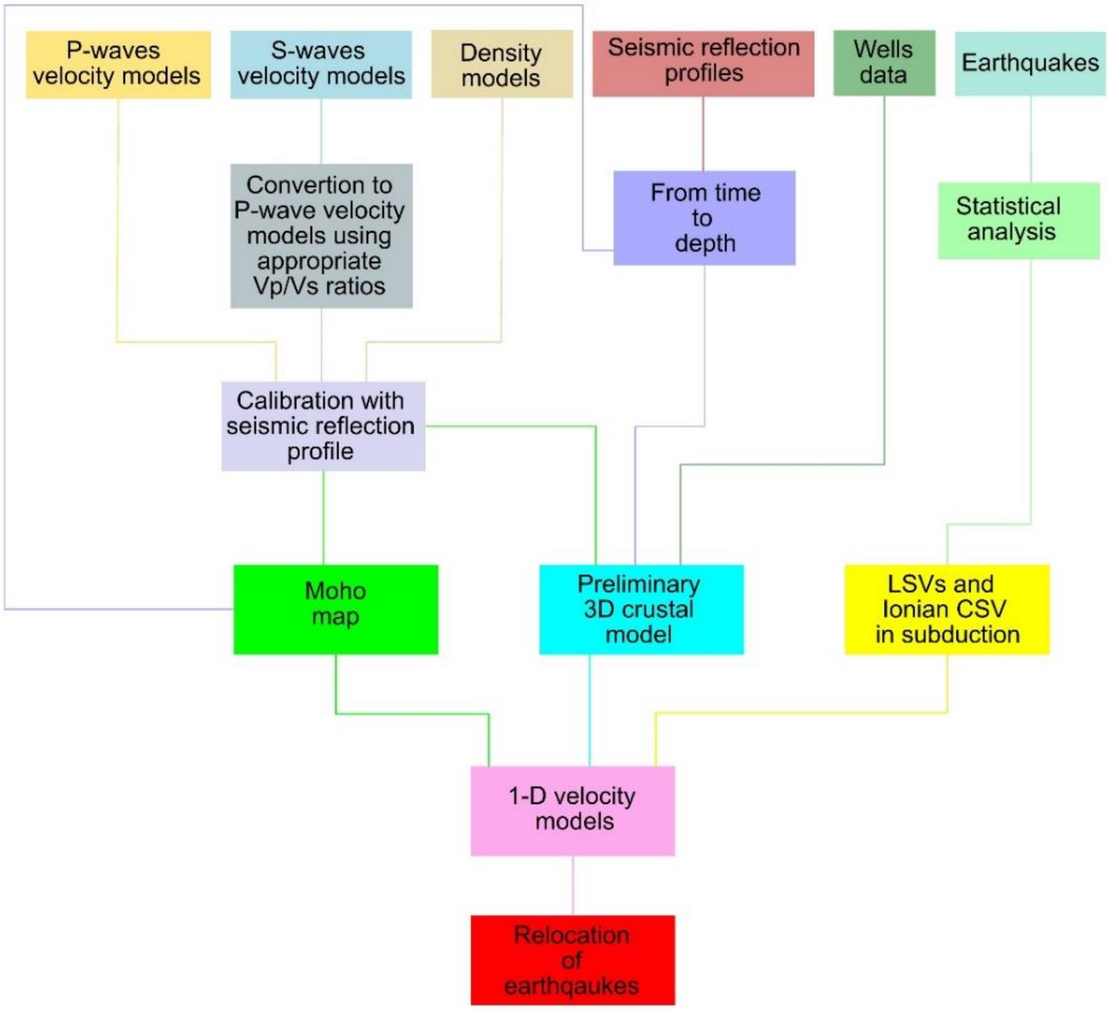

Figure 1: Flow diagram summarizing the main data and methods used in this study, along with the key results obtained. This diagram highlights the integration of various datasets and methodologies leading to significant findings in the research.

CHAPTER 1
INTRODUCTION

1.1 PURPOSES AND MOTIVATION OF THE THESIS

The Central Mediterranean is a geodynamically intricate region located at the convergence of the African and European tectonic plates, characterized by a different geological feature such as subducting lithosphere, continental collisions, volcanic arcs, and back-arc basins. These elements lead to significant lateral variations in crustal thickness and lithospheric properties, which complicate our understanding of the underlying mechanisms (Faccenna et al., 1996; Catalano et al., 2001; Rosenbaum et al., 2002; van der Meijde et al., 2003; Handy et al., 2010; Di Stefano et al., 2011; Jolivet et al., 2015).

Despite several studies in the literature, one of the major problems for a complete understanding of the Central Mediterranean area is that monodisciplinary investigations are often carried out rather than multidisciplinary approaches. This leads to not considering constraints highlighted by other disciplines and to lesser and heterogeneous data coverage.

Existing crustal models at European scale, often fail to capture the strong lateral variation that are at the Mediterranean scale (e.g., Tesauro et al., 2008; Molinari and Morelli, 2011; Artemieva and Thybo, 2013). The complex geodynamic of the region necessitates a high-resolution three-dimensional crustal model that integrates multidisciplinary datasets, including seismic reflection profiles, P- and S-wave velocity models, density models and well data.

Current Moho models, particularly those included in broader European crustal assessments (e.g., Tesauro et al., 2008; Molinari and Morelli, 2011; Artemieva and Thybo, 2013), are insufficient to capture the complex geodynamics of the central Mediterranean.

Some regional Moho maps cover parts of the Central Mediterranean but have many areas uncovered (e.g. Pontevivo and Panza, 2002; Lombardi et al., 2008; Piana Agostinetti and Amato, 2009; Di Stefano et al., 2011).

The most critical sectors are offshore areas, where data are limited. A notable example is the Sicily Channel. Recent work by Kherchouche et al. (2020) proposed a nearly constant Moho depth, contrast with known tectonic structures.

Understanding the characteristics of subduction zones is crucial, as they are the sites of the most intense seismic activity in the world. Previous global models (Syracuse and Abers, 2006; Hayes et al., 2012) have delineated slab geometries, but they often lack essential details, particularly for the Ionian subduction zone. Studies such as Maesano et al. (2017) and Hayes et al. (2018) provide some information about the Ionian slab but have poor resolution in the deeper sectors.

This PhD thesis aims to contribute to the current state of knowledge of the tectonic and geodynamic setting of the Central Mediterranean by building 3D models able to show shallow and deep structures at the Mediterranean scale. This was made possible through the use of data from different disciplines such as P-wave and S-wave velocity models, density models, seismic reflection profiles, and well data and earthquakes.

A preliminary 3D crustal model constrained at the base by the Moho surface has been proposed.

The map of the Moho presented here shows the highest resolution and areal extension currently available.

This thesis introduces, for the first time, the model of the Crustal Seismogenic Volume (CSV) derived from a statistical analysis of earthquakes, incorporating data from the CLASS catalog (Latorre et al., 2022) alongside the ISIDe database (ISIDe Working Group, 2016). This integrated approach allows for a more constrained model, extending the temporal range of earthquake data and improving the understanding of the top and bottom surfaces of the CSV.

From the models realized in this thesis, 1D-velocity models were extracted and tested to optimize the location of seismic events recorded by the national seismic network between 2005 and 2018.

The results obtained in this thesis project provide valuable insights about the complex geodynamics of the central Mediterranean, facilitating enhanced seismic and tsunami hazards assessments and supporting the construction of lithospheric-scale models. This work contributes to the ongoing effort to optimize earthquake location accuracy and improve seismic tomography studies in this geodynamically complex region.

1.2 TECTONIC AND GEODYNAMIC SETTING

The Central Mediterranean region has developed as a consequence of the trench rollback associated with the subduction of the African plate over the past 30 million years (Faccenna et al., 2001; Malinverno and Ryan, 1986). As a result of this tectonic process, the area is divided into various domains, each exhibiting distinct lithospheric thicknesses.

Continental collision is a key tectonic feature in Sicily and Calabria. This collision involves several distinct domains: the Sicilian-Maghrebian domain in central and western Sicily, the foreland domain in southeastern Sicily, the Kabilo-Peloritanian-Calabrian domain in northeastern Sicily and Calabria, and the volcanic region associated with Mount Etna and the Aeolian Islands (Billi et al., 2006, and references therein).

An arc-shaped tectonic feature known as the Calabrian Arc is observed in this region. Its extension into the Ionian offshore is marked by a thick accretionary wedge, about 300 km wide and several hundred kilometers in length (Cernobori et al., 1996; Polonia et al., 2011; Gallais et al., 2012; Corradino et al., 2020). This structure was defined as the "External Calabrian Arc" by Selli and Rossi (1975).

The Ionian subduction zone is among the narrowest in the world, measuring about 200 km wide, 500 km deep and dipping northwestward at about 70° (Anderson and Jackson, 1987; Giardini and Velonà, 1991; Selvaggi and Chiarabba, 1995; Wortel and Spakman, 2000; Chiarabba and Palano, 2017; Scarfì et al., 2018). Govers and Wortel (2005) and Nijholt and Govers (2015) noted the presence of shear subduction-transform edge propagator (STEP) zones along the edges of the subducting slab. Several studies (Govers and Wortel, 2005; Cocchi et al., 2017; Scarfì et al., 2018; De Ritis et al., 2019) have identified two key STEP zones along the edges of the Ionian plate: the Tindari-Letojanni STEP, a right-lateral shear zone located along the Aeolian Islands, and the Palinuro STEP, a left-lateral shear zone located along the Palinuro volcanic chain .

The Southern Tyrrhenian Sea is a retroarc basin that developed from northwest to southeast (Sartori, 1990; Gueguen et al., 1998; Argnani and Savelli, 1999; Carminati et al., 2004) as a result of the southeastward migration of the subduction system. This process initially led to the formation of the Vavilov Basin, followed by the development of the Marsili Basin (Sartori, 1990). The Southern Tyrrhenian Sea is predominantly characterized by thinned continental crust (Lliboutry, 2000; Pepe et al., 2000), though oceanic crust is also present in the Vavilov and Marsili basins (Neri et al., 2012; Sartori et al., 2004; Pontevivo and Panza, 2006; Cella et al., 2008; Scrocca et al., 2012). The exact extent of the oceanic crust remains somewhat uncertain, but Marani and Trua (2002) describe the Marsili Basin as nearly circular, with a diameter of around 120 km.

West of the Malta escarpment, in the offshore region of southern Sicily, lies the Sicilian Channel. This area is characterized by both contracting features, such as the Gela Thrust Front (GTF), and extensional structures, including the NW-SE oriented grabens of Pantelleria, Linosa, and Malta (e.g., Finetti et al., 1984; Civile et al., 2010; Sulli et al., 2021). Crustal thinning occurs at these, together with local uplift of the Moho (Scarascia et al., 1994; Agius et al., 2022). Volcanic activity is also present in this region, particularly in the northwestern part of the channel, between the southwestern coast of Sicily and the island of Linosa (Palano et al., 2020; Maiorana et al., 2023).

The eastern sector of the Malta escarpment hosts the Ionian Sea. Several authors (de Voogd et al., 1992; Faccenna et al., 2001, 2004; D'Agostino et al., 2008) describe the Ionian Sea as the last remaining fragment of subducting oceanic crust in the central Mediterranean. Refraction seismic data acquired in the Ionian Sea shows a thinned oceanic or continental crust (de Voogd et al., 1992).

1.3 STRUCTURE OF THE THESIS

This thesis is structured into six main chapters, each containing interconnected subsections that address different aspects of the research.

The first chapter outlines the objectives and motivations behind the thesis and the tectonic and geodynamic setting of the study area.

In the second chapter, one of the most critical areas of the central Mediterranean, the Sicily Channel, is examined due to its limited geological and geophysical data coverage. Using a multidisciplinary approach and statistical methods on earthquakes, a Moho map for the western sector of the Sicily Channel is constructed, along with an analysis of two lithospheric seismogenic volumes. This chapter also investigates the correlations between these models and volcanic activity, tectonic structures, and seismogenic volumes.

The third chapter employs a similar multidisciplinary strategy to develop a comprehensive Moho map of the central Mediterranean, filling existing gaps in literature and enhancing data coverage across the region. Through statistical analysis of seismic events, a Ionian crustal seismogenic volume in subduction is defined.

In the fourth chapter, improvements to the Moho model and the Ionian crustal seismogenic volume in subduction are presented. These advancements are achieved through the incorporation of new geological and geophysical data, as well as the use of re-localized seismic events extended over a longer time range.

The fifth chapter focuses on extracting velocity models from the results obtained in the previous chapters. These velocity models are then tested to accurately relocate seismic events recorded by the national seismic network in the central Mediterranean.

The sixth chapter is dedicated to conclusions and final remarks.

Collectively, these findings contribute significantly to unraveling the complex geodynamic puzzle of the central Mediterranean and provide valuable tools for seismic and tsunami hazards mitigation in the region.

CHAPTER 2
EXPLORING THE DEEP STRUCTURES OF THE CENTRAL WESTERN SICILY CHANNEL

2.1 INTRODUCTION

The Sicily Channel, a seismically active region, is characterized by moderate seismicity typically exhibiting magnitudes below 5. However, the precise location of earthquake hypocenters remains inadequately constrained due to the sparse distribution of permanent seismic stations and significant attenuation effects.

Understanding the Moho depth in this context is essential for elucidating the dynamics of the Earth's interior and assessing geohazards. Existing Moho maps for the region are either incomplete or derived from methodologies that inadequately capture the geological complexities of the Sicily Channel. This study aims to bridge these gaps through a multidisciplinary approach, incorporating seismic reflection profiles, P- and S- waves velocity models, density models and statistical earthquake analysis to enhance the understanding of the lithosphere's structure and its relationship with tectonic and volcanic activity.

The results underscore the necessity of continued multidisciplinary research to unravel the intricate geodynamic puzzle of the Central Mediterranean, providing a foundation for future studies aimed at mitigating the risks associated with seismic and tsunami events in this seismically active zone.

The content presented in this chapter has been submitted to the journal *Scientific Reports*.

2.2 A NEW MOHO MAP OF THE CENTRAL-WESTERN SICILY CHANNEL: CORRELATION WITH VOLCANOES, TECTONIC STRUCTURES AND SEISMOGENIC VOLUMES

scientific reports

A NEW MOHO MAP OF THE CENTRAL-WESTERN SICILY CHANNEL: CORRELATION WITH VOLCANOES, TECTONIC STRUCTURES AND SEISMOGENIC VOLUMES

S. Bongiovanni[1,*], M. Maiorana[1], A. D'Alessandro[2], R. Martorana[1], A. Sulli[1]
[1]Università di Palermo, Dipartimento di Scienze della Terra e del Mare, Palermo, Italy
[2]Istituto Nazionale di Geofisica e Vulcanologia, Osservatorio Nazionale Terremoti, Rome, Italy
**simona.bongiovanni@unipa.it*

ABSTRACT
A detailed Moho map is essential for understanding the deep structure of a given area, especially for a complex area such as the Sicily Channel, shaped by the Europa-Africa convergence. We built a new Moho map of the central-western Sicily Channel using a multidisciplinary approach, which comprises the analysis of crustal seismic reflection profiles and velocity models from multiple databases. We found two earthquake alignments that occurred in the study area from 1981 to the present that reach sub-Moho depths and through which we constructed two Lithospheric Seismogenic Volumes (LSVs). We then related these results with the location of the volcanoes, the tectonic structures, and the rheological profiles present in the literature. This work aims to expand the limited knowledge of the geodynamic setting and lithospheric structure of the Sicily Channel. Furthermore, it can constitute a starting point for future works regarding the seismic hazard of the area.

Keywords: Moho depth, Sicily Channel, Lithospheric seismogenic volume, Seismic reflection profiles

1. INTRODUCTION

The Sicily Channel is a seismically active area, characterized by moderate seismicity with a magnitude generally below 5. Unfortunately, the location of the earthquakes hypocenters in this area is poorly constrained because due to the sparse distribution of permanent seismic stations and the high attenuation [1].

As illustrated in Fig. 1a, an alignment of earthquakes with sinistral strike-slip focal mechanisms occurs in the western sector of the Sicily Channel as noted by several authors [2, 3, 4, 5].

The Sicily Channel hosts eight seismogenic sources (Fig. 1b): four with approximately N-S trends in the western sector and near the Sicilian coast (Fig. 1b within the blue dashed line) and four with N-S trends crossing the Grabens (Fig. 1b within the red dashed line). These are mapped in the DISS (Database of Individual Seismogenic Sources) [6].

The Sicily Channel has been greatly influenced by the interaction between Africa and Europe plates. Among the various deformation stages recorded, the most important one began in the Late Miocene with the formation of the Sicilian Fold and Thrust Belt (SFTB) [7]. In the Pliocene, an NNE-SSW-oriented extensional mechanism produced the Graben of Malta, Linosa and Pantelleria [8, 9, 10]; at the same time, the Gela Thrust System (GTS) emplacement occurred [11] as well as the formation of a N-S oriented left strike-slip mechanism [12], that extends from Capo Granitola-Sciacca to Linosa (CGSFZ) [5, 9] (Fig. 1c). The latter, physically separating the Graben of Pantelleria from those of Malta and Linosa (Fig. 1c), induced a different evolution between them; the earthquakes available in the area confirm that this structure is currently active and involves the lithosphere levels [9, 13]. Along this deformation belt, also a relevant magmatic activity is recorded, which was associated with the formation of magmatic manifestations, constituting several volcanoes and volcanic banks (Fig. 1a), scattered in the whole Sicily Channel [13, 14, 15, 16]. Near the coast of western Sicily, volcanic edifices of the Quaternary age were discovered by Lodolo *et al.* [17]. According to Civile *et al.* [5], in this system, the magma rises through the faults, acting as conduits, that cut across the entire lithosphere leading to a partial melting by decompression. The seismic section CROP M23 (location in Fig. 1a) of Catalano *et al.* [18] highlighted the deep structural layers of this highly deformed zone, revealing a mild Moho rising from west to east of the CGSFZ tectonic structure, and a Moho deepening beneath the Gela Thrust System. Civile *et al.* [19] also detected in the seismic line CROP M25 (location in Fig. 1a) a Moho rising under the Pantelleria Graben, probably linked to deep fluids rising causing several volcanic manifestations around Pantelleria Island (Fig. 1c). This interpretation is supported by the gravity model realized along the seismic profile showing a Moho rising to about 17 km, in the NW of Pantelleria Graben, and, to the N and S of the Pantelleria Graben, a Moho deepening at 24–25 km depth [19].

Knowledge of the Moho depth is crucial to gaining insights into the dynamics of the Earth's interior, the evaluation of geohazard, the reconstruction of the lithospheric pattern of a given area and the knowledge of deep structures. The Moho presents different characteristics and geometries depending on whether it lies in oceanic or continental region or is located in areas subjected to extensive or compressive processes [20].

The Moho is generally determined by means of seismic and/or gravimetric methods.

In the literature, many maps of Moho have been produced by different methods. Suhadolc & Panza [21] and Du *et al.* [22] generated a map of European Moho obtained from interpretations of CSS (Controlled Source Seismology) profiles.

Moho depth maps have also been created for other regions such as southern California [23], northern and northeastern China [24, 25, 26, 27], eastern Tibet [28, 29, 30] and southern China [31] , using Receiver Function (RF) analysis. Teng *et al.* [32] and Reddy & Rao [33] discussed and reviewed refraction seismic profiles for Moho determination in China and reflection seismic profiles for Indian shield Moho determination, respectively. Stankiewicz & De Wit [34] modeled the Moho below South Africa using reflection seismic profiles and RF analysis. These studies emphasize that obtaining reliable depths by using the RF method requires very accurate S-wave and P-wave velocities. Consequently, reliable results depend on velocity variations with depth, which are best constrained by seismic refraction data.

Mjelde *et al.* [35] and Aitken *et al.* [36] determined the Moho depth for South America and Australia, respectively, using gravity data from satellite observation. In addition, Aitken *et al.* [36] show a limitation of gravity inversion for crustal modeling. These authors noted the unreliability of the method, for example in areas with thick and dense crust or thin and low-density crust, adding that in such a case the method can be made reliable by defining the structure through seismic methods.

Other authors have created Moho maps by integrating data from various methods to overcome the limitations of individual techniques and to ensure better areal coverage. Grad *et al.* [37] made a Moho map of Europe using seismic and gravity data; Assumpção *et al.* [38] discussed crustal thickness models of South Africa using data extrapolated from seismic tomography, reflection seismic profiles and receiver function; Tugume *et al.* [39] made crustal thickness map in Africa and Arabia by interpolating gravity data, RF data and surface wave dispersion.

Regarding the Central Mediterranean area and the Italian region, Nicolich & Dal Piaz [40] and Scarascia *et al.* [41] produced a Moho isobath map using CSS profiles; Waldhauser *et al.* [42] and Lippitsch *et al.* [43], produced a detailed Moho map of the Alpine region using a method proposed by Waldhauser [44] and Waldhauser *et al.* [42] to determine 3-D P-wave velocity models; Pontevivo & Panza [45] used surface wave scattering to reconstruct the lithosphere-asthenosphere system of Italy; Lombardi *et al.* [46] and Piana Agostinetti &

Amato [47] proposed a Moho map applying the RF method for the Italian peninsula and the central-western Alps, respectively; Di Stefano *et al.* [48] and Spada *et al.* [49] show a Moho map for the Italian peninsula using both CSS and RF data.

However, these maps either partially or completely exclude the Sicily Channel, which lies on the periphery of these models and is poorly detailed. This is primarily because they are mainly produced on a seismological basis and the seismic network in the area is not adequately distributed because stations are located only on land.

Kherchouche *et al.* [50] proposed a Moho map for the Sicily Channel using ambient noise and earthquake tomography method, but the nearly constant value of about 30 km depth is incompatible with the geological structures in the area.

Jongsma *et al.* [51], Agius *et al.* [1], and Calò & Parisi [2] report information for this area through the study of earthquakes; Civile *et al.* [8, 19], Corti *et al.* [52], and Palano *et al.* [13] describe the area focusing on the analysis of the superficial part of seismic reflection profiles. As a result, the lithospheric knowledge of the Sicily Channel remains incomplete.

With the present work, we want to contribute to the knowledge of the deepest part of the Sicily Channel, specifically in an area where there are several banks and volcanoes, and to provide an instrument that can be used to understand the mechanisms influencing the variation in crustal thickness found in the study area and the possible connection between rising deep magmatic fluids and outcropping volcanoes.

To do this, we used joint analysis of multidisciplinary data. Specifically, we interpreted reprocessed ultra-high penetration seismic reflection profiles [18] calibrated with well-log data to observe detailed surface geometries down to Moho depth and used them to calibrate, in turn, P-wave velocity (Vp) and shear wave (Vs) models extrapolated from the literature. Further, to understand the connection with structures in the area we merged the seismological contribution using earthquakes with a statistical approach, using the Gaussian Kernel function. The location of this data is shown in Figure 1 a.

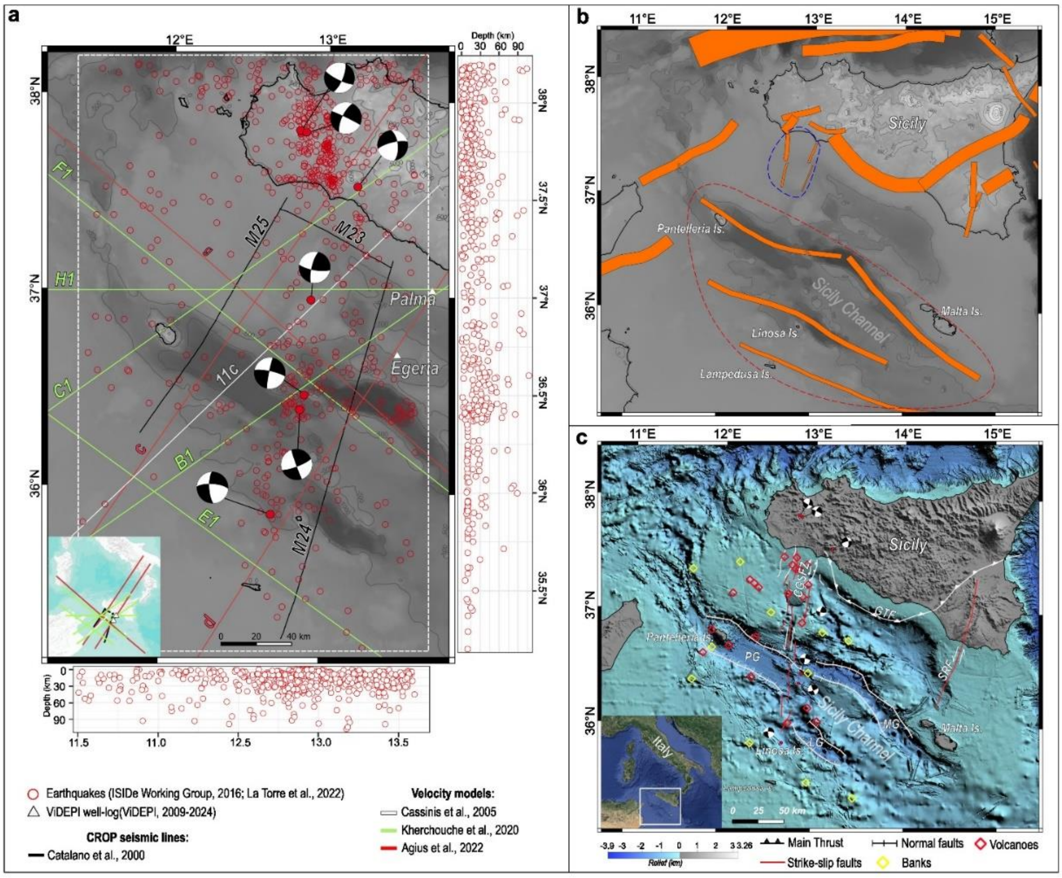

Figure 1. *a – Location of the dataset available for the study area. Focal mechanisms of the major events present in the Time Domain Moment Tensor (TDMT) database are also reported [53]; b - The seismogenic sources detected in the DISS (Database of Individual Seismogenic Source) [6] are shown in orange. The red and blue dashed lines contain the seismogenic sources located in the Sicily Channel; c - Geological and morpho-structural map of the study area. GTF (Gela Thrust Front) [54], LG (Linosa Graben), MG (Malta Graben), PG (Pantelleria Graben), CGSFZ (Capo Granitola-Sciacca fault zone) [5], SRF (Scicli-Ragusa Fault[5]. Focal mechanisms of the major events present in the Time Domain Moment Tensor (TDMT) database are also reported [53]. The location of banks and volcanoes is derived from Aïssi et al. [15] and Lodolo, et al. [17].*

2. RESULTS

2.1 SEISMO-STRATIGRAPHIC INTERPRETATION

We interpreted CROP seismic profiles M23, M24, and M25 to determine the thickness and the geometries of the main units and structures. On each seismic line, we projected Vp profiles from Cassinis *et al.* [55] and Agius *et al.* [56]. Key reflectors, limiting the main layers from Moho to the seabed, have been identified based on their amplitude, lateral continuity, and velocity variation. The correlation with well data (Egeria and Palma) (location in Fig. 1a) and literature data [5, 18, 57, 58] allowed us to characterize the shallower levels and attribute them to the respective age and feature. The deep layers were identified based on seismic reflection characteristics and velocity variation (Figs. 2),

From the seabed to the horizon corresponding to the Top of Miocene a wide Plio-Pleistocene sedimentary filling is observed; its maximum thickness (1.8 s/TWT) is reached in front of the GTS wedge (Fig. 2a). The reflectors show medium amplitude, high frequency, and parallel geometry, with onlap termination on the GTS and CGSFZ. This unit is composed of pelagic marls and marly limestones of the Zanclean Trubi Fm., and of the Piacenzian-Pleistocene shelf clayey deposits with sandy intercalations of the Ribera Fm. [5, 9].

In the northern sector of the study area, the GTS chaotic reflectors, dissected by different S-vergent thrust faults, exceeding 2 s/TWT of thickness, are observed (Fig. 2a).

Underneath this unit, the Miocene deposits are present, consisting of shelf siliciclastic deposits of the Terravecchia Fm. and evaporitic sediments of the Messinian Gessoso-Solfifera Group [5, 9]. The seismic signal is characterized by a high amplitude reflector, and medium frequency, with locally transparent zones (Fig. 2a).

Underlying these, the Mesozoic carbonates are observed; these are composed of: the Upper Triassic (Sciacca Fm.) and Lower Jurassic (Inici Fm.) deposits consisting of a carbonate platform succession overlain by Jurassic-Eocene pelagic limestones with marly and clayey intercalations (Buccheri, Chiaramonte, Hybla and Amerillo Fms.). Horizons show high lateral continuity, medium frequency, and a sub-parallel configuration (Fig. 2a).

Volcanic manifestations are widespread in the entire study area (Fig. 1a), and volcanic intrusions are visible in all the analyzed seismic lines (Figs. 2a and b). Those are characterized by wide diffraction hyperbolae zones and chaotic facies, sometimes reaching the seafloor.

The deep layers include the units occurring below 5 s/TWT. The crystalline basement is the top of the upper crust, the shallowest of the deep layers, and is identified by a discontinuous and strong reflector lying at an average depth of 6 s/TWT (10 km) in all the study area [18] and by a Vp velocity variation that goes above 6 km/s at it (Figs. 2a and b).

The top of the lower crust was identified below this, with numerous horizontal (near flat) and gently dipping reflections characterized by low continuity and medium amplitude, locally interrupted by wide diffraction hyperbolae zones. The velocity here increases to more than 7 km/s up to the Moho (Figs. 2a and b). A double laminated, laterally discontinuous reflector occurs at its base; this, according to Catalano *et al.* [18] interpretation, is assumed to be the

Moho horizon. Above the Moho, high amplitude reflectors are also observed, characterizing a high reflective lower crust, *sensu* Catalano *et al.* [7].

In seismic profiles M23, M24 and M25, the signal shows high amplitude, low frequency, and it is locally interrupted by diffraction hyperbolae (Figs. 2). The most prominent double reflection is visible in M24 and M25 (Fig. 2c). In proximity to the assumed Moho, the velocity increases up to 8 km/s.

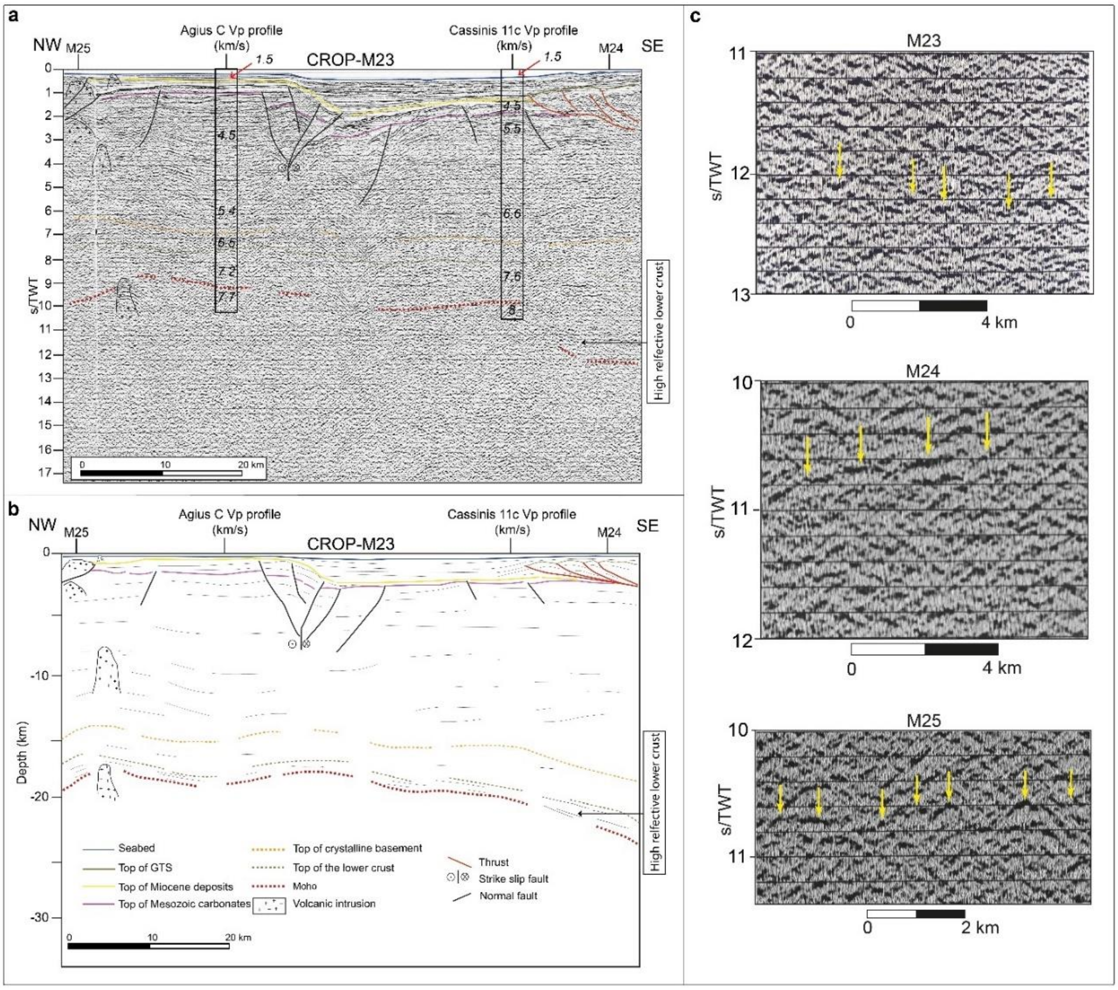

Figure 2. a - M23 seismic line interpretation after Catalano et al. [18] in time (TWT); b - Line drawing in depth (km). Crossing Vp profiles by Cassinis et al. [55] and Agius et al. [56] have been represented; c - Moho reflection characteristics (indicated by yellow arrows) in M23, M24 and M25 CROP profiles.

2.2 MOHO SURFACE IN TIME (S/TWT) AND IN DEPTH (KM)

From the Vs models of Agius *et al.* [56] and Kherchouche *et al.* [50] (location shown in Fig. 1a) we obtained Vp values for the Moho surface, which are respectively 8 km/s and 7.7 km/s.

The velocity models of Kherchouche *et al.* [50] were not used to construct the Moho surface as they did not align well with the other data used and therefore, we used only the 3 velocity models proposed by Agius *et al.* [56].

The obtained Moho surface in time ranges from ~6.7 to ~12.6 s/TWT (see Supplementary Fig. S1 online). The lowest values are found beneath the Pantelleria Graben (6.7 s/TWT): there, the contour lines follow the trend of the tectonic structures, which are normal faults at the rims of the Graben (Fig. 1a). Otherwise, between the Pantelleria Graben and the Linosa Plateau sector, the concavity of the contour lines shows a constant NW trend; and, on the contrary, in the proximity of the GTS and in the southern Linosa Graben, a variation in the concavity of the contour lines is observed (see Supplementary Fig. S1 online).

The Moho surface in depth shows strong lateral variation, with depths ranging from ~16.8 km to ~27.2 km (Fig. 3a).

In the Pantelleria Graben, the Moho reaches 16.8 km depth, maintaining a shallower trend than in the surrounding areas. Near the Linosa and Malta rims, it reaches depths of around 20 km (Fig. 3a).

Additionally, a Moho deepening is observed along the M23 profile from west to east. At the point where it intersects the orogenic wedge of the GTS, the Moho reaches ~27 km depth (Fig. 3a Supplementary Fig. S2 online).

The study area has a variable bathymetry that affects the Moho depth map. To get information about the crustal structure, we constructed a crustal thickness map (Fig. 3b). The pattern of the crustal thickness map is similar to that of the Moho map and shows greater thicknesses in the GTS sector (~27 km) and lesser thicknesses at the Pantelleria Graben (~18 km) and near Linosa and Malta rims (~19km).

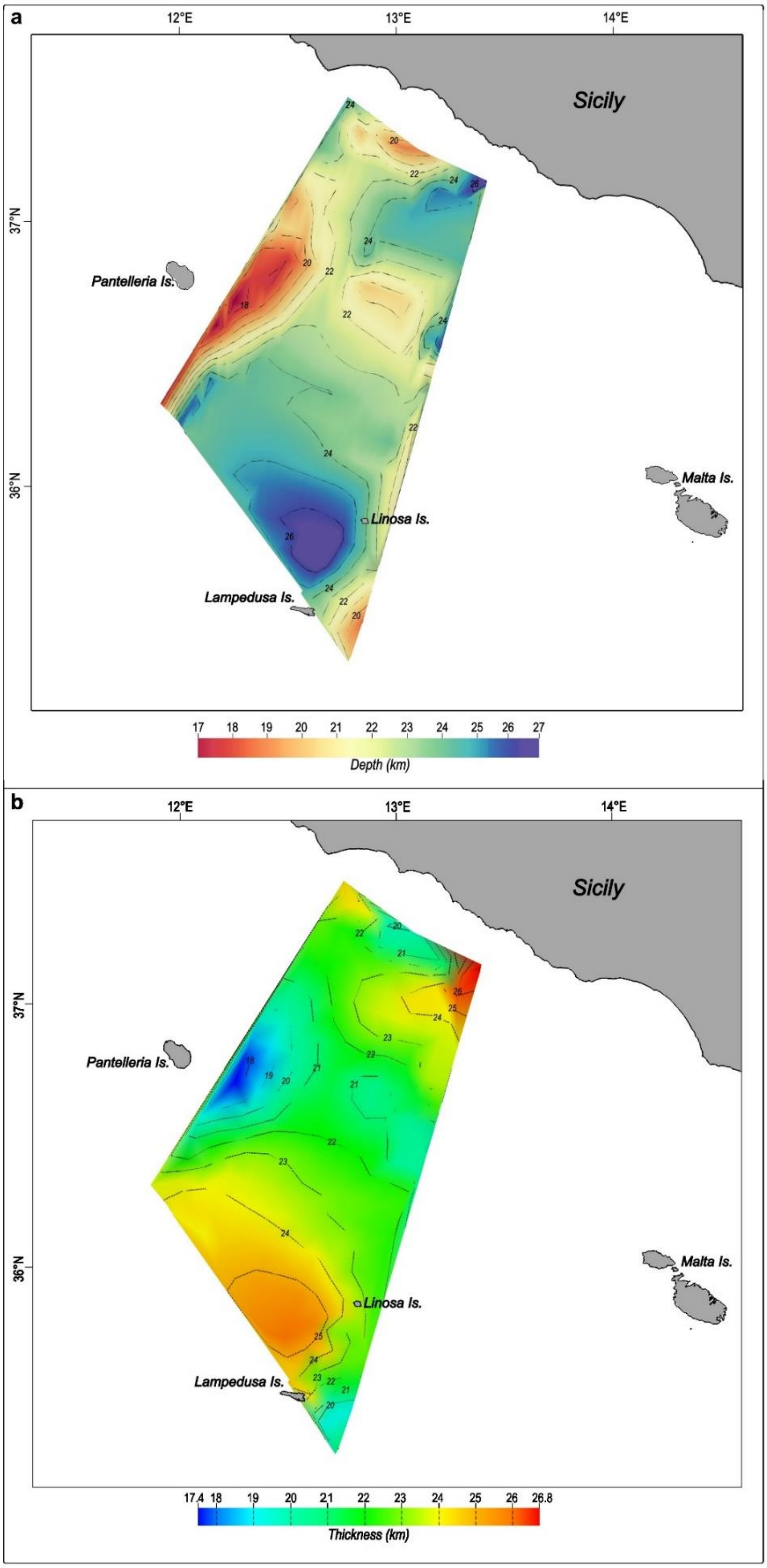

Figure 3. *Moho map in depth (a) and the crustal thickness map (b) of the central western sector of the Sicily Channel.*

2.3 LITHOSPHERIC SEISMOGENIC VOLUMES (LSVS)

From the statistical analysis of each dataset of earthquakes divided into depth ranges, we obtained density plots on which we calculated gradients (example in Fig. 4) and maximum gradient values. Using the isolines, obtained from the maximum density gradient values for each depth range, we determined two pairs of surfaces perpendicular to each other bordering two LSVs also perpendicular to each other: one with N-S trend (blue scale in Figs. 5) and one with E-W trend (red scale in Figs. 5). For lithospheric seismogenic volume, we mean the seismogenic zone where most earthquakes occur[59] involving the crust and upper mantle. The base of this volume corresponds to the brittle-ductile transition zone and is influenced by different factors including the geodynamics of the study area and the composition and physical state of the rocks [59, 60]

It is observed that the N-S-oriented LSV follows the trend of the tectonic structures located within the CGSFZ. Otherwise, the E-W volume shows a trend concordant with the normal faults bordering the Pantelleria, Malta, and Linosa Grabens.

In Fig. 5, the geometry of the N-S-trending LSV's bounding surfaces is well illustrated to the west and east. The volume extends from the northern coast of Sicily to the island of Linosa for about 240 km and from 5 km to about 60 km depth. In particular, the northernmost sector of the volume is present from a depth of 5 km to about 25 km; from the island of Pantelleria southward, the volume deepens to a depth of 60 km.

To the south of the Sicily coast, the volume decreases vertically and is only present from about 20 km depth to about 35 km depth. The minimum, average and maximum distance between the two surfaces, and thus the minimum, average and maximum value of the volume thickness are 35 km, 48 km and 55 km, respectively. The two surfaces also exhibit concavity facing toward the inside of the volume (Figs. 5b and d). The central sector of the NS-trending LSV perpendicularly intersects the EW-trending LSV (red scale in Figs. 5).

The latter extends from a depth of 50 km to 60 km and a length of 100 km. The minimum, average and maximum distance between the two surfaces and thus the minimum, average and maximum volume thickness are 50 km, 70 km and 90 km, respectively. The two surfaces bordering the volume exhibit a concavity facing toward the inside of the volume (Figs. 5a and c).

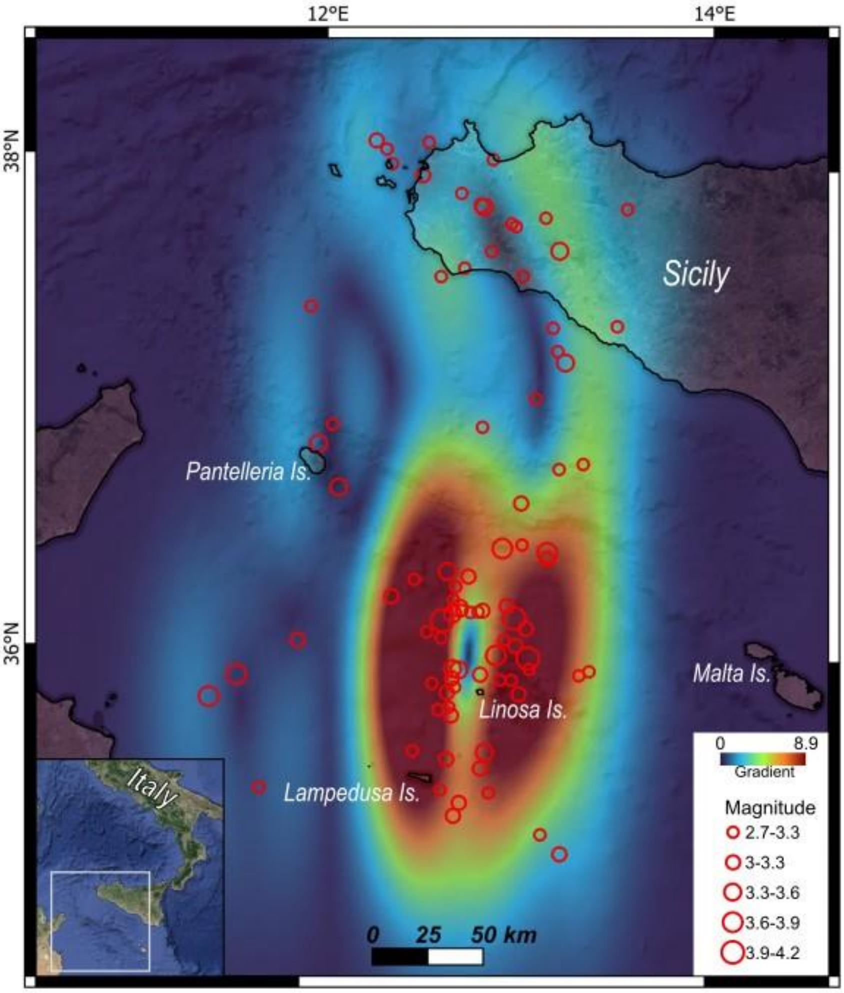

Figure 4. *An example of the density gradient (color scale) obtained from the density of earthquakes (red dots) located between 5 and 15 km depth.*

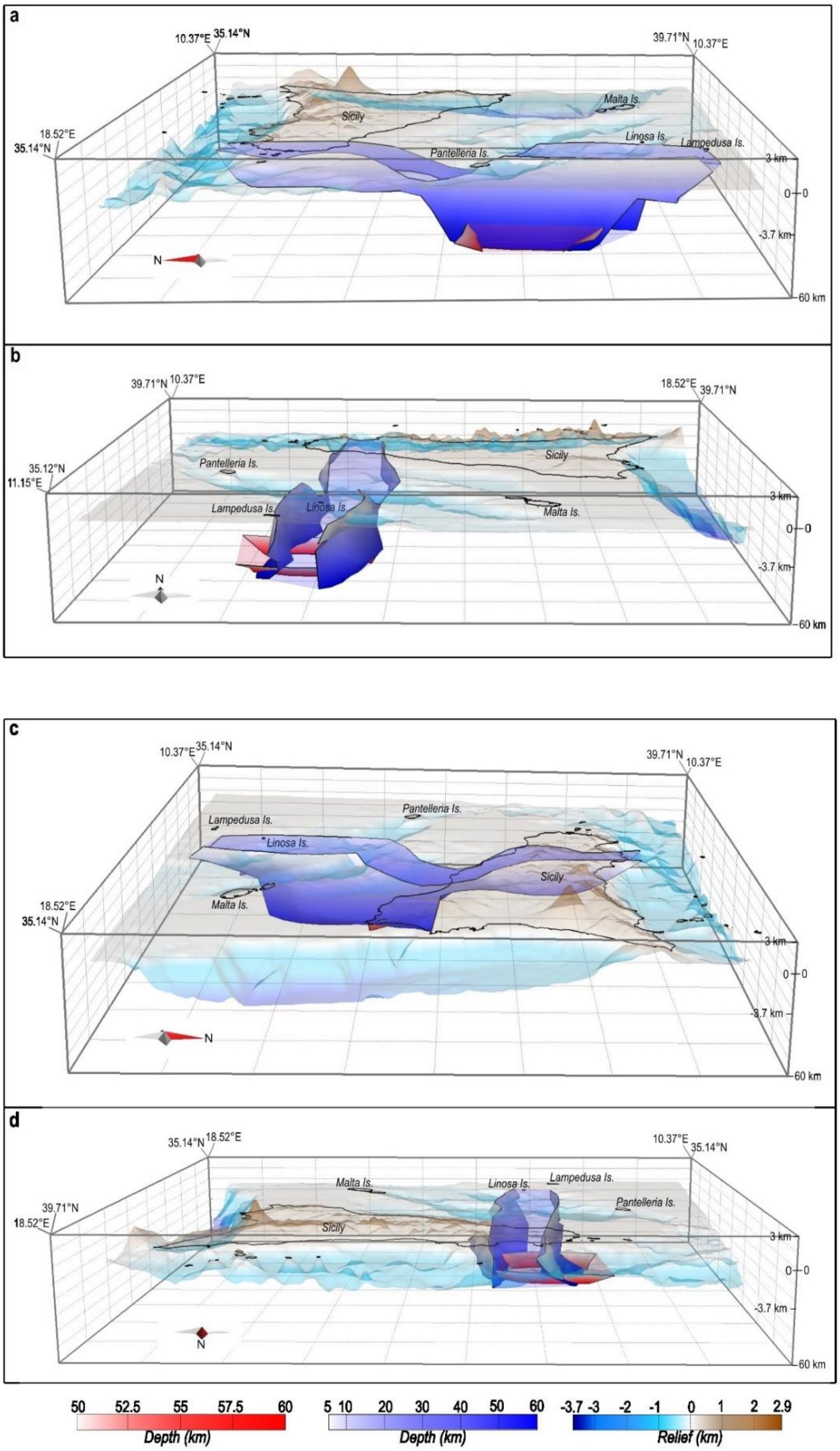

Figure 5 a, b, c, d. *Different views of the LSVs represented by the surfaces bordering them laterally. Topography (exaggeration x8) is represented in blue-brown color scale; in blue scale the LSV with NS trend, in red scale the LSV with EW trend. The fill between the surfaces in transparency represents the volume*

3. DISCUSSION

A new, reliable, high-resolution Moho map of the central-western sector of the Sicily Channel. We used data from different disciplines, which allowed us to have a greater data coverage than the Moho maps produced for the Italian peninsula that showed a gap in the Sicily Channel due to the poor data coverage due to the use of single-discipline data and techniques [41, 43, 46, 47, 48, 49].

In addition, the Delaunay triangulation method used, offers the advantage of generating a consistent triangular grid, improving the computational accuracy of the model and preserving the original data set without adding or removing data points.

Considering that this new map covers a smaller study area and was made using a wide dataset, it exhibits a higher resolution comparatively to other Moho maps of the Mediterranean and the Italian peninsula [55, 57, 61].

Moreover, the map reveals strong lateral variations (the depth ranges between 16.8 km and 27.2 km, see Fig. 3a) conversely to the map proposed by Kherchouche *et al.* [50] which shows a constant trend in Moho depth within the Sicily Channel, probably due to a not well-distributed seismic network in the area.

Furthermore, our map exhibits a strong correlation with the tectonic structures found in the literature and shown in Fig. 1c (e.g., Pantelleria, Malta, and Linosa Grabens) and with the location of volcanoes; in fact, a shallower Moho (16.8 km depth) is observed in correspondence with the Capo Granitola-Sciacca offshore, around the Pantelleria, Lampedusa, and Linosa islands and near the volcanoes (Fig. 6).

The two constructed LSVs, if compared with the other data analyzed, are a fundamental tool for understanding the lithosphere structure variation of the study area. Fundamental evidence is that both the N-S and the E-W LSVs show a concordant trend with both tectonic structures (Fig. 1c) and seismogenic sources from the DISS database (Fig. 1b).

Specifically, these LSVs exhibit (i) a NNE-oriented trend (in agreement with Calò & Parisi [2]; Di Stefano *et al.* [3]; Spampinato *et al.* [4]; Civile *et al.* [5], which follows the structures of the CGSFZ, interpreted by Civile et al. (2018) as lithospheric faults favoring the rise of magmas to the surface, and (ii) an EW-oriented trend, concordant with the normal faults delineating Pantelleria, Malta, and Linosa Grabens (Fig. 7).

Furthermore, the E-W alignment of seismic events, which has not been widely discussed by other authors, is supported by the presence of an E-W seismogenic source identified in the DISS database.

In detail, the N-S LSV extends from 5 km to 60 km depth, except in the northernmost region where it lies at a depth between 20 km and 35 km depth (Figs 5a and c). In this sector, morpho-bathymetric and seismic data from the literature [5, 15, 17, 62] indicate a high concentration of volcanoes, located outside the LSV. Conversely, some volcanoes are observed within the LSV, particularly around Linosa and Pantelleria Islands (Fig. 6). Hence, it is not possible to derive a direct relationship between the location of volcanoes and LSVs.

Viti *et al.* [63] suggest, in the rheological profiles realized for the Sicily Channel, an alternation between viscous and brittle behavior at various depths down to approximately 35 km; down to this value, they observe a predominantly viscous behavior, in agreement with the maximum Moho depth reconstructed in this work (see Fig. 3a).

Analysis of a large earthquake dataset, linked to the reconstruction of a detailed Moho map, has identified sub-moho earthquakes.

Except for subduction zones, the sub-Moho earthquakes in general are rare [64, 65]. Otherwise, they are observed in various parts of the world and across different tectonic regimes [66, 67, 68, 69]. The two LSVs shown in this paper indicate the presence of seismic events at depths greater than the Moho. Therefore, this is not anomalous as different tectonic regimes coexist in the study area as reported by Calò and Parisi [2], Corti *et al.* [52] and Maiorana *et al.* [10].

The presence of such sub-Moho events would also suggest the presence of rheological variation in the mantle, but this is not in agreement with the rheological profiles of Viti *et al.* [63] which give no evidence of brittle behavior under Moho. Therefore, these profiles should be updated.

However, if we consider the absence of a shallow LSV in the north of the Pantelleria volcanic island (Figs. 5 a and c) and the absence of it at great depth near to the Linosa volcanic island (Figs. 5 b and d), we see that the absence of LSV also gives important information about the mantle rheological nature.

In the first case, the absence of a shallow LSV to the north is in an area where a shallow magma chamber is present, at a depth of about 6 km, also inferred from a significant positive gravimetric anomaly in the complete Bouguer map [17, 70].

In contrast, the absence of a continuous LSV at depth around Linosa is related to the presence of deep magmatic intrusions as indicated by seismic reflection data [10] and to the absence of evolved rocks on Linosa Island indicating a deep magma reservoir [71].

Considering our results, optimizing the localization of earthquakes would be beneficial, thereby improving the accuracy of seismogenic volumes such as those we have produced. Extending the seismic network to include offshore areas could help achieve this goal.

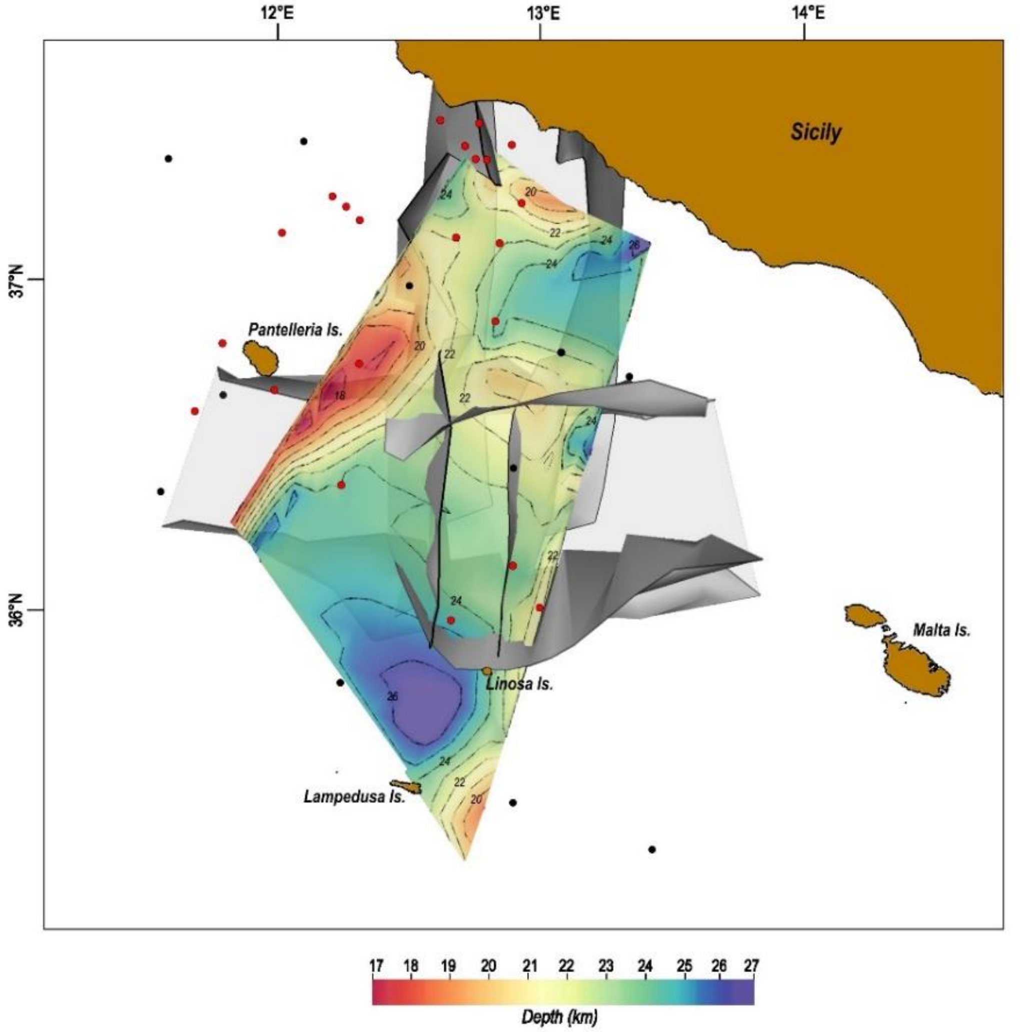

Figure 6. *Moho map in depth (color scale) and the LSVs (in grey scale) obtained. The red and black dots represent volcanoes and banks, respectively.*

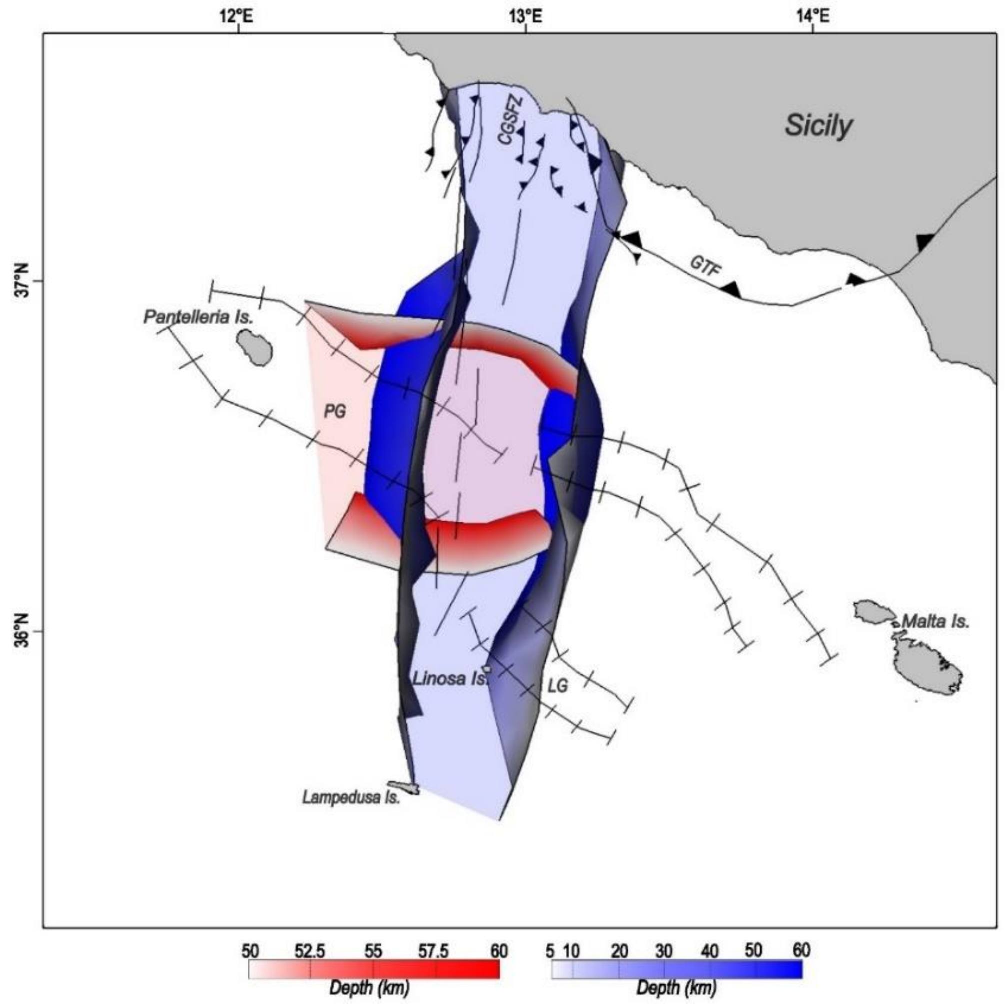

Figure 7. LSVs in plan. LSV with N-S trend, in red scale the LSV with E-W trend. PG (Pantelleria Graben), MG (Malta Graben), LG (Linosa Graben), CGSFZ (Capo Granitola-Sciacca Fault Zone) [5], GTF (Gela Thrust Front) [54].

In conclusion, our Moho map of the west-central sector of the Sicilian Channel represents a key tool for constraining to the bottom the crustal velocity models useful for earthquake localization. This is particularly important because, currently, earthquakes in the Sicily Channel are localized using a single velocity model that covers large areas with varying structural characteristics. Moreover, since the E-W trending seismogenic sources extend farther east than the sector we analyzed, it is necessary to extend the analysis to obtain a complete overview of the entire Sicily Channel.

Finally, based on our results, we suggest updating the rheological models proposed in the literature for the Sicily Channel to improve our understanding of the geodynamics and lithospheric structure, which remains still unclear.

4. METHODS

4.1 INTERPRETATION OF SEISMIC REFLECTION PROFILES AND WEEL-LOG DATA

We analyzed intermediate to ultra-high penetration seismic reflection profiles and well-logs data derived from ViDEPI (https://www.videpi.com/videpi/videpi.asp) and CROP databases [18] (Fig. 2). The CROP (CROsta Profonda) project (http://www.crop.cnr.it/) interpreted the deep crust reflection seismic profiles to map the deepest crustal reflectors. The seismic reflection profiles were acquired in collaboration with CNR-ENI and CNR-ENEL from 1988 to 1995 by the RV OGS-Explora using an Airgun array and a 4500 m long and 180-channel streamer. This represents a multidisciplinary geophysical research project aimed at understanding geodynamic processes, assessing geological hazard, and exploring energy resources in Italy. Approximately 10000 km of seismic reflection were acquired (about 1250 km on land and about 8700 km at sea). The dataset is publicly available for consultation (www.videpi.com/videpi/videpi.asp).

The interpretation of the dataset was carried out through a seismo-stratigraphic and structural analysis, applying Vail [72] 's method, and implementing a 2.5D geological model using MOVE Software (Midland Valley). The interpretation of the seismo-stratigraphic horizons was compared with the analysis of the seismic profiles by various authors [18, 73, 74]. In the first step the seismic reflection profiles were interpreted on the basis of their reflectivity. Subsequently, intersections with other seismic profiles and velocity profiles were evaluated. The interpretation of the seismo-stratigraphic horizons was compared with the analysis of the seismic profiles by various authors [18, 73, 74].

Literature data on the localization of volcanic banks [15, 17] were projected on a DEM downloaded from EMODnet (https://emodnet.ec.europa.eu/geoviewer/#) (Fig. 1c).

4.2 VELOCITY DATA AND TIME TO DEPTH CONVERSION

We digitized and analyzed, through the 3D modeling software MOVE Software (Midland Valley Ltd.) which allows 2D data to be visualized in a 3D environment, 5 2D shear velocity models (Vs) obtained from ambient noise and earthquake tomography method by Kherchuche *et al.* [50], 3 2D shear velocity models (Vs) inferred from seismic surface waves by Agius *et al.* [56] and a 2D P-wave velocity model inferred from the WARR (Wide-Angle Reflection-Refraction) profiles by Cassinis *et al.* [55] (Fig. 1a) (see Supplementary Fig. S3 online)

Initially, we converted 2D shear velocity models (Vs) to 2D P-wave velocity models (Vp) using the relationship between Vp and Vs proposed by Menichelli *et al.* [75] for southern Italy. Since the latter focuses on southern Italy in general and not specifically in off-shore areas, we also used the empirical law proposed by Brocher [76] (see Supplementary Fig. S4.1, S4.2 online). The results obtained from the two methods are comparable, so we used the model proposed by Menichelli *et al.* [75]. Subsequently, we converted these 2D velocity models from depth-to-time through the 3D Time Conversion Tool (see Supplementary Fig. S5 online). In particular, we used the Database method where rock properties, such as the velocity and velocity decay with depth, are assigned to each layer.

We calibrated the P-wave velocity models with seismic reflection profiles. To construct the Moho surface in times (s/TWT), we interpolated- the recognized Moho horizon on each individual profile by Delaunay triangulation method. This method offers the advantage of creating a uniform grid of triangles for better model computation quality, without adding or removing data points from the original dataset. A grid with 4 km x 4 km cells was used for resampling the interpolated surfaces and simplifying it.

For the construction of the Moho surface in depth, we converted velocity models and reflection seismic profiles from time to depth using the 3D Depth Conversion tool and Database method. Velocity values (Table 1) extrapolated from literature [18, 41, 74] were used to depth-convert the reflection seismic profiles.

We realized a Moho surface in depth (km) with the same method used for the construction of the surface of the Moho in times (s/TWT). In addition, since the depth of the Moho is conditioned by the depth of the seafloor, to provide more information about the crustal structure we constructed the crustal thickness map. The thickness at each point was calculated using the bathymetry as the top and the Moho surface as the bottom.

	M23			M24			M25		
	MIN (m/s)	AVE (m/s)	MAX (m/s)	MIN (m/s)	AVE (m/s)	MAX (m/s)	MIN (m/s)	AVE (m/s)	MAX (m/s)
Water	1500	1500	1500	1500	1500	1500	1500	1500	1500
Seabed	1574	1659,57	1887	1615	1983,93	2718	1770	2032,14	1977
GTF	4036	4036	4036	4036	4036	4036	N.A.	N.A.	N.A.
Oligo-Miocene	1160	1851,33	2545	1657	2094,92	2859	1618	2104,93	3290
Meso-Cenozoic	5300	5600	5800	2030	2879,45	3966	1997	2975,91	3951
Upper Crust	6000	6000	6000	6000	6000	6000	5788,94	6090,47	6392
Lower Crust	6800	7100	7400	7000	7000	7000	7000	7000	7000
Crust/mantle discontinuity	7700	7922,67	8068	8000	8000	8000	8000	8000	8000

Table 1. Velocity values obtained for each layer detected in the CROP seismic reflection profiles. Values derive from sonic logs (Egeria and Palma) analysis, interval velocities tables of the seismic profile, and Vp velocities from Cassinis *et al.* [55] and Agius *et al.* [56].

4.3 ANALYSIS OF EARTHQUAKES

We considered seismic events from 2005 to 2023 extrapolated from the ISIDe [77] database, which contains the parametric data of all seismic events localized by the INGV. To extend the dataset's temporal range, we also included earthquakes from 1981 to 2018, extrapolated from the CLASS (Catalogo delle Localizzazioni ASSolute) catalog [78], which contains earthquakes with optimized localizations. For this reason, we removed from the ISIDe catalog those earthquakes with the same ID as the events from 2005 to 2018 in the CLASS catalog (see Supplementary Fig. S6 online for more details regarding seismic events extrapolated from CLASS catalog and associated location errors).

Our research was conducted in the area between latitudes between 35.2° and 38.2° N and longitudes between 11.5° and 13.6° E. The location of epicenters on a horizontal plane and vertical planes of this dataset that we created is shown in Figure 1a. The same figure also shows focal mechanisms of the major events, extrapolated from Time Domain Moment Tensor (TDMT) dataset [53].

At first, we calculated the magnitude of completeness (Mc) of the dataset created using the MAXimum Curvature method (MAXC) [79] implemented in the Tremors software-app [80] and we captured STAI (Short-term aftershock incompleteness) periods using the same software-app to avoid overestimation of Mc.

We implemented a MATLAB code to organize the obtained database of earthquakes into 10-km depth ranges with a 50% overlap. We then analyzed these data through a statistical approach using the R statistical software [81], a language and environment for statistical processing and graphics.

We implemented a code on R statistical software using a Kernel smoothed intensity function from a point pattern with 0.01 x 0.01-pixel grid to obtain a density plot of the seismicity for each of these depth ranges.

The intensity estimate has been computed with a *Gaussian* Kernel function and bandwidth chose with the rule of thumb by Scott [82]. The latter determines the width of the window within which the points affecting the calculation of the intensity estimate are located.

In addition, in the computation of density plots, we assigned weights to each seismic event based on magnitude. Specifically, since the energy of an earthquake increases exponentially as the magnitude increases, we assigned an exponentially increasing value for each increasing value of magnitude.

The functions employed here are found in the *raster* [83] and *spatsat* [84] packages of the R statistical software.

For each density plot calculated for each depth range, we obtained the density gradient. Finally, we extrapolated the isolines of the maximum values of the density gradient, interpolated them using the Delaunay triangulation method, and obtained two perpendicular pairs of vertical surfaces bordering two Lithospheric Seismogenic Volumes (LSVs).

ACKNOWLEDGMENTS

The authors would like to thank Salvatore Scudero (INGV-ONT) for the useful discussions and suggestions on this paper.

AUTHOR CONTRIBUTIONS STATEMENT

S.B, M.M.: data analysis and interpretation of results, review of literature data, preparation of the figures, writing the main text of the manuscript; A.S.: interpretation of results, initial idea, work planning and review of the manuscript; R.M, A.D.: work planning and review of the manuscript.

DATA AVAILABILITY

The source of the datasets used in this paper are cited in the paragraph ‘Data and Methods’.

ADDITIONAL INFORMATION

Competing Interests: All authors declare that they have no conflicts of interest.

REFERENCES

1. Agius, M. R., Galea, P., Farrugia, D. & D’Amico, S. An instrumental earthquake catalogue for the offshore Maltese islands region, 1995–2014. *Annals of Geophysics*, 63(6), 658. https://doi.org/10.4401/ag-8383 (2020).
2. Calò, M. & Parisi, L. Evidences of a lithospheric fault zone in the Sicily Channel continental rift (southern Italy) from instrumental seismicity data. *Geophysical Journal International*, 199(1), 219-225 (2014).
3. Di Stefano R., *et al.* A regional-scale discontinuity in western Sicily revealed by a multidisciplinary approach: A new piece for understanding the geodynamic puzzle of the southern Mediterranean. *Tectonics*, 34(10), 2067-2085 (2015).
4. Spampinato, S., *et al.* A reappraisal of seismicity and eruptions of Pantelleria Island and the Sicily Channel (Italy). *Pure and Applied Geophysics,* 174, 2475-2493 (2017).
5. Civile, D., *et al*. Capo Granitola-Sciacca fault zone (Sicilian Channel, Central Mediterranean): structure vs magmatism. *Marine and Petroleum Geology,* 96, 627-644. (2018).
6. DISS Working Group. Database of Individual Seismogenic Sources (DISS), Version 3.3.0: A compilation of potential sources for earthquakes larger than M 5.5 in Italy and surrounding areas. Istituto Nazionale di Geofisica e Vulcanologia (INGV). https://doi.org/10.13127/diss3.3.0 (2021).
7. Catalano, R., *et al.* Sicily’s fold–thrust belt and slab roll-back: the SI. RI. PRO. seismic crustal transect. *Journal of the Geological Society*, 170(3), 451-464 (2013).

8. Civile, D., *et al.* The Pantelleria graben (Sicily Channel, Central Mediterranean): an example of intraplate 'passive'rift. *Tectonophysics*, 490(3-4), 173-183 (2010).
9. Civile, D., *et al.* Morphostructural setting and tectonic evolution of the central part of the Sicilian channel (Central Mediterranean). *Lithosphere*, 2021(1), https://doi.org/10.2113/2021/7866771 (2021).
10. Maiorana, M., Artoni, A., Le Breton, E., Sulli, A., Chizzini, N. & Torelli, L. Is the Sicily Channel a simple Rifting Zone? New evidence from seismic analysis with geodynamic implications. *Tectonophysics*, 864, 230019. (2023).
11. Di Stefano, E., Infuso, F. & Scarantino, S. Plio-Pleistocene sequence stratigraphy of south western offshore Sicily from well-logs and seismic sections in a high-resolution calcareous plankton biostratigraphic framework. In: Max, M.D., Colantoni, P. (Eds.), Geological Development of the Sicilian-Tunisian Platform: *Unesco Report in Marine Science* 58, 105–110 (1993a).
12. Fedorik, J., Toscani, G., Lodolo, E., Civile, D., Bonini, L. & Seno, S. Structural analysis and Miocene-to-Present tectonic evolution of a lithospheric-scale, transcurrent lineament: The Sciacca Fault (Sicilian Channel, Central Mediterranean Sea). *Tectonophysics*, 722, 342-355 (2018).
13. Palano, M., Ursino, A., Spampinato, S., Sparacino, F., Polonia, A. & Gasperini, L. Crustal deformation, active tectonics and seismic potential in the Sicily Channel (Central Mediterranean), along the Nubia–Eurasia plate boundary. *Scientific reports,* 10(1), 21238 (2020).
14. Beccaluva, L., Colantoni, P., Di Girolamo, P. & Savelli, C. Upper Miocene submarine volcanism in the Strait of Sicily (Banco Senza Nome). *Bull. Volcanol*. 44, 573–581 (1981).
15. Aïssi, M., Rovere, M. & Würtz, M. Sardinia channel—Strait of Sicily—Ionian Sea—Adriatic Sea seamounts. *Atlas of Mediterranean Seamounts and Seamount-Like Structures* (2014).
16. Cavallaro, D. & Coltelli, M. The Graham volcanic field offshore southwestern Sicily (Italy) revealed by high-resolution seafloor mapping and ROV images. *Frontiers in Earth Science*, 311 (2019).
17. Lodolo, E., Zampa, L. & Civile, D. The Graham and Terrible volcanic province (NW Sicilian Channel): gravimetric constraints for the magmatic manifestations. *Bulletin of Volcanology*, 81, 1-11 (2019).

18. Catalano, R., Franchino, A., Merlini, S. & Sulli, A. A crustal section from the Eastern Algerian basin to the Ionian ocean (Central Mediterranean). *Mem. Soc. Geol. It*, 55, 71-85 (2000).
19. Civile, D., Lodolo, E., Tortorici, L., Lanzafame, G. & Brancolini, G. Relationships between magmatism and tectonics in a continental rift: The Pantelleria Island region (Sicily Channel, Italy). *Marine Geology*, 251(1), 32–46, https://doi.org/10.1016/j.margeo.2008.01.009 (2008).
20. Carbonell, R., Levander, A. & Kind, R. The Mohorovičić discontinuity beneath the continental crust: An overview of seismic constraints. *Tectonophysics*, 609, 353-376 (2013).
21. Suhadolc, P. & Panza G. Physical properties of the lithosphere-asthenosphere system in Europe from geophysical data, in *The Lithosphere in Italy*, edited by A. Boriani et al., pp. 15–40, Acad. Naz. dei Lincei, Rome (1989).
22. Du, Z., Michelini, A. & Panza G. F. EurId: A regionalized 3-D seismological model of Europe, Phys. Earth *Planet. Inter*., 106, 31–62, doi:10.1016/S0031-9201(97)00107-6 (1998).
23. Zhu, L. & Kanamori, H. Moho depth variation in southern California from teleseismic receiver functions. *Journal of Geophysical Research: Solid Earth*, 105(B2), 2969-2980 (2000).
24. Chen, L., Wang, T., Zhao, L. & Zheng, T. Distinct lateral variation of lithosphere thickness in the northeastern north China craton, *Earth planet. Sci. Lett*., 267, 56–68 (2008).
25. Liu, H. & Niu, F. Receiver function study of the crustal structure of Northeast China: seismic evidence for a mantle upwelling beneath the eastern flank of the Songliao Basin and the Changbaishan region, *Earthq. Sci.*, 24(1), 27–33 (2011).
26. He, C.S., Dong, S.W., Chen, X.H., Santosh, M. & Li, Q.S. Crustal structure and continental dynamics of Central China: a receiver function study and implications for ultrahigh-pressure metamorphism, *Tectonophysics*, 610, 172–181 (2014).
27. Wang, C., Sandvol, E., Zhu, L., Lou, H., Yao, Z. & Luo, X. Lateral variation of crustal structure in the ordos block and surrounding regions, North China, and its tectonic implications, *Earth planet. Sci. Lett*., 387, 198–211 (2014).
28. Xu, L., Rondenay, S. & Van der Hilst, R.D. Structure of the crust beneath the southeastern Tibetan Plateau from teleseismic receiver functions, *Phys. Earth planet. Inter.,* 165, 176–193 (2007).

29. Zhang, Z., *et al.* Crustal structure across Longmenshan fault belt from passive source seismic profiling, *Geophys. Res. Lett.*, 36, L17310, doi:10.1029/2009GL039580 (2009).

30. Sun, Y., Niu, F., Chen, Y. & Liu, J. Crustal structure and deformation of the SE Tibetan plateau revealed by receiver function data, *Earth planet. Sci. Lett.,* 349, 186–197 (2012).

31. He, C.S., Donga, S.W., Santosh, M. & Chen, X.H. Seismic evidence for a geosuture between the Yangtze and Cathaysia Blocks, South China, *Sci. Rep.,* 3, 200,doi:10.1038/srep02200 (2013).

32. Teng, J., *et al.* Investigation of the Moho discontinuity beneath the Chinese mainland using deep seismic sounding profiles. *Tectonophysics*, 609, 202-216 (2013).

33. Reddy, P. R. & Rao, V. Seismic images of the continental Moho of the Indian shield. *Tectonophysics*, 609, 217-233 (2013).

34. Stankiewicz, J. & de Wit, M. 3.5 billion years of reshaped Moho, southern Africa. *Tectonophysics*, 609, 675-689 (2013).

35. Mjelde, R., Goncharov, A. & Müller, R. D. The Moho: boundary above upper mantle peridotites or lower crustal eclogites? A global review and new interpretations for passive margins. *Tectonophysics*, 609, 636-650 (2013).

36. Aitken, A. R. A., Salmon, M. L. & Kennett, B. L. N. Australia's Moho: A test of the usefulness of gravity modelling for the determination of Moho depth. *Tectonophysics*, 609, 468-479 (2013).

37. Grad, M., Tiira, T. & ESC Working Group. The Moho depth map of the European Plate. *Geophysical journal international*, 176(1), 279-292 (2009).

38. Assumpção, M., Feng, M., Tassara, A. & Julià, J. Models of crustal thickness for South America from seismic refraction, receiver functions and surface wave tomography. *Tectonophysics*, 609, 82-96 (2013).

39. Tugume, F., Nyblade, A., Julià, J. & van der Meijde, M. Precambrian crustal structure in Africa and Arabia: evidence lacking for secular variation. *Tectonophysics*, 609, 250-266 (2013).

40. Nicolich, R. & Dal Piaz, G. Isobate della Moho in Italia, in Structural Model of Italy, 6 fogli 1:500,000, Progetto Finalizzato 'Geodinamica' CNR, Rome (1991).

41. Scarascia, S., Lozej, A. T. & Cassinis, R. Crustal structures of the Ligurian, Tyrrhenian and Ionian seas and adjacent onshore areas interpreted from wide-angle

seismic profiles. *Bollettino di Geofisica Teorica ed Applicata*, 36(141-44), 5-19 (1994).

42. Waldhauser, F., Kissling E., Ansorge J. & Muller S. Three-dimensional interface modeling with two-dimensional seismic data: The Alpine crust-mantle boundary, *Geophys. J. Int*., 135, 264–278, doi:10.1046/j.1365-246X.1998.00647.x (1998).
43. Lippitsch, R., Kissling E. & Ansorge J. Upper mantle structure beneath the Alpine orogen from high-resolution teleseismic tomography, J. *Geophys. Res.,* 108(B8), 2376, doi:10.1029/2002JB002016 (2003).
44. Waldhauser, F. A parameterized three-dimensional Alpine crustal model and its application to teleseismic wavefront scattering, *Ph.D. thesis*, Swiss Fed. Inst. of Technol., Zurich, Switzerland (1996).
45. Pontevivo, A. & Panza G. Group velocity tomography and regionalization in Italy and bordering areas, *Phys. Earth Planet. Inter*., 134, 1–15, doi:10.1016/S0031-9201 (02)00079-1 (2002).
46. Lombardi, D., Braunmiller J., Kissling E. & Giardini D. Moho depth and poissons ratio in the western central Alps from receiver functions, Geophys. J. Int., 173, 249–264, doi:10.1111/j.1365-246X.2007.03706.x (2008).
47. Piana Agostinetti, N., & Amato, A. Moho depth and Vp/Vs ratio in peninsular Italy from teleseismic receiver functions. *Journal of Geophysical Research: Solid Earth*, 114(B6) (2009).
48. Di Stefano, R., Bianchi, I., Ciaccio, M. G., Carrara, G. & Kissling, E. Three-dimensional Moho topography in Italy: New constraints from receiver functions and controlled source seismology. *Geochemistry, Geophysics, Geosystems*, 12(9) (2011).
49. Spada, M., Bianchi, I., Kissling, E., Agostinetti, N. P. & Wiemer, S. Combining controlled-source seismology and receiver function information to derive 3-D Moho topography for Italy. *Geophysical Journal International*, 194(2), 1050-1068 (2013).
50. Kherchouche, R., Ouyed, M., Aoudia, A., Mellouk, B. & Saadi, A. Structure of the crust and uppermost mantle beneath the Sicily Channel from ambient noise and earthquake tomography. *Annals of Geophysics*, 63(6), SE666-SE666 (2020).
51. Jongsma, D., van Hinte, J. E. & Woodside, J. M. Geologic structure and neotectonics of the North African continental margin south of Sicily. *Marine and Petroleum Geology*, 2(2), 156–179. https://doi.org/10.1016/0264-8172(85)90005-4 (1985).
52. Corti, G., Cuffaro, M., Doglioni, C., Innocenti, F. & Manetti, P. Coexisting geodynamic processes in the Sicily Channel. In Postcollisional tectonics and

magmatism in the Mediterranean region and Asia. *Geological Society of America*, https://doi.org/10.1130/2006.2409(05) (2006).

53. Scognamiglio, L., Tinti, E., Quintiliani, M. Time Domain Moment Tensor (TDMT) [Data set]. Istituto Nazionale di Geofisica e Vulcanologia (INGV). https://doi.org/10.13127/TDMT (2006).
54. Sulli, A., Morticelli, M. G., Agate, M. & Zizzo, E. Active north-vergent thrusting in the northern Sicily continental margin in the frame of the quaternary evolution of the Sicilian collisional system. *Tectonophysics*, 802, 228717 (2021).
55. Cassinis, R., Scarascia, S., Lozej, A. & Finetti, I. R. Review of seismic wide-angle reflection–refraction (WARR) results in the Italian region (1956–1987). *CROP PROJECT: Deep seismic exploration of the central Mediterranean and Italy*, 31-55 (2005).
56. Agius, M. R., *et al.* Shear-Velocity Structure and Dynamics Beneath the Sicily Channel and Surrounding Regions of the Central Mediterranean Inferred From Seismic Surface Waves. *Geochemistry, Geophysics, Geosystems*, 23(10), e2022GC010394 (2022).
57. Finetti I. R. Depth Contour Map Discontinuity in the Central Mediterranean Region from New CROP Seismic Data. *CROP PROJECT: Deep seismic exploration of the central Mediterranean and Italy*, 31-55 (2005).
58. Cavallaro, D., Monaco, C., Polonia, A., Sulli A. & Di Stefano A. Evidence of positive tectonic inversion in the north-central sector of the Sicily Channel (Central Mediterranean). *Nat Hazards* 86 (Suppl 2), 233–251. https://doi.org/10.1007/s11069-016-2515-6 (2016).
59. Scholz, C. The Mechanics of Earthquakes and Faulting. Cambridge University Press, Cambridge. https://doi.org/10.1017/9781316681473 (2019).
60. Watts, A.B., Burov, E.B. Lithospheric strength and its relationship to the elastic and seismogenic layer thickness. Earth Planet. Sci. Lett. 213, 113–131. https://doi.org/10.1016/S0012-821X(03)00289-9 (2003).
61. Locardi, E. & Nicolich, R., Geodinamica del Tirreno e dell'Appennino centro-meridionale: la nuova carta della Moho. Memorie della Società Geologica Italiana, 41, 121-140 (1988).
62. Spatola, D., *et al.* The Graham Bank (Sicily Channel, central Mediterranean Sea): seafloor signatures of volcanic and tectonic controls. *Geomorphology*, 318, 375-389 (2018).

63. Viti, M., Albarello, D. & Mantovani, E. Rheological profiles in the central-eastern Mediterranean. *Annali di geofisica*, 40(4) (1997).
64. Maggi, A., Jackson J., McKenzie D.& Priestley K. Earthquake focal depths, Effective elastic thickness and the strength of the continental lithosphere, *Geology*, 28, 495–498 (2000).
65. Jackson, J. Strength of the continental lithosphere: Time to abandon the jelly sandwich?, *GSA Today*, 12, 4 –10 (2002).
66. Déverchère, J., Houdry, F., Diament, M., Solonenko, N. V. & Solonenko, A. V. Evidence for a seismogenic upper mantle and lower crust in the Baikal rift. *Geophysical Research Letters*, 18(6), 1099-1102 (1991).
67. Chen, W. & Yang Z. Earthquakes beneath the Himalayas and Tibet: Evidence for strong lithospheric mantle, *Science*, 304, 1949– 1952 (2004).
68. Schulte-Pelkum, V., Monsalve G., Sheehan A., Pandey M., Sapkota S. & Bilham R. Imaging the Indian subcontinent beneath the Himalaya, *Nature*, 435, 1222– 1225 (2005).
69. Monsalve, G., Sheehan, A., Schulte-Pelkum, V., Rajaure, S., Pandey, M. R. & Wu, F. Seismicity and one-dimensional velocity structure of the Himalayan collision zone: Earthquakes in the crust and upper mantle. *Journal of Geophysical Research: Solid Earth*, 111(B10) (2006).
70. Civile, D., Mangano, G., Micallef, A., Lodolo, E., & Baradello, L. A Failed Rift in the Eastern Adventure Plateau (Sicilian Channel, Central Mediterranean). *Journal of Marine Science and Engineering*, *12*(7), 1142 (2024).
71. Bindi, L., Tasselli, F., Olmi, F., Peccerillo, A., & Menchetti, S. Crystal chemistry of clinopyroxenes from Linosa Volcano, Sicily Channel, Italy: implications for modelling the magmatic plumbing system. *Mineralogical Magazine*, *66*(6), 953-968 (2002).
72. Vail, P.R. Seismic Stratigraphy Interpretation Procedures. In: Bally, A.W., Ed., Atlas of Seismic Stratigraphy, AAPG Studies in Geology, Vol. 1, No. 27, 1-10 (1987).
73. Chironi, C., *et al.* Crustal structures of the Southern Tyrrhenian Sea and the Sicily Channel on the basis of the M25, M26, M28, M39 WARR profiles. *BOLLETTINO-SOCIETA GEOLOGICA ITALIANA*, 119(1), 189-204 (2000).
74. Finetti, I. R. & Del Ben, A. Crustal tectono-stratigraphic setting of the Adriatic Sea from new CROP seismic data. *CROP PROJECT: Deep seismic exploration of the Central Mediterranean and Italy,* 1, 519-548 (2005).

75. Menichelli, I. et al. Minimum 1D VP and VP/VS models and hypocentral determinations in the central Mediterranean area. *Seismological Society of America*, 93(5), 2670-2685 (2022).
76. Brocher, T. M. A Regional View of Urban Sedimentary Basins in Northern California Based on Oil Industry Compressional-Wave Velocity and Density Logs. Bulletin of the Seismological Society of America; 95 (6): 2093–2114. doi: https://doi.org/10.1785/0120050025 (2005).
77. ISIDe Working Group. ISIDe, Italian Seismological Instrumental and Parametric Database, version 1.0. DOI:10.13127/ISIDe (2016).
78. Latorre D., Di Stefano R., Castello B., Michele M. & Chiaraluce L. Catalogo delle Localizzazioni ASSolute (CLASS): locations (Version 1). Istituto Nazionale di Geofisica e Vulcanologia (INGV) https://doi.org/10.13127/class.1.0 (2022).
79. Wiemer S. & Wyss M.,. Minimum magnitude of completeness in earthquake catalogs: Examples from Alaska, the western United States and Japan. *Bull. Seismol. Soc. Am*., 90(4), 859– 869 (2000).
80. Figlioli, A., Vitale, G., Taroni, M., & D’Alessandro, A. Tremors—A Software App for the Analysis of the Completeness Magnitude. *Geosciences*, 14(6), 149 (2024).
81. RStudio Team. Integrated Development for R. RStudio, PBC, Boston, MA URL http://www.rstudio.com/ (2020).
82. Scott, D.W. *Stima della densità multivariata. Teoria, pratica e visualizzazione* . New York: Wiley (1992).
83. Hijmans R.J. Raster: geographic data analysis and modeling, r package version 2.8-4 (2018).
84. Baddeley, A., Turner, R. Spatstat: an R package for analyzing spatial point patterns. *Journal of statistical software*, 12: 1-42 (2005).

SUPPLEMENTARY INFORMATION

1. Moho in time

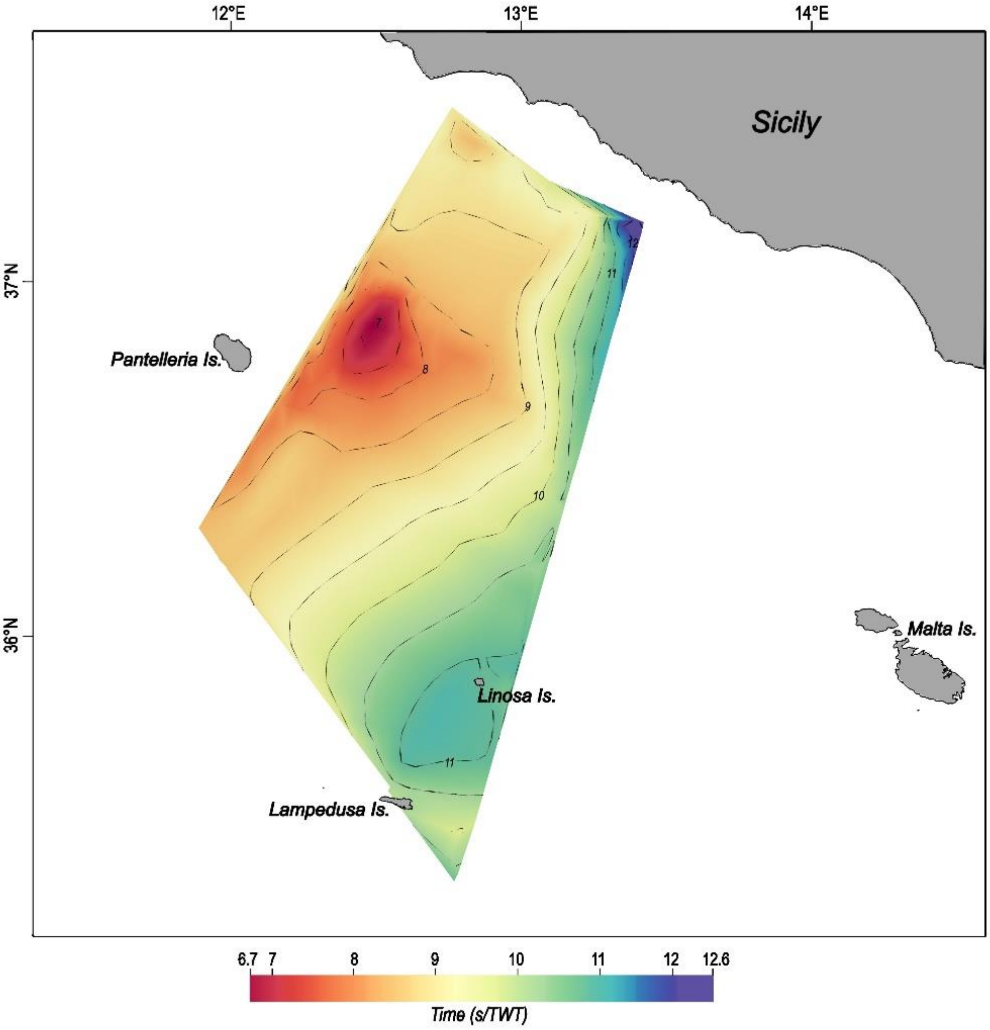

Figure S1. Moho map in time of the central western sector of the Sicily Channel.

2. Moho in depth

To better observe where the Moho information was acquired from the input data and where it was obtained from the interpolation, we show in Figure S2 the location of the seismic reflection profiles and the S- and P-wave velocity models with respect to the Moho map.

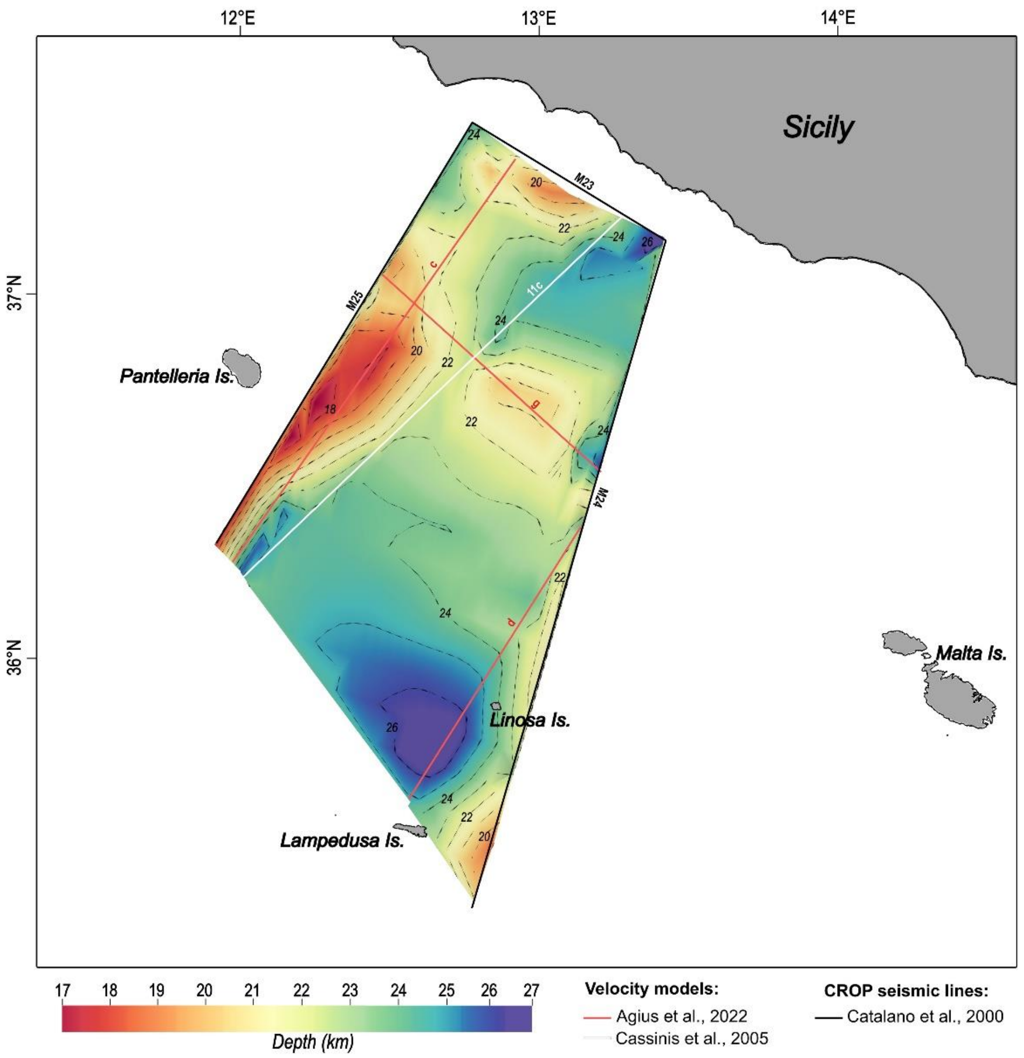

Figure S2. Moho map of the central western sector of the Sicily Channel.

3. S- and P- wave velocity models

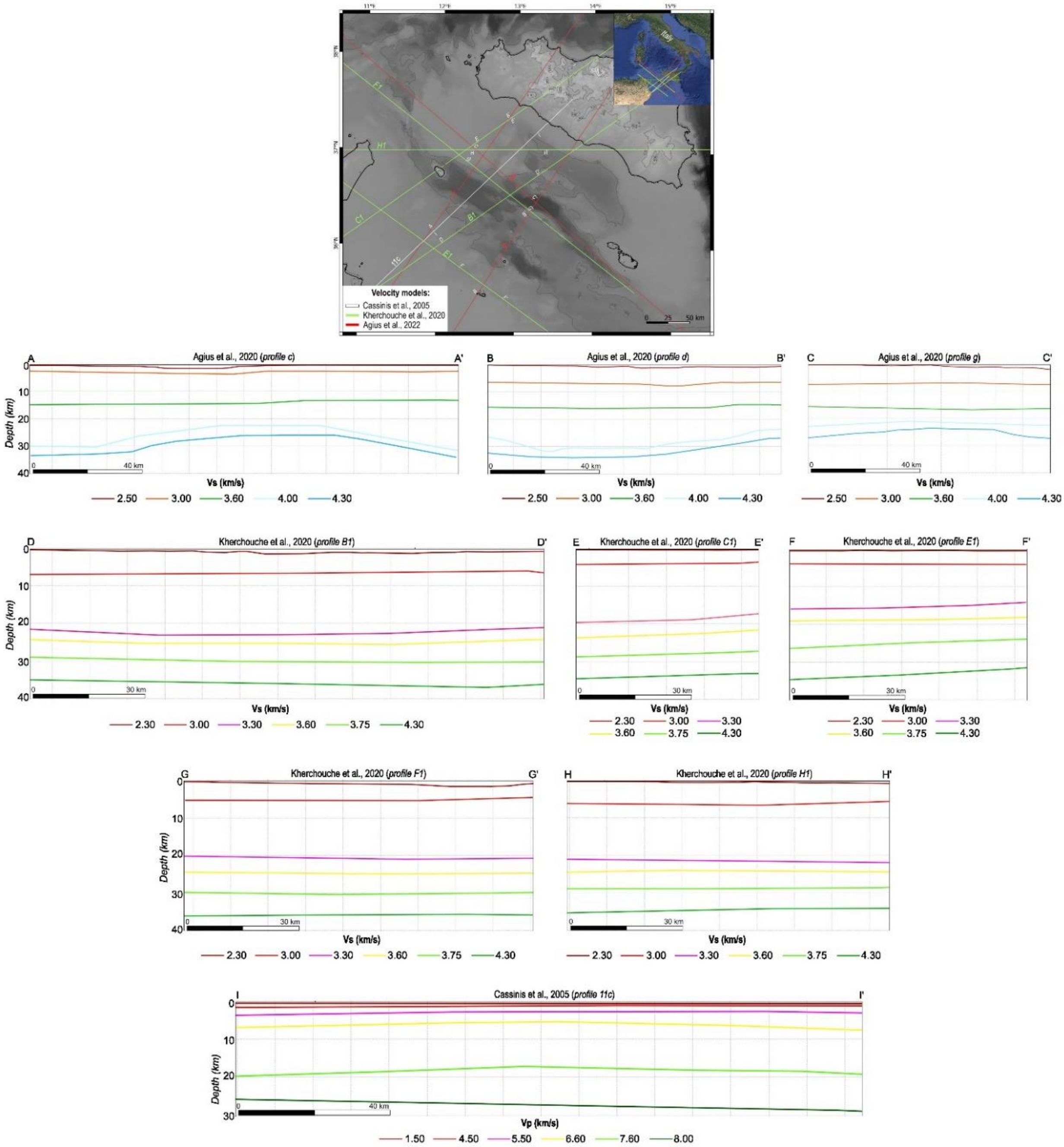

Figure S3. S- wave velocity models (Vs) [1, 2] and P-wave velocity models (Vp) [3] used in this paper.

4. From S-wave velocity models (Vs) to P-wave velocity models (Vp)

We converted Vs values to Vp values using the Vp/Vs ratio proposed by Menichelli *et al.* [4]. Since the latter is defined for southern Italy in general and not specifically for offshore areas, we also used empirical law proposed by Brocher [5]. Figure S4.1 shows the Vs and related Vp values obtained using the model of Menichelli *et al.* [4] (red circles) and the Brocher [5] law (green circles). It is observed that the results obtained from the two methods are comparable with an R^2 close to 1.

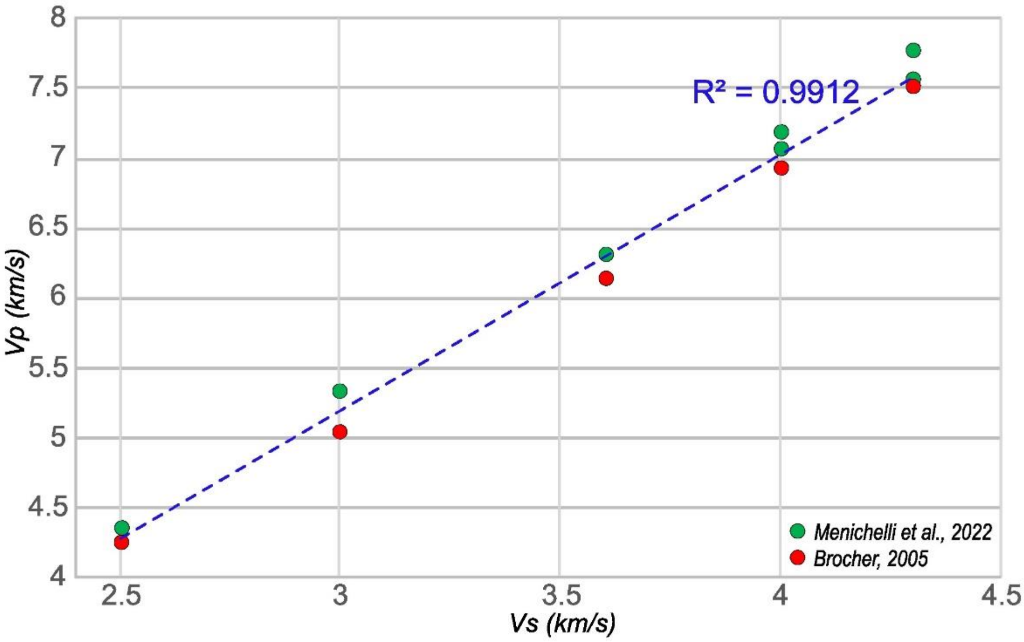

Figure S4.1. Comparison of Vp values obtained using the Vp/Vs ratio of Menichelli *et al.* [4] (red circles) and the Brocher [5] law (green circles) and the corresponding Vs values.

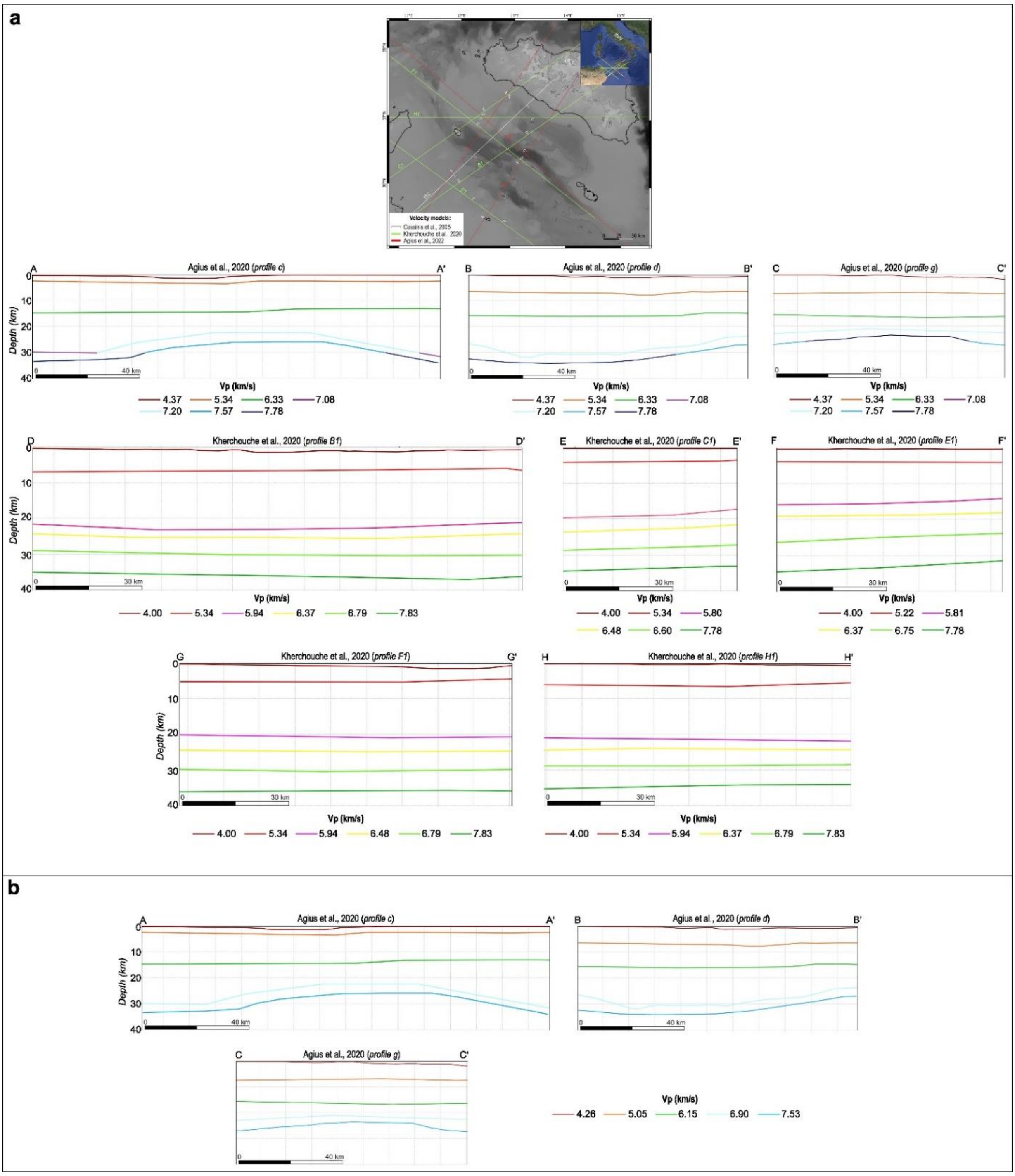

Figure S4.2. a – P-wave velocity models of Agius *et al.* [1] and Kherchouche *et al.* [2] obtained using the Vp/Vs ratio of Menichelli *et al* [4]; b - P-wave velocity profiles of Agius *et al.* [1] obtained using Brocher [5] law

5. Depth-to-time models

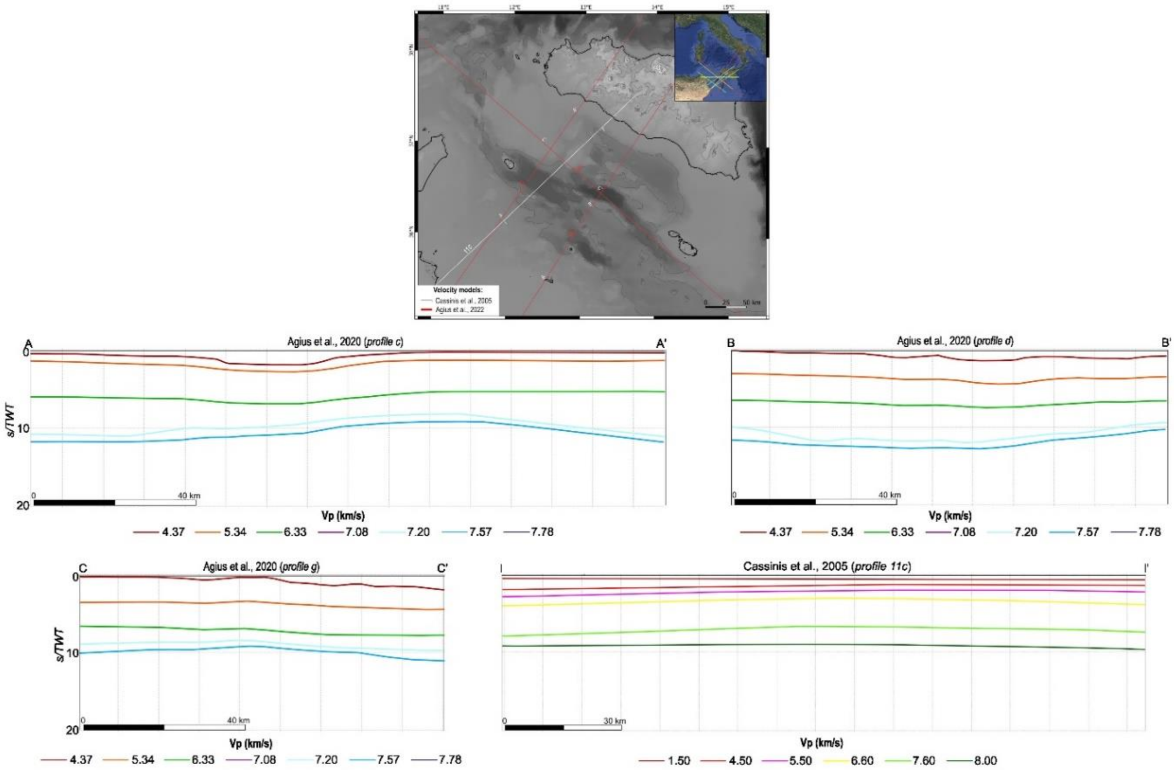

Figure S5. P-wave velocity models of Agius *et al.* [1] obtained by conversion from Vs to Vp, and of Cassinis *et al.* [3], converted from depth to times. Vertical exaggeration x2.

6. Seismic events and associated location errors

In this paper we considered events extrapolated from the ISIDe [6] database and from the CLASS [7] catalog. The latter catalog provides location quality classes, from *A* (top) to *E* (depth not for any use), and hypocentral errors in the horizontal and vertical planes for each seismic event (Fig. S6). For the building of LSVs, we excluded events belonging to quality class *E* and we considered only seismic events with M ≥ Mc (≥ 2.9).

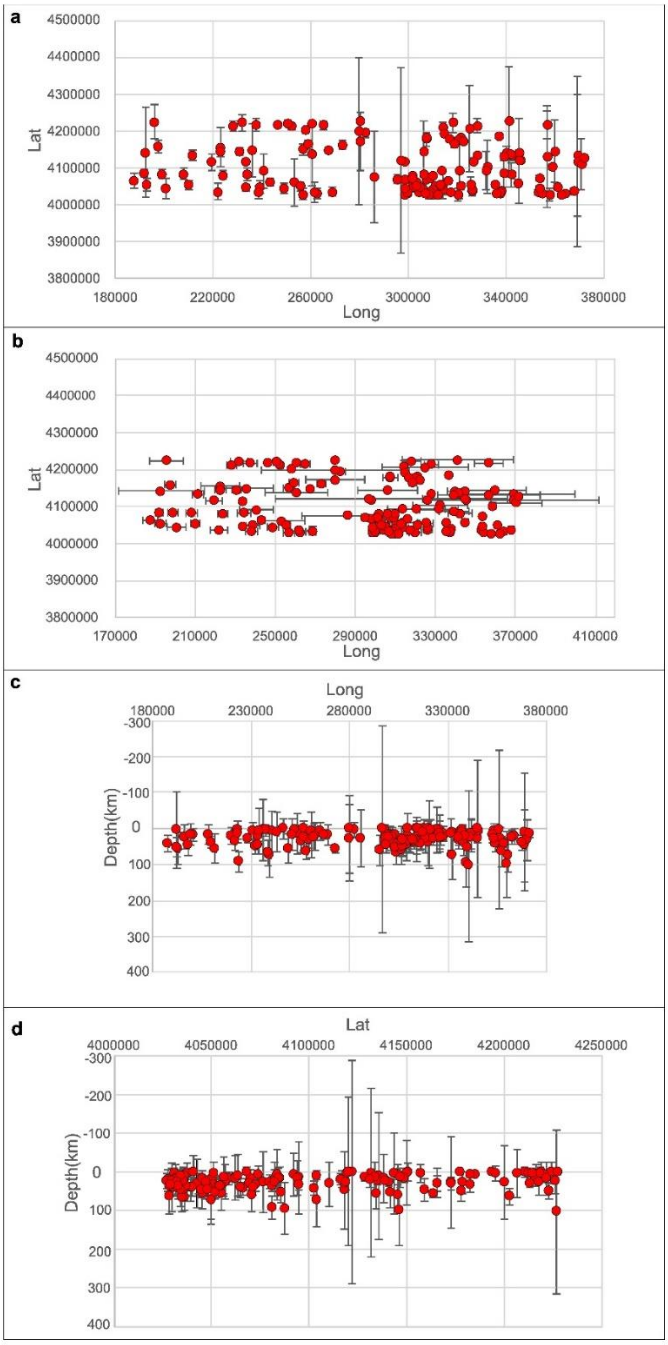

Figure S6. Seismic events extrapolated from the CLASS [7] catalog from 1981 to 2018 (red circles). Error bars represent hypocenter uncertainties along the horizontal planes (a, b) and the vertical plane (c, d).

References

1. Agius, M. R., *et al.* Shear-Velocity Structure and Dynamics Beneath the Sicily Channel and Surrounding Regions of the Central Mediterranean Inferred From Seismic Surface Waves. *Geochemistry, Geophysics, Geosystems*, 23(10), e2022GC010394 (2022).

2. Kherchouche, R., Ouyed, M., Aoudia, A., Mellouk, B. & Saadi, A. Structure of the crust and uppermost mantle beneath the Sicily Channel from ambient noise and earthquake tomography. *Annals of Geophysics*, 63(6), SE666-SE666 (2020).

3. Cassinis, R., Scarascia, S., Lozej, A. & Finetti, I. R. Review of seismic wide-angle reflection–refraction (WARR) results in the Italian region (1956–1987). *CROP PROJECT: Deep seismic exploration of the central Mediterranean and Italy*, 31-55 (2005).

4. Menichelli, I. et al. Minimum 1D VP and VP/VS models and hypocentral determinations in the central Mediterranean area. *Seismological Society of America*, 93(5), 2670-2685 (2022).

5. Brocher, T. M.; A. Regional View of Urban Sedimentary Basins in Northern California Based on Oil Industry Compressional-Wave Velocity and Density Logs. *Bulletin of the Seismological Society of America*; 95 (6): 2093–2114 (2005).

6. ISIDe Working Group. ISIDe, Italian Seismological Instrumental and Parametric Database, version 1.0. DOI:10.13127/ISIDe (2016).

7. Latorre D., Di Stefano R., Castello B., Michele M. & Chiaraluce L. Catalogo delle Localizzazioni ASSolute (CLASS): locations (Version 1). Istituto Nazionale di Geofisica e Vulcanologia (INGV) https://doi.org/10.13127/class.1.0 (2022).

CHAPTER 3
MOHO MODELING AND ANALYSIS OF THE SEISMOGENIC VOLUME IN SUBDUCTION IN THE CENTRAL MEDITERRANEAN

3.1 INTRODUCTION

The Central Mediterranean is a region marked by geodynamic complexity, resulting from the intricate interactions between the African and European tectonic plates. This convergence generates a variety of geological features, including subducting lithosphere, volcanic arcs, and back-arc basins, all contributing to significant lateral variations in lithospheric thickness and crustal structures (Faccenna et al., 1996; Catalano et al., 2001; Rosenbaum et al., 2002; van der Meijde et al., 2003; Handy et al., 2010; Di Stefano et al., 2011; Jolivet et al., 2015). These variations are reflected in a lateral variation in the depth of the Moho.

In geologically complex regions like the Central Mediterranean, a robust Moho topography map and a high-resolution model of the subducting lithosphere are essential tools for seismological, geodynamic, and geophysical investigations.

Subduction zones, recognized as some of the most seismically active areas on Earth, host the largest earthquakes and pose considerable risks for seismic and tsunami hazards (Hayes et al., 2018). Accurately describing the location and geometry of subduction slabs is fundamental for analyzing these hazards and comprehending the geodynamic context.

This thesis, present a new, detailed, and comprehensive three-dimensional map of the Moho topography of the Central Mediterranean. This model integrates various datasets, including velocity models, gravimetric profiles, and interpreted seismic reflection profiles, as well as conversions of seismic data from time to depth.

Currently, existing literature lacks a comprehensive Moho map that covers the entire Central Mediterranean region. Many available models either partially address this area or are embedded within broader regional studies, limiting their resolution and the ability to discern local geological complexities. The model shown in this thesis aims to fill this gap, revealing pronounced lateral variations in Moho depth and structure.

Furthermore, it was obtained for the first time a detailed three-dimensional model of the Ionian Crustal Seismogenic Volume (CSV) in subduction, derived from statistical method.

These results provide a vital resource for furthering the understanding of the Central Mediterranean's complex geodynamics, informing seismic and tsunami hazard assessments, and aiding the construction of lithospheric-scale models. These models can optimize earthquake location analyses and constrain seismic tomography studies, thereby contributing to a more comprehensive understanding of this geologically rich area.

The content of this chapter is in submission to the journal *Tectonophysics*

3.2 A NEW THREE-DIMENSIONAL MOHO MODEL OF THE CENTRAL MEDITERRANEAN AREA AND A RECONSTRUCTION OF THE IONIAN CRUSTAL SEISMOGENIC VOLUME IN SUBDUCTION

S. Bongiovanni[1], A. D'Alessandro[2], R. Martorana[1], A. Sulli[1]

[1]Università di Palermo, Dipartimento di Scienze della Terra e del Mare, Palermo, Italy

[2]Istituto Nazionale di Geofisica e Vulcanologia, Osservatorio Nazionale Terremoti, Rome, Italy

Abstract:

The Central Mediterranean is a geodynamically complex area resulting from the interaction between the African and European plates. Due to its complexity, the study area shows strong lateral variation in the geometry of the Moho.

In this paper, we propose the fullest Moho map currently available for the Central Mediterranean. We obtained this model using velocity models, gravimetric profiles, interpreted seismic profiles, and conversion of seismic profiles from time (TWT) to depth. Furthermore, using hypocenters of earthquakes that occurred from 2005 to 2023 with M≥2, we reconstructed the Crustal Seismogenic Volume of the subducting Ionian sector.

As a result, we obtained the surface of the top and bottom of the Crustal Seismogenic Volume and we analyzed its characteristics such as dip, azimuth, curvature, and distance between the two surfaces.

The surface of the slab was also compared with other surfaces available in the literature, and we analyzed the differences.

1 Introduction:

The Central Mediterranean is a geodynamically complex region for which all the mechanisms are not yet well understood, because it is located at a convergent margin between two plates: the African plate and the European plate.

The Central Mediterranean area is characterized by different sectors that include subducting lithosphere, continental collision, volcanic arc, back-arc basins and is therefore characterized by strong lateral variation in lithosphere thickness and in the crustal structures (Faccenna et al., 1996; Catalano et al., 2001; Rosenbaum et al., 2002; van der Meijde et al., 2003; Handy et al., 2010; Di Stefano et al., 2011; Jolivet et al., 2015). This consequently implies a strong lateral variation of the Moho depth. In such complex regions, a robust Moho topography map and a high-resolution model of the subducting lithosphere are indispensable instruments for seismological, geodynamic, and geophysical modeling.

For example, the geometry and the characteristics of the Moho are different depending on if it is oceanic or continental or if it is in zones where extensional or compressional processes are occurring (Carbonell et al., 2018).

Regarding the subduction zones, these are the most seismically active zones on the globe in which the largest earthquakes occur (Hayes et al., 2018). Describing the exact location and geometry of the subduction slab is fundamental to analyzing seismic hazard, tsunami hazard, and understanding the geodynamic setting of a subduction zone.

In addition, it is important to study as many characteristics of the subduction slab as possible such as, for example, curvature and width. In fact, Bletery et al., (2016) show that the curvature of the subduction system is one of the major controlling factors of high magnitude earthquakes. They suggest that earthquake size is limited in highly curved subduction zones. According to Schellart and Rawlinson (2013), more but smaller intensity earthquakes occur at narrow slab contrast to wide subduction zones, which support large stresses and release a large amount of energy in the form of large earthquakes.

In this paper we propose a new, detailed, and robust 3D map of the Moho topography of the Central Mediterranean. We constructed it by merging data of different nature (velocity models, gravimetric profiles, interpreted seismic reflection profiles, conversion of seismic profiles from time to depth) which allowed us to have optimal coverage of the area. In addition, the multidisciplinary approach we use allows for a more robust and reliable result because some methods require very precise a priori models and it is therefore important to constrain these results with those obtained from other methods (e.g. Aitken et al., 2013; Stankiewicz and Dewit, 2013).

Today, there are no maps in literature that cover the entire Central Mediterranean area, or the latter is within models that cover a larger area. For this reason, our model has a higher resolution that allows us to observe more clearly the strong lateral variations.

We also proposed for the first time a detailed 3D model of the Crustal Seismogenic Volume (*CSV*) of the Ionian subduction zone obtained by statistical earthquake modeling using the Gaussian kernel function. We analyzed the characteristics of the slab we obtained and compared it with those present in the literature.

Our results are a useful resource to understand the complex geodynamics of this area, to seismic and tsunami hazard analysis, and to construct lithospheric-scale models that can be used, for example, to optimize the location of earthquakes and constrain seismic tomography studies.

2 Previous studies:

Moho is generally identified by seismic and/or gravimetric methods. In the literature through the years, several authors have used Controlled Source Seismology to construct the European Moho map (Suhadolc and Panza, 1989; Du et al., 1998). Other authors used Receiver Function (RF) analysis to determine the Moho depth of Southern California (Zhu and Kanamori, 2000), northern and northeastern China (Chen et al., 2008; Liu and Niu, 2011; He et al, 2014; Wang et al., 2014), southern China (He et al., 2013), the Anatolian Plate (Vanacore et al., 2013), the Northern Canadian Cordillera (Audet et al., 2020), and eastern Tibet (Xu et al., 2007; Zhang et al., 2009; Sun et al., 2012). Stankiewicz and Dewit (2013) suggest that the use of RF analysis produces results that are not very robust because they require very accurate S-wave and P-wave velocity models, and it is therefore important to constrain these data with the seismic reflection method. Other authors used gravity data to identify the Moho in the Hellenic Arc area (Tirel et al., 2004), France (Lefort and Agarwal, 2002), South America (Mjelde et al., 2013) and Australia (Aitken et al., 2013). The latter suggest that, when possible, it is appropriate to constrain gravimetric data with seismic methods to improve the confidence of the results, especially in areas with dense and thick crust or thin and low-density crust.

To overcome the limits of these methodologies and to have a greater number of available data, several authors constructed lithospheric models and Moho maps using joint analysis of data from different methodologies. Tugume et al. (2013) made a crustal thickness map of Arabia and Africa using gravity data, RF data and surface wave dispersion; Assumpção et al. (2013) built a crustal thickness model of South Africa based on seismic tomography, RF data and seismic reflection profiles; Zhao et al. (2020), Li et al. (2014) and Huang et al. (2023) obtained a depth model of the Moho beneath Tibetan Plateau, Taiwan orogen and South China Sea basin, respectively, using gravimetric and seismic data.

The Mediterranean Moho topography models are included in European crustal models (e.g., Tesauro et al., 2008; Molinari and Morelli, 2011; Artemieva and Thybo, 2013) in which the scale of detail is inadequate to appreciate the strong lateral variations due to the complicated geodynamic setting.

Moho models containing portions of the Mediterranean are present in the literature and were produced by different methodologies. Some authors have realized maps of the Moho isobaths with poor resolution from CSS profiles (Nicolich and Dal Piaz, 1991; Scarascia et al., 1994), others have used surface wave scattering (Pontevivo and Panza, 2002), and some others used RF method (Lombardi et al., 2008; Piana Agostinetti and Amato, 2009).

More detailed and complete models were produced by Di Stefano et al. (2011) and Spada et al. (2013) using CSS and RF data. However, these models continue to be incomplete as some portions of the Central Mediterranean are not included. The area that is most incomplete is the Sicily Channel. In this area, Kherchouche et al. (2020) propose a map of the Moho obtained by environmental noise and earthquake tomography methos that shows a near-constant Moho depth, incompatible with the tectonic structures that are present. More recently, Bongiovanni et al. (2023, 2024) proposed a detailed map of the Moho using gravimetric data, velocity models, and crustal seismic reflection profiles, but it covers only the western portion of the Sicily Channel.

Regarding the subduction zones, many authors produced a global model because they host the highest intensity earthquakes and understanding their geometry and exact location is important for earthquake hazards analysis. Syracuse and Abers (2006) modeled most of the subduction zones present on the globe, but their models are poorly detailed as they have a resolution of 50 km; Hayes et al. (2012) modeled about 80% of the subduction zones present on the globe with a higher resolution (20 km). In both studies, the Ionian slab is not present. The latter was described in the literature by various authors (e.g., Rossi and Sartori, 1981; Gudmundsson and Sambridge, 1998; Doglioni et al., 1999; Minelli and Faccenna, 2010; Neri et al., 2012; van der Meer et al., 2018) who did not show and describe the exact geometry and boundaries.

More recently, Maesano et al. (2017) reconstructed the slab geometry up to a depth of about 300 km without showing the bottom of the subduction seismogenic volume, knowledge of which remains incomplete to present day. Hayes et al. (2018) describe the geometry of the slab up to 480 km depth with a resolution of 20 km, which precludes observing the strong variations present both laterally and at depth. Finally, the Database of Individual Seismogenic Sources (DISS) (2021) extends the slab model of Maesano et al. (2017) to 440 km depth but simplifies the last 140 km, which are modeled with nearly constant slope and width with increasing depth.

3 Geological and geodynamic setting

The Central Mediterranean is the result of the trench rollback of the African subducting slab that occurred during the last 30 Ma (Faccenna et al., 2001; Malinverno e Ryan, 1986). Consequently, the Central Mediterranean area consists of several domains characterized by different lithospheric thickness.

The Southern Tyrrhenian Sea (Fig. 1) is a retroarc basin which development occurred from NW to SE (Sartori, 1990; Gueguen et al., 1998; Argnani and Savelli, 1999; Carminati et al., 2004) due to the southeastward migration of the subduction system. This led to the formation first of the Vavilov Basin and then of the Marsili Basin (Sartori, 1990). The Southern Tyrrhenian Sea is characterized by thinned continental crust (Lliboutry, 2000; Pepe et al., 2000) but also by oceanic crust in the Vavilov and Marsili basins (Neri et al., 2012; Sartori et al., 2004; Pontevivo and Panza, 2006; Cella et al., 2008; Scrocca et al., 2012). The size of the latter is not very clear although Marani and Trua (2002) describe the Marsili basin as near-circular in shape with a diameter of 120 km.

Continental collision is present in Sicily and Calabria. It consists of the Sicilian-Maghrebian domain in central and western Sicily, the foreland domain in southeastern Sicily, the Kabilo-Peloritanian-Calabrian domain in northeastern Sicily and Calabria and the volcanic area in correspondence of the Mt Etna and the Aeolian Island (Billi et al., 2006 and references therein included) (Fig. 1).

An arc-shaped tectonic wedge called Calabrian Arc is identified in correspondence with the latter. Its extension into the Ionian offshore consists of a thick accretionary wedge about 300 km wide and several hundred km long (Cernobori et al., 1996; Polonia et al., 2011; Gallais et al., 2012; Corradino et al., 2020), referred to as the "External Calabrian Arc" by Selli and Rossi (1975) (Fig. 1).

In the offshore area of southern Sicily, to the west of the Malta escarpment, we find the Sicily Channel. This sector contains both contractional structures such as the Gela Thrust Front (GTF) and extensional structures such as the NW-SE oriented grabens of Pantelleria, Linosa and Malta (e.g. Finetti et al., 1984; Civile et al., 2010; Sulli et al., 2021) (Fig. 1). This area is characterized by shallow waters that deepen at the grabens (up to 1700 m), where there is crustal thinning with local uplift of the Moho (Scarascia et al., 1994; Agius et al., 2022). Volcanic manifestations are also present within the Sicily Channel, especially in the northwestern sector between the southwestern coast of Sicily and Linosa Island (Palano et al., 2020; Maiorana et al., 2023).

To eastern sector of the Malta escarpment hosts the Ionian Sea (Fig. 1). Several authors (de Voogd et al., 1992; Faccenna et al., 2001, 2004; D'Agostino et al., 2008) describe the Ionian Sea as the last remaining fragment of subducting oceanic crust in the Central Mediterranean. Refraction seismic data acquired in the Ionian Sea show a thinned oceanic or continental crust (de Voogd et al., 1992).

The Ionian subduction is one of the narrowest in the world of about 200 km wide, 500 km deep and dipping northwestward at about 70° (Anderson and Jackson, 1987; Giardini and Velonà, 1991; Selvaggi and Chiarabba, 1995; Wortel and Spakman, 2000; Chiarabba and Palano, 2017; Scarfì et al., 2018). Govers and Wortel (2005); Nijholt and Govers (2015) indicate the presence of subduction-transform edge propagator (STEP) shear zones in subduction slab edges. Some authors (Govers and Wortel, 2005; Cocchi et al., 2017; Scarfì et al., 2018; De Ritis et al., 2019) identified two STEP zones in both Ionian slab edges: the Tindari-Letojanni STEP, a right-lateral shear zone located along some of the Aeolian islands, and the Palinuro STEP, a left-lateral shear zone located along the Palinuro volcanic chain (Fig. 1).

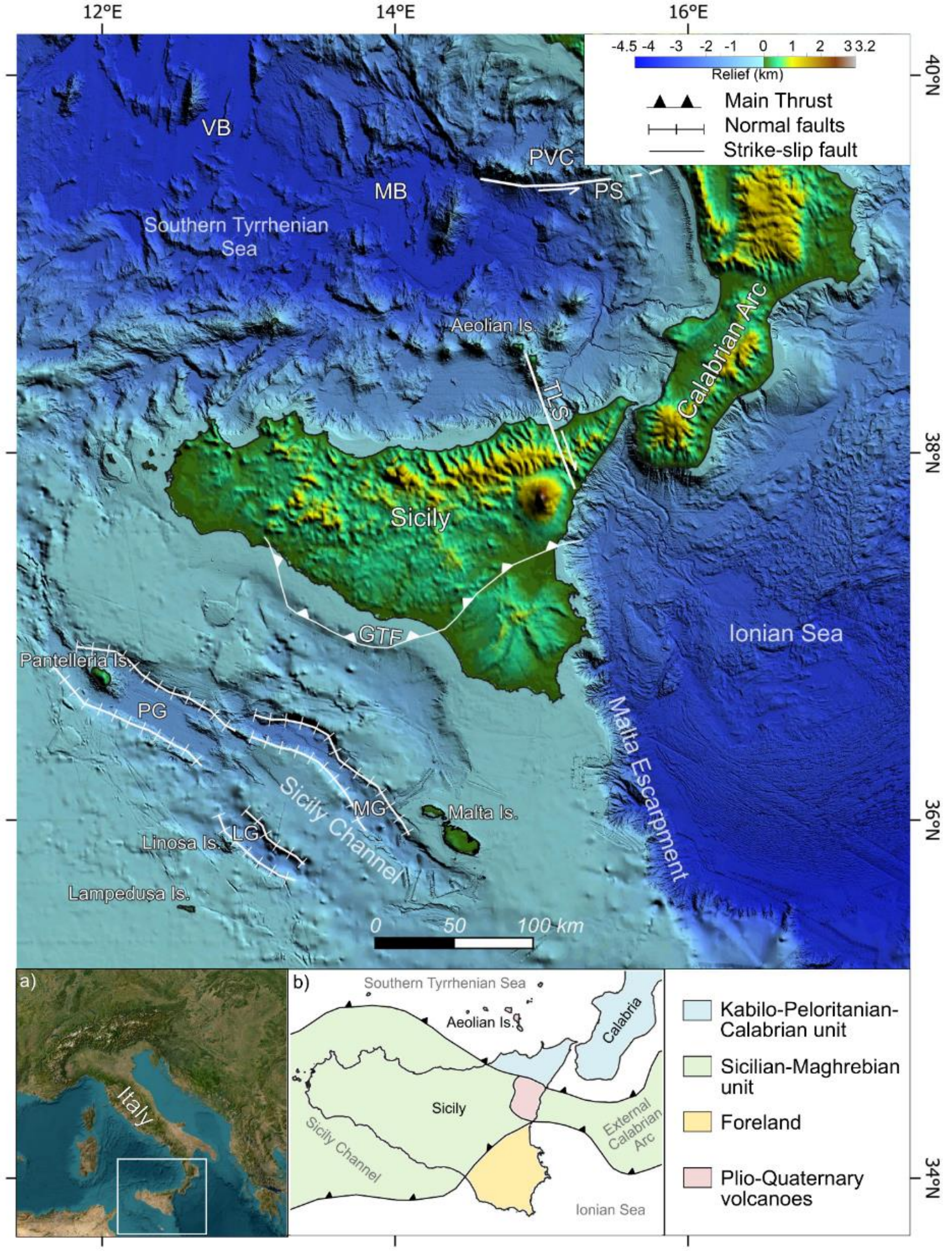

Figure 1: Geological setting of the Central Mediterranean area. VB: Vavilov Basin, MB: Marsili Basin; PVC: Palinuro volcano chain, PS: Palinuro STEP, TLS: Tindari-Letojanni STEP (Cocchi et al., 2017; De Ritis et al., 2019), GTF: Gela Thrust Front (Sulli et al., 2021); MG: Malta Graben, PG: Pantelleria Graben, LG: Linosa Graben (Civile et al., 2018). The inset (a) shows the location of the study area; the inset (b) shows the tectonic sketch of the study area (modified from Sulli, 2000). Bathymetric data were downloaded from EMODnet (https://emodnet.ec.europa.eu/geoviewer/#).

4 Data and methods

We constructed the surface of the Moho using different kinds of data (location in Fig. 2).

At the first, we consulted the catalog of seismic reflection profiles (ViDEPI 2009-2022). We used the 3D modeling software "MOVE 2017" (Midland Valley Ltd.) to digitize the profile traces that are in the study area and to plot the Moho horizons interpreted by several authors (Finetti, 2005; Catalano et al., 2013; Tugend et al., 2019; Sulli et al., 2021).

We then converted these horizons from times (TWT) to depth using the 3D Depth Conversion tool. For this purpose, we initially created a database in which we inserted the velocity value at the top of each horizon and, where possible, the velocity gradient and density (Tab.1), extrapolated from the literature (Makris et al, 1986; Scarascia et al., 1994; Bello et al., 2000; Catalano et al., 2000; Chironi et al., 2000; Nicolich et al., 2000; Catalano et al., 2002; Cassinis et al., 2005; Tassis et al., 2013; Dellong et al., 2018; Dellong et al., 2020; Akimbekova et al., 2023).

Table 1: P-wave velocities, density and velocity gradient used to time-depth conversion of seismic reflection profiles:

Horizon	**Vp (km/s)**	**Density (g/cm^3)**	**Velocity gradient (s^{-1})**
Water	1.5	-	
Plio-Pleistocene	1.8 - 2.2	2.2 - 2.35	0.08 - 1.1
Oligo-Miocene	3.4 - 4	-	-
Meso-Cenozoico	4.3 - 5	-	-
Volcanic bodies	5.5	2.86 - 3.3	-
Upper crust	6 - 6.3	2.63 - 2.75	0.005 - 0.01
Lower Crust	6.7 - 7	2.85	0.07 – 0.02
Oceanic Crust	6.9 - 7.2	2.85 - 3.1	-
Crust/mantle discontinuity	7.45 - 8.3	3.2 - 3.37	0.03

We used 16 P-wave velocity models inferred from Deep Seismic Soundings (DSS) profiles, Wide-Angle Reflection or Refraction (WARR) profiles, seismic information recorded from Ocean Bottom Seismometers (OBS) and Expanding Spread Profiles (ESP) (Makris et al., 1986; De Voogd et al., 1992 Scarascia et al., 1994; Chironi et al., 2000; Nicolich et al., 2000;

Cassinis et al., 2005; Dellong et al., 2018). We digitized these profiles using the 3D modeling software "MOVE 2017" (Midland Valley Ltd.) and traced horizons connectable to the Moho surface at abrupt changes in P-wave velocity. The P-wave velocities used for Moho horizon recognition are shown in Tab. 2. We then calibrated the horizons of the velocity models by constraining them to those of the seismic reflection profiles.

Table 2: P-wave velocities reported in literature used to identify the Moho surface:

	Vp (km/s)
Makris et al., 1986	8.1
Scarascia et al., 1994	8
Chironi et al., 2000	7.8 – 8.3
Nicolich et al., 2000	8
Cassinis et al., 2005	7.7 – 8.1
Dellong et al., 2018	8.1
De Voogd et al., 1992	7.45

We also used 4 gravimetric interpretations (Chironi et al., 2000; Dellong et al., 2018) to increase the coverage of the area. We implemented them on the "MOVE 2017" software (Midland Valley Ltd.), we plotted the Moho horizons, and we calibrated them using the Moho horizons of seismic reflection profiles as constraints.

To build the Moho surface of the Central Mediterranean area, we interpolated the horizons we previously plotted in each profile using the Delaunay triangulation method. This method has the advantages of providing more uniform geometry of triangles in a grid and not adding or removing data points from the dataset used as input. We then simplified the surface obtained by resampling it using a 10 km x 10 km grid.

To build the model of the Ionian slab and the *CSV*, we considered earthquakes that occurred from 2005 to 2023, with M ≥ 2 and depth ≥ 40 km (location in Fig. 2). We extracted them from the ISIDe database (ISIDe Working Group, 2016) considering a latitude between 35.15° and 39.6° N and a longitude between 11.5° and 17.6° E. Figure 2 also shows the focal mechanisms of the major events reported by the Time Domain Moment Tensor (TDMT) catalog (Scognamiglio et al., 2006) and the European-Mediterranean Catalog of Regional Centroid Moment Tensor (RCMT) (Pondrelli et al., 2004), which show two patterns at the subducting Ionian slab: a strike-slip in the NE and SW sectors and a normal one in the central zone.

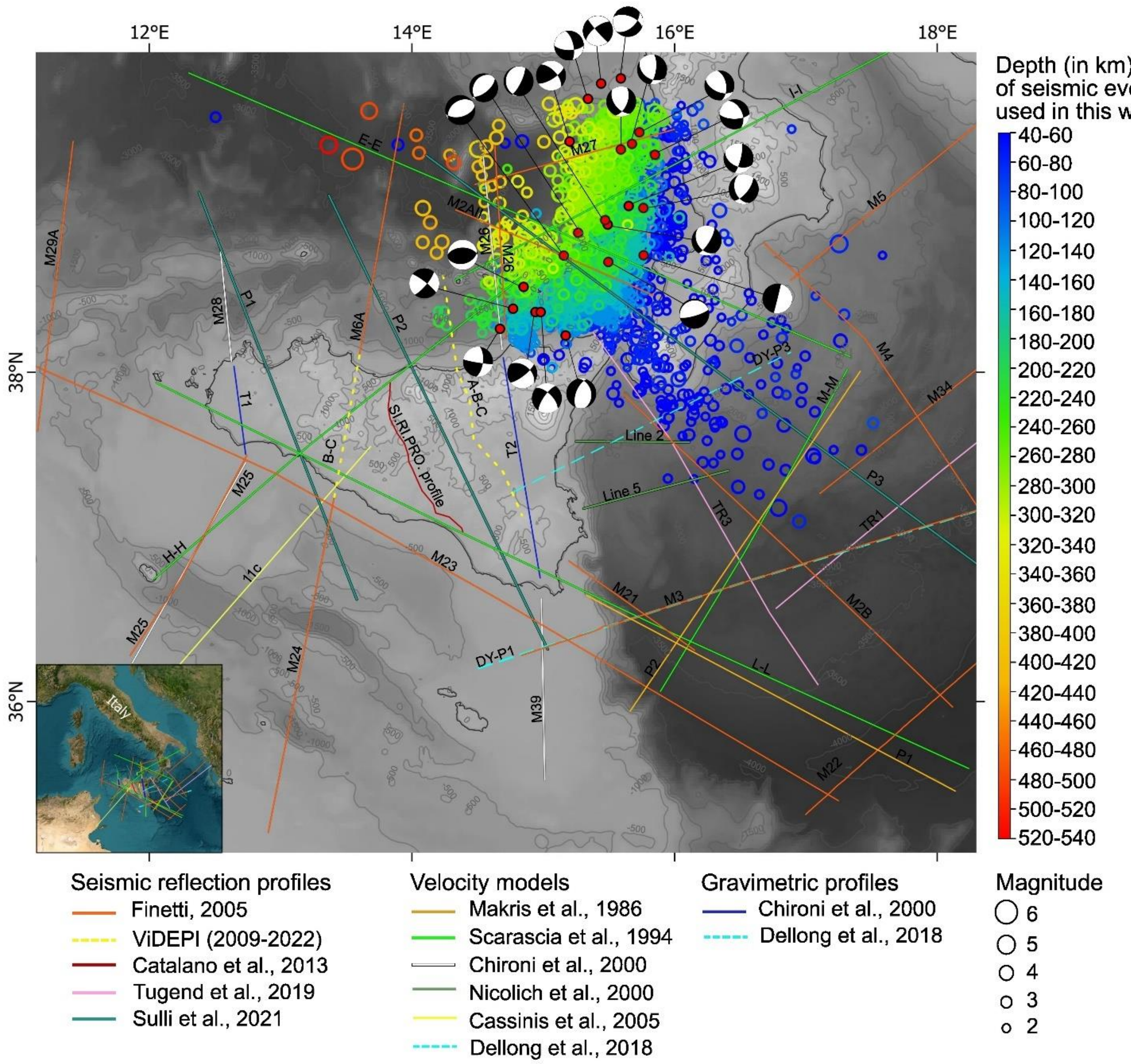

Figure 2: Map showing location of datasets used in this work (see text for details). Focal mechanism of the major events present in the Time Domain Moment Tensor (TDMT) catalog (Scognamiglio et al., 2006) and in the European-Mediterranean catalog of Regional Centroid Moment Tensor (RCMT) (Pondrelli et al., 2004) are also reported.

We divide the earthquakes dataset into 10 km depth ranges with 50% overlap. We used a statistical approach to obtain a density plot for each of these datasets by implementing a Kernel smoothed intensity function from a point pattern with 0.01 x 0.01-pixel grid, which is a spatial function representing the number of random points per unit area. We used a Gaussian Kernel function that allows for smoothing patterns obtained from highly heterogeneous points especially in areas where there are few observation points (Davies et al., 2018). We then calculated the density gradients for each density plot and extrapolated the maximum values of the gradient.

Data were organized using a MATLAB script and processed by implementing a code on the statistical software R through the *spatsat* (Baddeley and Turner, 2005) and *raster* (Hijmans, 2018) packages.

For each density gradient plot, we obtained two isolines from the gradient maxima, corresponding to the top and bottom of the *CSV*. We imported these into the 3D modeling software "MOVE 2017" (Midland Valley Ltd.) and we interpolated the top and bottom isolines of the *CSV* using the Delaunay interpolation method. We then simplified the surface obtained by resampling mode using a 10 km x 10 km grid.

In order to analyze the *CSV* in detail, we extrapolated geometric properties from its top and bottom surfaces using the “Surface Geometry Analysis Tool” in MOVE 2017 (Midland Valley Ltd.).

Specifically, we calculated Dip and Azimuth to orient in space each Delaunay triangle composing the surfaces. Considering each triangle as a planar surface, the Dip is the angle at which each triangle surface is inclined with respect to the horizontal plane and varies from 0° (horizontal) to 90° (vertical) (see sketch in Fig. 3 a). Azimuth ranges between 0° and 360° and it is the angle measured clockwise between the geographic North and the projection on the horizontal plane of the maximum dip (dip direction in Fig. 3 a) of the surface. We also calculated the curvature for each triangle constituting the surfaces using the "Simple method," which provides a measure of the rate of change of dip across a surface. For this purpose, we considered the normals of each triangle surrounding a vertex and calculated an average normal, giving a weight according to the size of the triangles. The curvature values are produced by the divergence of the normals of the triangles surrounding a vertex from the mean normal.

To observe the patterns of these parameters we constructed their Kernel density estimate curves. To do this we implemented a code on the statistical software R using a bandwidth with Silverman's (1986) rule and Gaussian Kernel.

To understand the effective size of the *CSV*, we calculated its thickness through the "Parallel construction method." Through this method, we created normal lines at the barycenter of each triangle constituting the top surface of the *CSV* up to the conjunction with the bottom surface (green lines in Fig. 3 b). To each triangle constituting the *CSV* top surface we then assigned a thickness value corresponding to the length of the line joining that triangle of the *CSV* top surface with the *CSV* bottom surface.

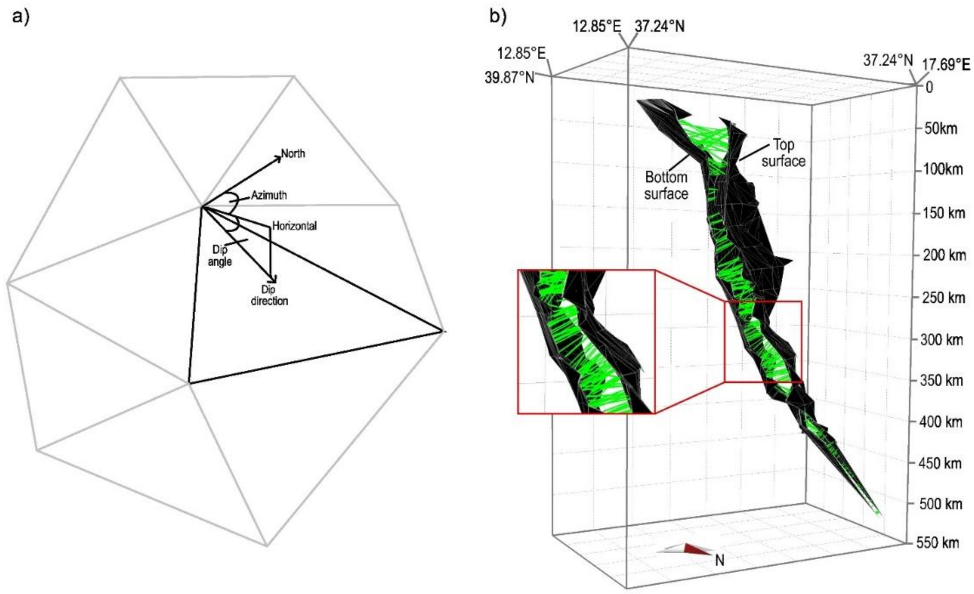

Figure 3: a) Sketch showing an example of a triangular Delaunay grid of which the top and bottom surfaces of the CSV are composed, and the dip and azimuth angles calculated for each triangle of the surfaces; b) Calculation of the thickness of the CSV. The top and bottom surfaces of the CSV are represented in black. The green lines are line normals to the barycenters of the triangles forming the top surface and reaching the bottom surface (zoom into the red square box). The length of each green line represents the value of the thickness of the CSV in that triangle.

5 Results

5.1 Moho surface:

The surface of the central Mediterranean Moho we obtained shows strong lateral variation throughout the study area in addition to the boundary at the plate interaction (Fig. 4). This edge is marked by the blue line in Figure 4 and separates the European Moho (to the north) from the African Moho (to the south).

The area of the European Moho that we have produced in this paper hosts the southern Tyrrhenian Sea, the northeastern sector of Sicily, and the Calabrian Arc. Below the latter and in part of the Southern Tyrrhenian, there is coexistence of the European and African Moho. The European Moho shows values between 15 km and 25 km depth except in the Marsili Basin, where it reaches 10 km depth, and in the northeastern sector of Sicily, where it reaches about 600 m depth.

The depth of the Moho in the Tyrrhenian Sea increases toward the Aeolian Arc. The latter is traced by the contourline that defines the 19 km depth of the Moho.

The African Moho hosts the Ionian Sea, the Sicily Channel, Sicily, and part of the offshore to the west of Sicily in which the Egadi Islands are located. In the Ionian Sea, the depth of the Moho varies between 15 km and 20 km (Fig. 4). It rapidly deepens in the northern sector at the edge of the European Moho where it reaches about 35 km depth, and in the western sector at the Malta escarpment (location in Fig. 1) where it rapidly reaches about 27 km depth.

In the Sicily Channel, the Moho shows strong lateral variation with depth values ranging from 18 km to 30 km. The lowest values are found in the central sector of the Sicily Channel that hosts the Grabens of Pantelleria, Linosa and Malta (location in Fig. 1) while the highest values are found at the GTF (location in Fig. 1). In the latter area the Moho deepens rapidly as shown by the very close isobaths. The African Moho reaches the greatest depths in Sicily with values of 38 km along the south-central sector and shows gentle uplift in the east and west where it reaches about 26 km and 28 km depth, respectively.

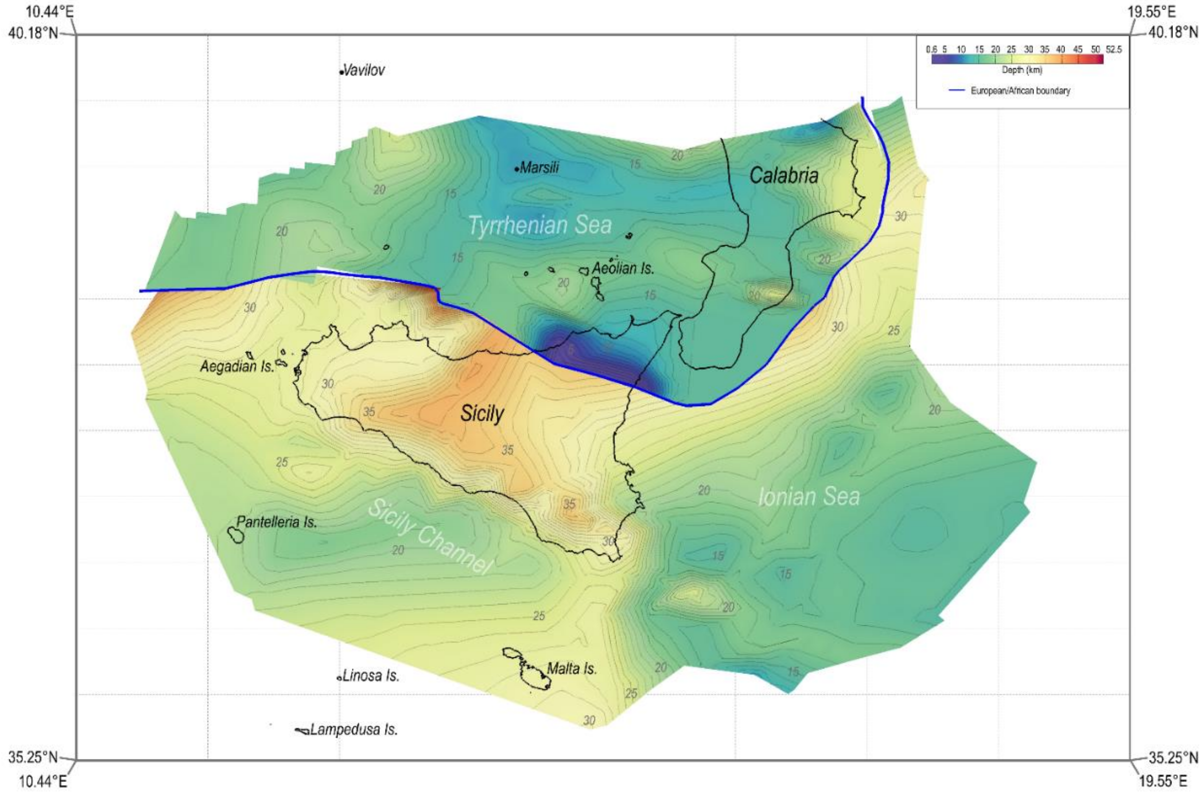

Figure 4: Map showing Moho surface represented in colour scale. The blue line indicates the boundary between African (to the north) and European (to the south) Moho.

5.2 Crustal Seimogenic Volume

The distribution of earthquakes used in this work appears rather homogeneous except in an oblique band oriented NE-SW where a seismic gap is present (dashed red line in Fig. 5).
This distribution influences the geometry of the top and the bottom surfaces of the *CSV*, which shows an articulated geometry.

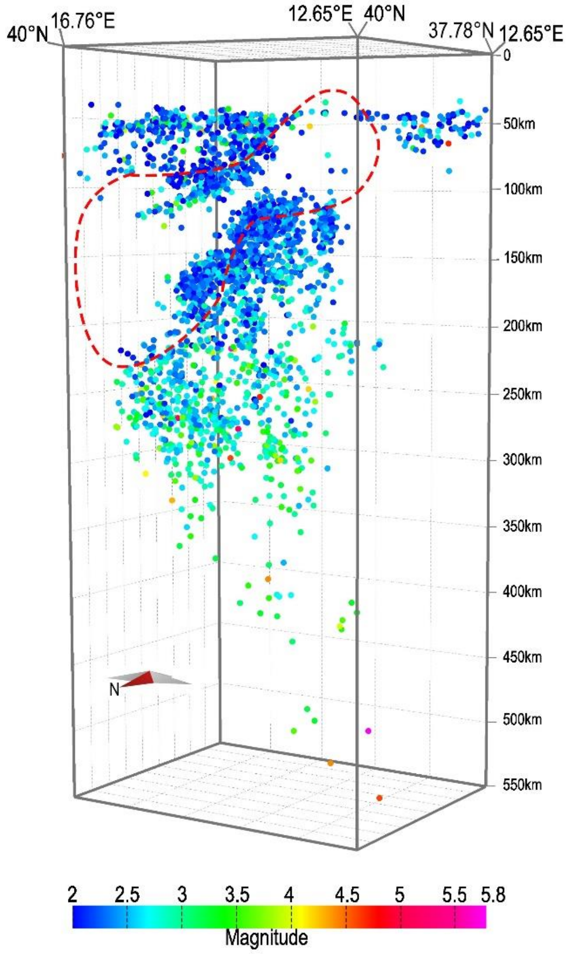

Figure 5: Distribution of earthquakes in the subduction zone extrapolated from the ISIDe catalog (Working Group 2016) from 2005 to 2023, with M ≥ 2 and depth ≥ 40 km. These are represented in color scale based on magnitude. The dashed red line highlights the seismic gap.

5.2.1 Top of CSV:

The surface of the CSV top is shown in gray by four different 3D views in Figs. 6.

It consists of 519 Delaunay triangles, and it extends to a depth of 525.7 km, which corresponds to the depth of the deepest earthquake in the seismic catalog used in this paper. At its shallowest part, it shows a width of about 170 km. Between 130 km and 230 km depth, the surface width decreases to about 100 km. Between 200 km and 250 km depth, the surface reaches a width similar to the upper part (~175 km). From 300 km to 525.7 km depth, the few seismic events suggest a narrowing of the surface.

From the dip calculation, the surface shows the highest values, reaching ~90°, up to a depth of 400 km. After this depth, the surface shows values between 70° and 75° (Fig. 7 a).

The distribution of dip values is negatively skewed and trimodal with a small peak at about 28° and two major peaks at 62° and 85° (Fig. 7 b).

The azimuth values are almost homogeneous along the entire surface (~300°) except at the upper part (~100°) and at the S-W edge (~340°) (Fig. 7c). The distribution is therefore negatively skewed and trimodal, with two peaks around 104° and 155° and a major peak at about 300° (Fig. 7 d). The slab surface is curved with a concavity toward the NW. It does not show strong variation in curvature, which remains uniform except in its edge (Fig. 7 e). Indeed, the distribution of curvature values (Fig. 7 f) is positively skewed, with peak values close to zero (see Section 4 for the curvature calculation method).

5.2.2 Bottom of the CSV:

The surface of the CSV bottom is shown in black from four different 3D perspectives in Figs. 6.

It consists of 515 Delaunay triangles and shows a geometry similar to that of the *CSV* top. Up to 200 km depth shows a width of about 100 km. Its maximum width, about 164 km, occurs between 220 km and 270 km depth. After this depth, there is a progressive narrowing of the surface which reaches a minimum width of 10 km. The highest dip values (~ 90°) occur between 100 km and 220 km. Above 100 km depth and below 220 km depth, values around 45° are observed (Fig. 8 a). The distribution of this parameter is negatively skewed and bimodal with two peaks at about 45° and 80° (Fig. 8 b). The surface shows azimuth values of ~300° except for a small upper part and the NW edge where it shows values of 120° and 350°, respectively (Fig. 8 c). The azimuth parameter distribution is negatively skewed with a high peak at ~300° (Fig. 8 d). Also, the *CSV* bottom surface shows a uniform curvature without abrupt changes, with concavity toward the NW (Fig. 8 e). Therefore, the distribution (Fig. 8 f) is positively skewed with values close to zero (see section 4 for the curvature calculation method).

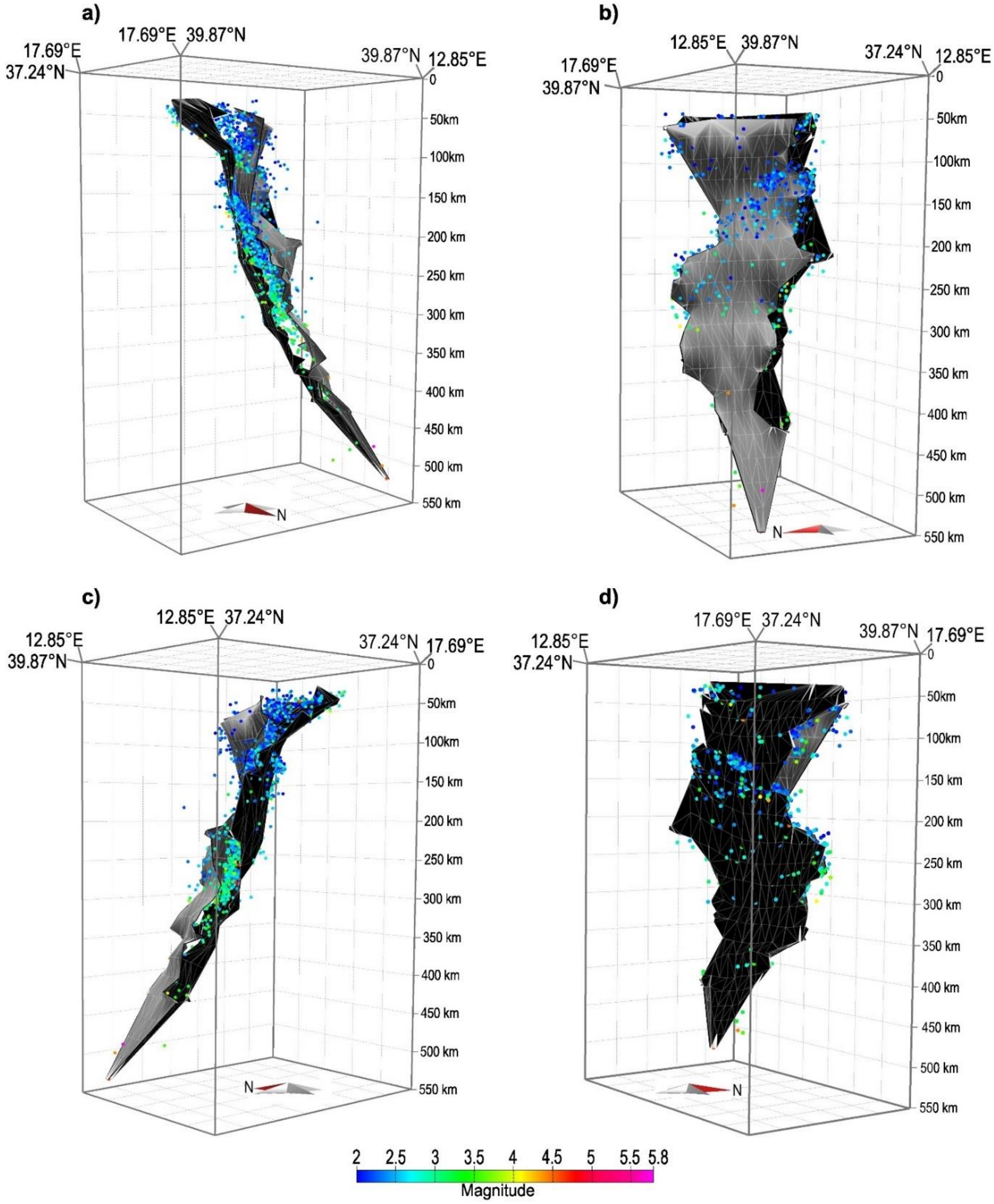

Figure 6 a, b, c, d: Different views of the 3D model of the top (in gray) and bottom (in black) surfaces of the CSV. Seismic events are represented in color scale based on magnitude.

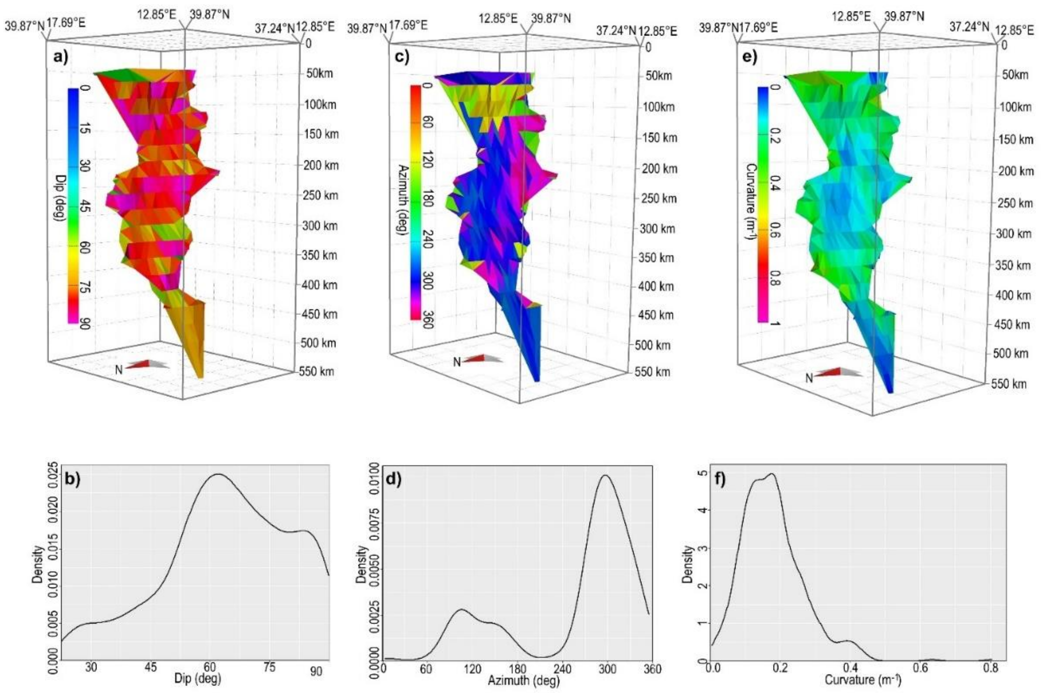

Figure 7: Representation of dip (a), azimuth (c) and curvature (d) of the CSV top and their Kernel density estimation (b, d, f).

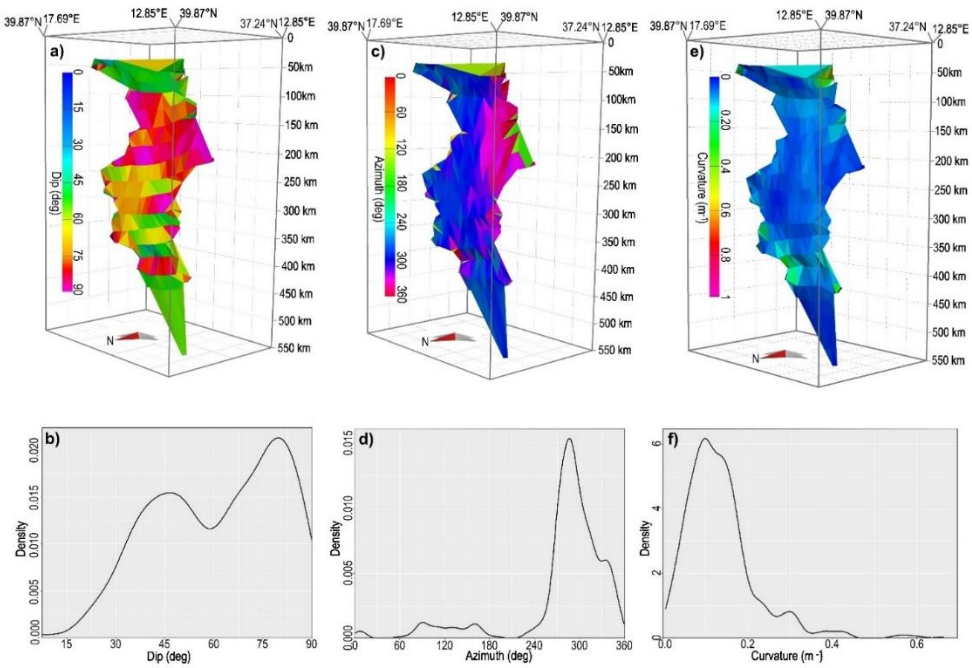

Figure 8: Representation of dip (a), azimuth (b) and curvature (c) of the CSV bottom and their Kernel density estimation (b, d, f).

To better observe the lateral and vertical variations of dip and azimuth of the CSV top and bottom surfaces, we plotted these parameters on the horizontal plane (Fig. 9 a) and the vertical planes (Figs. 9 b and c).

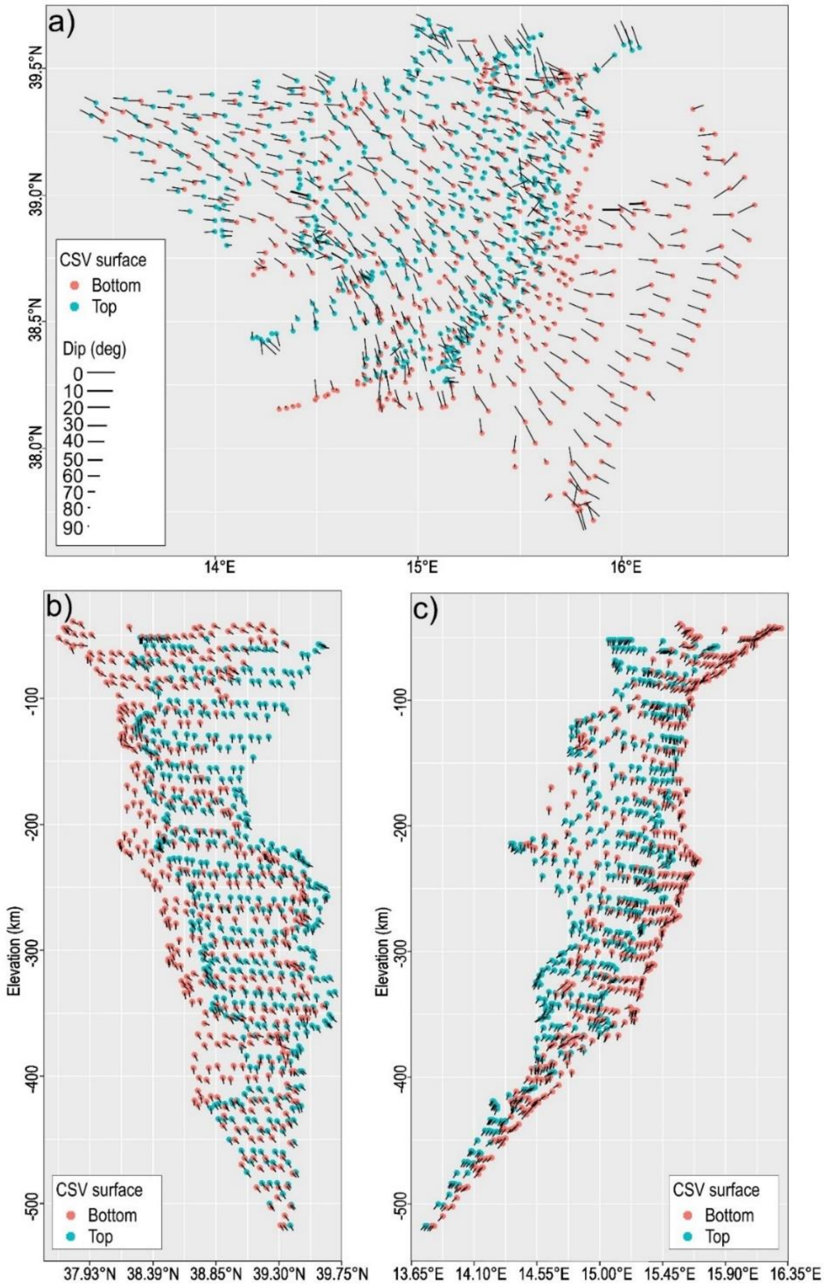

Figure 9: Representation of dip and azimuth of the top and bottom CSV surfaces on a horizontal plane (a) and vertical planes (b and c). Each point (blue and red for the top and bottom of the CSV, respectively) represents the barycenter of each Delaunay triangle constituting the two surfaces. In (a) each black segment is oriented respect to azimuth and the length of each segment indicates the value of dip; in (b) the black segments represent the dip angle. The figure was obtained using the statistical software R (version 4.3.2).

We determined the thickness of the *CSV* by calculating the distance between its top and bottom surfaces (Fig. 10 a, b).

The CSV shows its maximum thickness in the first 100 km of depth. It reaches a thickness of 90 km at a depth of 85 km and a median of 75 km at approximately 60 km depth. Between 100 km and 180 km depth, its thickness decreases with values ranging from 8 km to 25 km. From 180 km to approximately 350 km depth, the CSV shows thickness values between 25 km and 45 km and median values from 27 km to 35 km. The thickness of the remaining portion of the CSV decreases with depth, until reaching thickness values of about 5 km.

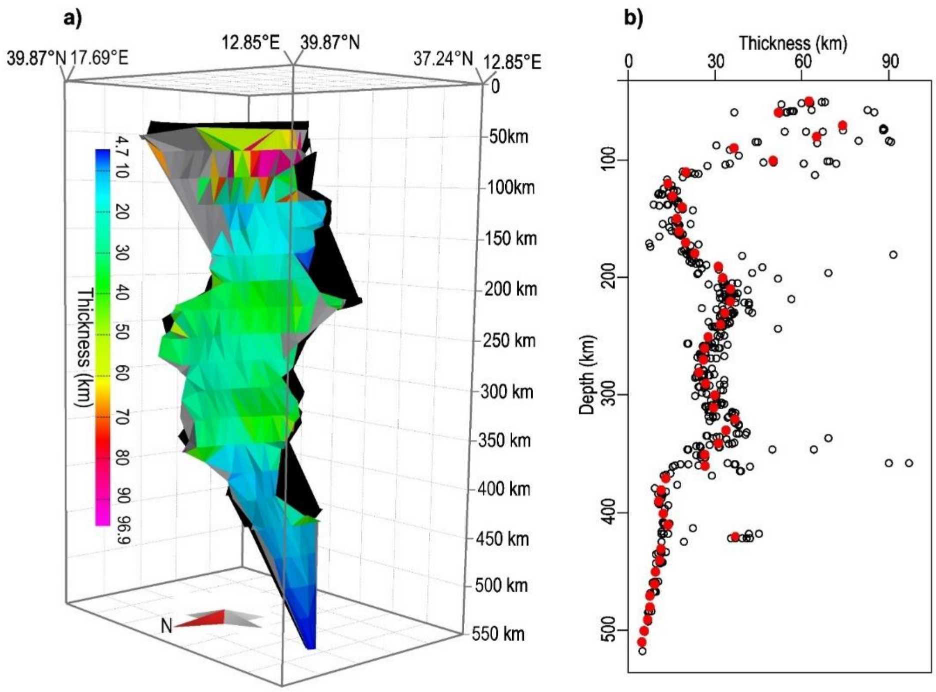

Figure 10: a) Representation of the thickness of the CSV. The black surface is the CSV bottom; the top surface is shown in color scale representing the thickness of the CSV. No data are shown in gray; b) Scatter plot showing the relationship between CSV thickness and depth. Red dots indicate the median thickness value each 10 km depth range.

6 Discussion

In this paper we propose a new and high-resolution map of the Moho of the Central Mediterranean realized by means of the joint analysis of data derived from different methodologies.

The advantages of this new map are (i) the greater areal coverage that, through the use of data from different methodologies, has allowed the Moho map of the entire Central Mediterranean to be made by also covering areas previously partially uncovered or absent in the literature (e.g. Piana Agostinetti and Amato, 2009; Di Stefano et al., 2011; Spada et al., 2013; Kherchouche et al., 2020) , and (ii) higher resolution than maps which include the Central Mediterranean but are at the European scale (e.g. Grad et al., 2009; Molinari and Morelli, 2011; Artemieva and Thybo, 2013).

The African Moho map proposed in this paper (to the south of the blue line in Fig. 4) shows high lateral variation and a close correlation with the tectonic structures. In particular, the African Moho shows minimum values (18 km depth) in the Sicily Channel at the Pantelleria Graben (see location in Fig. 1), and maximum values at the GTF (see location in Fig. 2) where the Moho reaches about 30 km depth. This strong lateral variation in the Sicily Channel is absent in the Moho map proposed by Kherchouche et al. (2020), probably due to poor seismic network coverage and lack of coverage in the offshore.

In the Ionian sector, Moho depth shows a decrease from about 35 km in the Calabrian domain to values between 15 km and 20 km in the western Ionian Sea, in agreement with Sgroi et al. (2021). Steep slopes are observed to the southwest, at the Malta escarpment, and to the north, bordering the European Moho. Depths reached by the Moho in Sicily range from about 26 km to 38 km. The largest values are found in the central southern sector, and the distribution of isobaths agrees with the distribution of negative Bouger anomalies of Accaino et al. (2011) and Milano et al. (2020).

The European Moho proposed in this paper (north of the blue line in Fig. 4) shows abrupt variations in the NE sector of Sicily and in the southern Tyrrhenian Sea at the Marsili Basin. In the NE sector of Sicily, the Moho rapidly reaches depth values less than one km. This result is in disagreement with the Moho isobaths proposed by various authors for this area (e.g., Piana Agostinetti et al., 2009; Di Stefano et al., 2011; Spada et al., 2013), which instead show values between 30 km and 35 km depth. This probably occurs because these authors consider the base of the lithosphere belonging to the African plate, whereas in this area refer to the lower limit of the crystalline basement belonging to the European units involved in deformation as Moho. In this sector, in fact, there is overlapping of units belonging to both the African and European plates. In particular, the Kabilo-Peloritanian-Calabrian unit belonging to the European plate overlaps on the Sicilian-Maghrebian unit belonging to the African plate (inset b of Fig. 1), forming a wedge. As a result, the African Moho deepens below the European Moho. The latter reaches very shallow depths until it is exhausted. This setting can be observed in the geologic profiles shown in this sector by Bianchi et al. (1987) and Roure et al. (1990). Furthermore, a shallow Moho in this sector is in agreement with the distribution of positive Bouger anomalies by Accaino et al. (2011) and Milano et al. (2020).

In the southern Tyrrhenian Sea, the Moho shows values between 15 km and 20 km with the exception of the Marsili Basin where it reaches 10 km depth. In this area, the distribution of Moho isobaths shows a nearly circular basin with a diameter of about 100 km, in agreement with Marani and Trua (2002) and Sartori (2003).

In this paper, we propose the Ionian CSV in subduction for the first time. Compared with 3D models of the Ionian slab in the literature (Maesano et al., 2017; Hayes et al., 2018; DISS Working Group, 2021), we propose a much more detailed model by also showing the CSV bottom surface. In particular, we obtained the geometric features of each Delaunay triangle composing the two surfaces (Figs. 7, 8, 9) and the thickness of the CSV (Fig. 10). It is observed that between about 110 km and 180 km depth the CSV is thinned with respect to the upper and lower portions (Fig. 10). We assume that above 110 km depth the CSV has difficulty subducting and that thinning below 110 km is caused by the weight of the slab that is subducting. Pre-existing structures, such as the presence of an oceanic ridge going into subduction, could explain the greater thickness at the shallowest part and the greater resistance to subduction. For example, Catalano et al. (2001) found an anomaly in the Ionian that could be related to an aborted oceanic ridge. Another reason could be the high rate of uplift and strong plate coupling in the eastern sector of the External Calabrian Arc, as shown by seismic line M-4 (Polonia et al., 2011).

Although the Ionian slab is among the steepest in the world (Dellong et al., 2020), the CSV extends areally toward the Tyrrhenian Sea reaching the portion between the Vavilov and Marsili basins (Fig. 11).

The top and bottom surfaces of the CSV obtained in this work show an articulated geometry. They narrow in the NE sector between about 100 km and 230 km depth and in the SW sector between about 200 km and 400 km depth (Figs. 6 b and d). From their plan projection (Fig. 11) these two constrictions appear to be horizontally propagating CSV tears.

In agreement with other authors (Neri et al., 2012; Calò et al., 2012; Gallais et al., 2013; Scarfì et al., 2018; Maesano et al., 2017, 2020) we interpret these lateral tears as the result of an initial process of CSV detachment.

At the surface, there are two tectonic structures at the edges of the CSV: the TLS (Tindari-Letojanni STEP) and the PS (Palinuro STEP) (Cocchi et al., 2017; De Ritis et al., 2019).

Some authors (e.g., Neri et al., 2012, Gallais et al., 2013; Calderoni et al., 2020) consider these two fault zones as STEP faults according to the Subduction-Transform Edge Propagator model introduced by Govers and Wortel (2005). When subduction rollback occurs, as in the case of the Ionian sector, segmentation of the subduction slab may occur

(Govers and Wortel, 2005; Rosenbaum et al., 2008) and lithospheric-scale sub-vertical tear faults may develop, referred to as STEP faults by Govers and Wortel (2005). These are generally faults with strike-slip motion, such as the TLS and PS structures (Fig. 1) and as shown by the focal mechanisms located at the edges of the CSV (Fig. 2). We therefore consider a possible relationship between the deep tectonic structures of the subduction zone and the surface tectonic structures located at the edges of the slab.

We also compared the slab obtained in this work with those proposed by Hayes et al. (2018) and the DISS (DISS Working Group, 2021) (Figs. 12).

Our slab model (Figs. 12 in blue) is narrower and more articulated than that proposed by Hayes et al. (2018) (Figs. 12 in yellow), which maintains the same width up to its maximum depth (~440 km) (Fig. 12 a). The edges of the slab proposed in this paper are discontinuous in sections 1, 2, 3, and 7 (Fig. 12 c), as suggested by the distribution of earthquake epicenters, differently to the model of Hayes et al. (2018), which shows regular and continuous edges in all sections in Figure 12 c. In addition, it is observed that from about 200 km depth, our slab model has a steeper slope.

The lonian slab model proposed by the DISS (DISS Working Group, 2021) (Fig. 12 in red) is more articulated than the model of Hayes et al. (2018) and is closer to our model although it shows differences: up to 200 km depth our model was extended laterally than that of the DISS (DISS Working Group, 2021) (Fig. 12 a), it was verticalized from about 250 km depth (Fig. 12 b, c) and it was narrowed after 300 km depth (Fig. 12 a). As shown in the section in Figure 12 c, the slab proposed by DISS (DISS Working Group, 2021) is also not continuous and up to 300 km depth has a similar trend as the one we proposed.

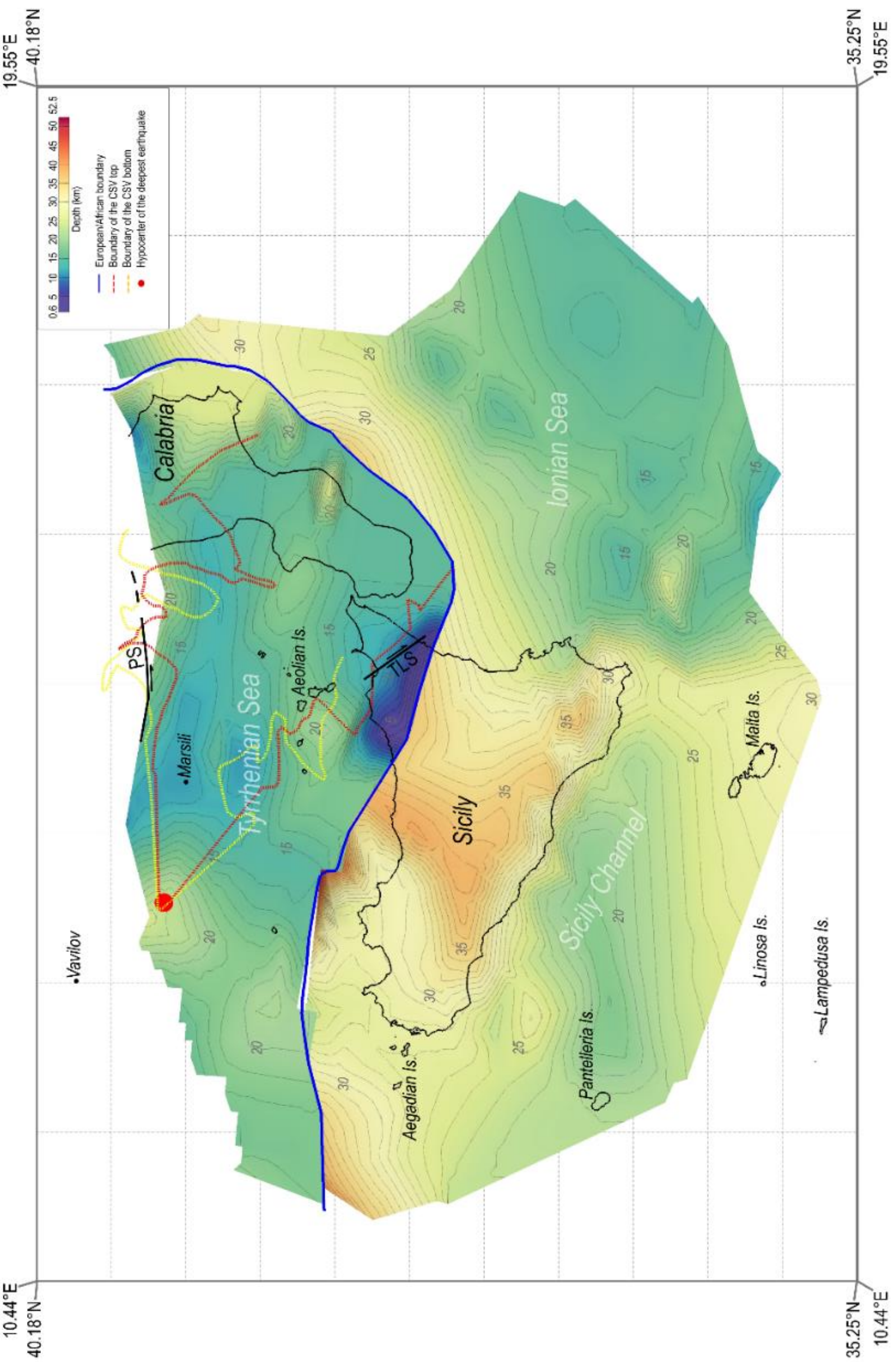

Figure 11: Moho map of the central Mediterranean and plan projection of the top (red) and bottom (yellow) surface boundary of the CSV. PS: Palinuro STEP, TLS: Tindari-Letojanni STEP (Cocchi et al., 2017; De Ritis et al., 2019).

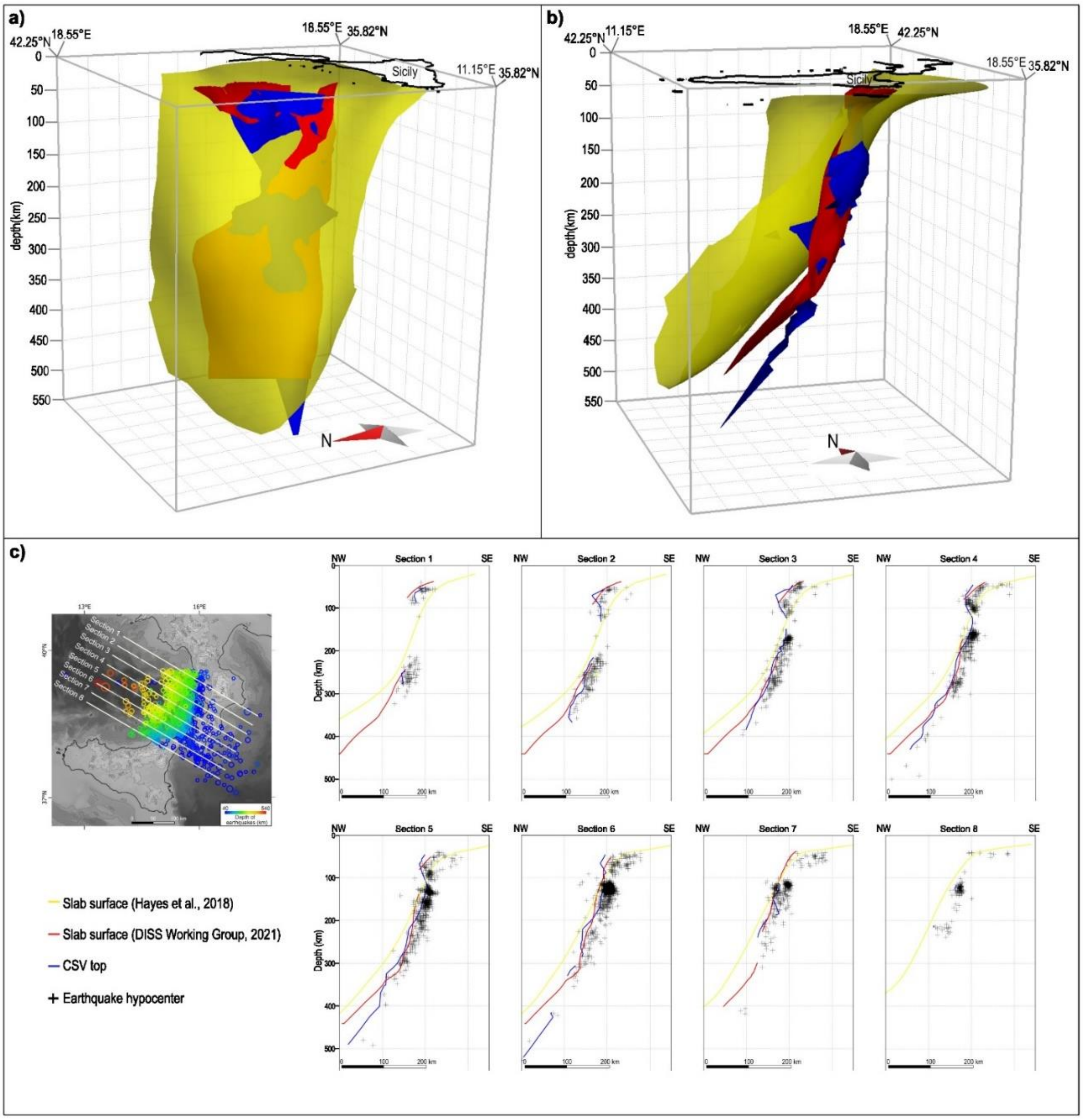

Figure 12: a, b: 3D views of the CSV top surfaces (blue) obtained in this work and the slab surfaces proposed by Hayes et al., (2018) (yellow) and DISS (DISS Working Group, 2021) (red); c: cross sections used to observe and compare the slab surfaces.

7 Conclusion

In this paper we propose the fullest Moho map currently available for the Central Mediterranean, including sectors that are partially uncovered or absent today.

A detailed model of the Moho with this areal coverage is an important instrument for the studies of the crustal structure of the Central Mediterranean and for the construction of velocity models essential for improving the accuracy of earthquake location.

We also propose for the first time the model of the subducting Ionian CSV showing in detail the lateral and vertical variations of the top and bottom surfaces that make up it.

Knowledge of the geometry and characteristics of the subducting CSV is a useful constraint to understanding the subduction mechanism occurring in the Ionian sector, to seismic and tsunami hazard studies, and to constructing geodynamic models of the area.

Finally, the model can be easily updated. New velocity models, seismic profiles and gravimetric profiles can be used to further enhance the detail of the Moho surface; new seismic events, their relocation and deep tomography data can be added to improve the detail of the subducting CSV.

References

- Accaino, F., Catalano, R., Di Marzo, L., Giustiniani, M., Tinivella, U., Nicolich, R., Sulli, A., Valenti, V., & Manetti, P. (2011). A crustal seismic profile across Sicily. Tectonophysics, 508(1-4), 52-61.
- Agius, M. R., Magrini, F., Diaferia, G., Kästle, E. D., Cammarano, F., Faccenna, C., Funiciello, F., & van der Meijde, M. (2022). Shear-Velocity Structure and Dynamics Beneath the Sicily Channel and Surrounding Regions of the Central Mediterranean Inferred From Seismic Surface Waves. Geochemistry, Geophysics, Geosystems, 23(10), e2022GC010394.
- Aitken, A. R. A., Salmon, M. L. & Kennett, B. L. N. (2013). Australia's Moho: A test of the usefulness of gravity modelling for the determination of Moho depth. Tectonophysics, 609, 468-479
- Akimbekova, A., Carboni, F., Mancinelli, P., Barreca, G., Scarfì, L., Pauselli, C., Monaco, C., & Barchi, M. R. (2023). Gravity modelling of the Tyrrhenian-Calabrian-Ionian subduction system. Frontiers in Earth Science, 11.
- Anderson, H., & Jackson, J. (1987). Active tectonics of the Adriatic region. Geophysical Journal International, 91(3), 937-983.Argnani, A., & Savelli, C. (1999). Cenozoic volcanism and tectonics in the southernTyrrhenian sea: Space-time distribution and geodynamicsignificance. Journal of Geodynamics, 27(4-5), 409-432.
- Artemieva, I. M., & Thybo, H. (2013). EUNAseis: A seismic model for Moho and crustal structure in Europe, Greenland, and the North Atlantic region. Tectonophysics, 609, 97-153.
- Assumpção, M., Feng, M., Tassara, A., & Julià, J. (2013). Models of crustal thickness for South America from seismic refraction, receiver functions and surface wave tomography. Tectonophysics, 609, 82-96.

- Audet, P., Schutt, D. L., Schaeffer, A. J., Estève, C., Aster, R. C., & Cubley, J. F. (2020). Moho variations across the northern Canadian Cordillera. Seismological Society of America, 91(6), 3076-3085.
- Baddeley A., & Turner R. (2005). Spatsat: an r package for analyzing spatial point patterns. J. Stat Softw 12, i06
- Bello, M., & Merlini, S. (2000). Structual model of central eastern Sicily. In EAGE Conference on Geology and Petroleum Geology of the Mediterranean and Circum-Mediterranean Basins (pp. cp-109). European Association of Geoscientists & Engineers.
- Bianchi, F., Carbone, S., Grasso, M., Invernizzi, G., Lentini, F., & Longaretti, G. (1987). Sicilia orientale. Profilo geologico Nebrodi-Iblei. Memorie della Società Geologica Italiana, 38, 429-458.
- Billi, A., Barberi, G., Faccenna, C., Neri, G., Pepe, F., & Sulli, A. (2006). Tectonics and seismicity of the Tindari Fault System, southern Italy: Crustal deformations at the transition between ongoing contractional and extensional domains located above the edge of a subducting slab. Tectonics, 25(2).
- Bongiovanni, S., Maiorana, M., D'Alessandro, A., Martorana, R., & Sulli, A. (2023). Multidisciplinary approach to the study of a crustal tectonic discontinuity: an example from the Central Mediterranean offshore (Sicily channel). In EGU General Assembly Conference Abstracts (pp. EGU-11843).
- Bongiovanni, S., Maiorana, M., D’Alessandro, A., Martorana, R. & Sulli., A. (2024). a new Moho map of the central-western Sicily Channel: correlation with volcanoes, tectonic structures and seismogenic volumes. Submitted to Scientific Reports.
- Bletery, Q., Thomas, A. M., Rempel, A. W., Karlstrom, L., Sladen, A., & De Barros, L. (2016). Mega-earthquakes rupture flat megathrusts. Science, 354(6315), 1027-1031.
- Calderoni, G., Gervasi, A., La Rocca, M., & Ventura, G. (2020). Strike-Slip Earthquakes at the Northern Edge of the Calabrian Arc Subduction Zone. Seismological Society of America, 92(2A), 1023-1035.
- Calò, M., Dorbath, C., Luzio, D., Rotolo, S. G., & D'anna, G. (2012). Seismic velocity structures of southern Italy from tomographic imaging of the Ionian slab and petrological inferences. Geophysical Journal International, 191(2), 751-764.
- Carbonell, R., Levander, A., & Kind, R. (2013). The Mohorovičić discontinuity beneath the continental crust: An overview of seismic constraints. Tectonophysics, 609, 353-376.
- Carminati, E., Cavazza, W., Roure, F., Spakman, W., Stampfli, G. M., & Ziegler, P. A. (2004). TRANSMED Transect III: Massif Central-Provence-Gulf of Lion-Provençal Basin-

Sardinia-Tyrrhenian Basin-Southern Apennines-Apulia-Adriatic Sea-Albanides-Balkans-Moesian Platform. In W. Cavazza, F. Roure, W. Spakman, G. M. Stampfli, & P. A. Ziegler (Eds.), The TRANSMED Atlas: The Mediterranean Region from crust to mantle. Heidelberg: Springer-Verlag.

- Catalano, R., Franchino, A., Merlini, S., & Sulli, A. (2000). Central western Sicily structural setting interpreted from seismic reflection profiles. Mem. Soc. Geol. It, 55, 5-16.
- Catalano, R., C. Doglioni, & S. Merlini (2001). On the Mesozoic Ionian basin, Geophys. J. Int., 144, 49–64, doi:10.1046/j.0956-540X.2000.01287.x.
- Catalano, R., Merlini, S., & Sulli, A. (2002). The structure of western Sicily, central Mediterranean. Petroleum Geoscience, 8(1), 7-18.
- Catalano R., Valenti V., Albanese C., Accaino F., Sulli A., Tinivella U., Gasparo Morticelli M., Zanolla C., & Giustiniani M. (2013). Sicily's fold–thrust belt and slab roll-back: the SI. RI. PRO. seismic crustal transect. Journal of the Geological Society, 170(3), 451-464.
- Cassinis R., Scarascia S., & Lozej A. (2005). Review of Seismic Wide-Angle Reflection—Refraction (WARR) Results in the Italian Region (1956-1987). CROP PROJECT: Deep Seismic Exploration of the Central Mediterranean and Italy , pp. 31–55, Elsevier.
- Cella, F., M. Fedi, G. Florio, V. Paoletti, & A. Rapolla (2008). A review of the gravity and magnetic studies in the Tyrrhenian basin and itsvolcanic districts,Ann. Geophys.,51(1), doi:10.4401/ag-3035.
- Cernobori, L., A. Hirn, J. H.McBride, R. Nicolich, L. Petronio, M. Romanelli, & Streamers/Profiles Working Groups (1996). Crustal image of the Ionian basin and its Calabrian margins, Tectonophysics, 264, 175–189, doi:10.1016/S0040-1951(96)00125-4.
- Chen, L., Wang, T., Zhao, L., & Zheng, T. (2008). Distinct lateral variation of lithosphere thickness in the northeastern north China craton, Earth planet. Sci. Lett., 267, 56–68.
- Chiarabba, C., & Palano, M. (2017). Progressive migration of slab break-off along the southern Tyrrhenian plate boundary: Constraints for the present day kinematics. Journal of Geodynamics, 105, 51-61.
- Chironi C., De Luca L., Guerra I., Luzio D., Moretti A., Vitale M., & Sealand Group. (2000). Crustal structures of the Southern Tyrrhenian Sea and the Sicily Channel on the basis of the M25, M26, M28, M39 WARR profiles. Boll. Soc. Geol. It., 119(1), 189-204.
- Civile, D., Lodolo, E., Accaino, F., Geletti, R., Schiattarella, M., Giustiniani, M., Fedorik, J., & Zampa, L. (2018). Capo granitola-sciacca fault zone (Sicilian Channel, Central Mediterranean): structure vs magmatism. Marine and Petroleum Geology, 96, 627-644.

- Civile, D., Lodolo, E., Accettella, D., Geletti, R., Ben-Avraham, Z., Deponte, M., Facchin, L., Ramella, R., & Romeo, R. (2010). The Pantelleria graben (Sicily Channel, Central Mediterranean): an example of intraplate ‘passive’rift. Tectonophysics, 490(3-4), 173-183.
- Cocchi, L., S. Passaro, F. C. Tontini, & G. Ventura (2017). Volcanism in slab tear faults is larger than in island-arcs and back-arcs, Nat. Commun. 8, no. 1, 1451, doi: 10.1038/s41467-017-01626-w.
- Corradino, M., Pepe, F., Bertotti, G., Picotti, V., Monaco, C., & Nicolich, R. (2020). 3-D architecture and Plio-Quaternary evolution of the Paola Basin: Insights into the forearc of the Tyrrhenian-Ionian subduction system. Tectonics, 39(2), e2019TC005898.
- Civello S., & Margheriti L. (2004). Toroidal mantle flow around the Calabrian slab (Italy) from SKS splitting. Geophysical Research Letters, 31(10).
- D’Agostino, N., A. Avallone, D. Cheloni, E. D’Anastasio, S. Mantenuto, & G. Selvaggi (2008). Active tectonics of the Adriatic region from GPS and earthquake slip vectors, J. Geophys. Res., 113, B12413, doi:10.1029/2008JB005860.
- Davies, T. M., Marshall, J. C., & Hazelton, M. L. (2018). Tutorial on kernel estimation of continuous spatial and spatiotemporal relative risk. Statistics in medicine, 37(7), 1191-1221.
- Dellong, D., Klingelhoefer, F., Kopp, H., Graindorge, D., Margheriti, L., Moretti M., Murphy, S., & Gutscher, M. A. (2018). Crustal structure of the Ionian basin and eastern Sicily margin: Results from a wide-angle seismic survey. J. Geophys.. Res.: Solid Earth, 123(3), 2090-2114, DOI: 10.1002/2017JB015312.
- Dellong, D., Klingelhoefer, F., Dannowski, A., Kopp, H., Murphy, S., Graindorge, D., Margheriti, L., Moretti, M., Barreca, G., Scarfì, L., Polonia, A., & Gutscher, M. A. (2020). Geometry of the deep Calabrian subduction (Central Mediterranean Sea) from wide-angle seismic data and 3-D gravity modeling. Geochemistry, Geophysics, Geosystems, 21(3).
- De Ritis, R., F. Pepe, B. Orecchio, D. Casalbore, A. Bosman, M. Chiappini, F. Chiocci, M. Corradino, R. Nicholich, E. Martorelli, C., Monaco, Presti, D., & Totaro, C. (2019). Magmatism along lateral slab edges: Insights from the Diamante–Enotrio–Ovidio volcanic-intrusive complex (southern Tyrrhenian Sea), Tectonics 38, 2581–2605, doi: 10.1029/2019TC005533.
- de Voogd, B., C. Truffert, N. Chamot-Rooke, P. Huchon, S. Lallemant, & X. Le Pichon (1992). Two-ship deep seismic soundings in the basins of the eastern Mediterranean Sea (Pasiphae cruise), Geophys. J. Int., 109, 536–552, doi:10.1111/j.1365-246X.1992.tb00116.x.

- Di Stefano, R., Bianchi, I., Ciaccio, M. G., Carrara, G., & Kissling, E. (2011). Three-dimensional Moho topography in Italy: New constraints from receiver functions and controlled source seismology. Geochemistry, Geophysics, Geosystems, 12(9).
- DISS Working Group (2021). Database of Individual Seismogenic Sources (DISS), Version 3.3.0: A compilation of potential sources for earthquakes larger than M 5.5 in Italy and surrounding areas. Istituto Nazionale di Geofisica e Vulcanologia (INGV). https://doi.org/10.13127/diss3.3.0
- Doglioni, C., S. Merlini, & G. Cantarella (1999). Foredeep geometries at the front of the Apennines in the Ionian Sea (central Mediterranean), Earth Planet. Sci. Lett., 168, 243–254, doi:10.1016/S0012-821X(99) 00059-X.
- Du, Z., A. Michelini, & G. Panza (1998). EurId: A regionalized 3-D seismological model of Europe, Phys. Earth Planet. Inter., 106, 31–62, doi:10.1016/S0031-9201(97)00107-6.
- Faccenna, C., Davy, P., Brun, J. P., Funiciello, R., Giardini, D., Mattei, M., & Nalpas, T. (1996). The dynamics of back-arc extension: an experimental approach to the opening of the Tyrrhenian Sea. Geophysical Journal International, 126(3), 781-795.
- Finetti, I.R. (Ed.) (2005). CROP project: deep seismic exploration of the Central Mediterranena and Italy. Elsevier.
- Faccenna, C., T. W. Becker, F. P. Lucente, L. Jolivet, & F. Rossetti (2001). History of subduction and back-arc extension in the central Mediterranean, Geophys. J. Int., 145, 809–820, doi:10.1046/j.0956- 540x.2001.01435.x.
- Faccenna, C., C. Piromallo, A. Crespo-Blanc, L. Jolivet, & F. Rossetti (2004). Lateral slab deformation and the origin of the western Mediterranean arcs, Tectonics, 23, TC1012, doi:10.1029/2002TC001488.
- Finetti I. R. (1984). Geophysical study of the Sicily Channel Rift Zone. Boll. Geofis. Teor. Appl., 26, pp. 3-28
- Finetti, I. R. (Ed.). (2005). CROP project: deep seismic exploration of the central Mediterranean and Italy. Elsevier.
- Gallais F., Gutscher M. A., Klaeschen D., & Graindorge D. (2012). Two-stage growth of the Calabrian accretionary wedge in the Ionian Sea (Central Mediterranean): Constraints from depth-migrated multichannel seismic data. Marine Geology, 326-328, 28-45, http://dx.doi.org/10.1016/j.margeo.2012.08.006.
- Gallais, F., Graindorge, D., Gutscher, M. A., & Klaeschen, D. (2013). Propagation of a lithospheric tear fault (STEP) through the western boundary of the Calabrian accretionary wedge offshore eastern Sicily (Southern Italy). Tectonophysics, 602, 141-152.

- Giardini, D., & M. Velonà (1991). Deep seismicity of the Tyrrhenian Sea, Terra Nova, 3, 57–64.
- Govers, R., & Wortel, M. J. R. (2005). Lithosphere tearing at STEP faults: Response to edges of subduction zones. Earth and Planetary Science Letters, 236(1-2), 505-523.
- Grad, M., T. Tiira, & the ESC Working Group (2009). The Moho depth map of the European Plate, Geophys. J. Int., 176, 279–292, doi:10.1111/j.1365-246X.2008.03919.x.
- Gudmundsson, Ó., & Sambridge, M. (1998). A regionalized upper mantle (RUM) seismic model. Journal of Geophysical Research: Solid Earth, 103(B4), 7121-7136.
- Gueguen, E., Doglioni, C., & Fernandez, M. (1998). On the post-25 Ma geodynamic evolution of the western Mediterranean. Tectonophysics, 298(1-3), 259-269.
- Handy, M. R., Schmid, S. M., Bousquet, R., Kissling, E., & Bernoulli, D. (2010). Reconciling plate-tectonic reconstructions of Alpine Tethys with the geological-geophysical record of spreading and subduction in the Alps. Earth-Science Reviews, 102(3-4), 121–158.
- Hayes, G. P., Moore, G. L., Portner, D. E., Hearne, M., Flamme, H., Furtney, M., & Smoczyk, G. M. (2018). Slab2, a comprehensive subduction zone geometry model. Science, 362(6410), 58-61.
- Hayes, G. P., Wald, D. J., & Johnson, R. L. (2012). Slab1. 0: A three-dimensional model of global subduction zone geometries. Journal of Geophysical Research: Solid Earth, 117(B1).
- He, C.S., Dong, S.W., Chen, X.H., Santosh, M. & Li, Q.S., (2014). Crustal structure and continental dynamics of Central China: a receiver function study and implications for ultrahigh-pressure metamorphism, Tectonophysics, 610, 172–181
- He, C.S., Donga, S.W., Santosh, M. & Chen, X.H., (2013). Seismic evidence for a geosuture between the Yangtze and Cathaysia Blocks, South China, Sci. Rep., 3, 200,doi:10.1038/srep02200
- Hijmans R.J. (2018). Raster: geographic data analysis and modeling, r package version 2.8-4
- ISIDe Working Group; 2016: ISIDe, Italian Seismological Instrumental and Parametric Database, version 1.0. DOI:10.13127/ISIDe.
- Jolivet, L., C. Gorini, J. Smit, & S. Leroy (2015), Continental breakup and the dynamics of rifting in back-arc basins: The Gulf of Lion margin,Tectonics,34, 662–679, doi:10.1002/2014TC003570
- Kherchouche, R., Ouyed, M., Aoudia, A., Mellouk, B. & Saadi, A. (2020). Structure of the crust and uppermost mantle beneath the Sicily Channel from ambient noise and earthquake tomography. Annals of Geophysics, 63(6), SE666-SE666.

- Lefort, J. P., & Agarwal, B. N. P. (2002). Topography of the Moho undulations in France from gravity data: their age and origin. Tectonophysics, 350(3), 193-213.
- Li, Z., Roecker, S., Kim, K., Xu, Y., & Hao, T. (2014). Moho depth variations in the Taiwan orogen from joint inversion of seismic arrival time and Bouguer gravity data. Tectonophysics, 632, 151-159.
- Liu, H. & Niu, F. (2011). Receiver function study of the crustal structure of Northeast China: seismic evidence for a mantle upwelling beneath the eastern flank of the Songliao Basin and the Changbaishan region, Earthq. Sci., 24(1), 27–33
- Lliboutry, L. (2000). Quantitative geophysics and geology. Springer Science & Business Media.
- Lombardi, D., J. Braunmiller, E. Kissling, & D. Giardini (2008). Moho depth and poissons ratio in the western central Alps from receiver functions, Geophys. J. Int., 173, 249–264, doi:10.1111/j.1365-246X.2007.03706.x
- Maesano, F. E., Tiberti, M. M., & Basili, R. (2017): The Calabrian Arc: three-dimensional modelling of the subduction interface. Scientific reports, 7(1), 8887.
- Maesano, F. E., Tiberti, M. M., & Basili, R. (2020). Deformation and fault propagation at the lateral termination of a subduction zone: The Alfeo fault system in the Calabrian Arc, Southern Italy. Frontiers in Earth Science, 8, 107.
- Maiorana, M., Artoni, A., Le Breton, E., Sulli, A., Chizzini, N., & Torelli, L. (2023). Is the Sicily Channel a simple Rifting Zone? New evidence from seismic analysis with geodynamic implications. Tectonophysics, 864, 230019.
- Makris, J., Nicolich, R., & Weigel, W. (1986). A seismic study in the Western Ionian Sea. In Annales geophysicae. Series B. Terrestrial and planetary physics (Vol. 4, No. 6, pp. 665-678).
- Malinverno, A., & Ryan, W. B. (1986). Extension in the Tyrrhenian Sea and shortening in the Apennines as result of arc migration driven by sinking of the lithosphere. Tectonics, 5(2), 227-245.245.
- Marani, M. P., Gamberi, F., & Bonatti, E. (2004). From seafloor to deep mantle: architecture of the tyrrhenian backarc basin. memorie descrittive della carta geologica d'italia. vol. lXIV.
- Marani, M. P., & Trua, T. (2002). Thermal constriction and slab tearing at the origin of a superinflated spreading ridge: Marsili volcano (Tyrrhenian Sea). Journal of Geophysical Research: Solid Earth, 107(B9), EPM-3.

- Milano, M., Kelemework, Y., La Manna, M., Fedi, M., Montanari, D., & Iorio, M. (2020). Crustal structure of Sicily from modelling of gravity and magnetic anomalies. Scientific Reports, 10(1), 16019.
- Minelli, L., & C. Faccenna (2010). Evolution of the Calabrian accretionary wedge (central Mediterranean), Tectonics, 29, TC4004, doi:10.1029/2009TC002562.
- Mjelde, R., Goncharov, A., & Müller, R. D. (2013). The Moho: boundary above upper mantle peridotites or lower crustal eclogites? A global review and new interpretations for passive margins. Tectonophysics, 609, 636-650.
- Molinari, I., & Morelli, A. (2011). EPcrust: a reference crustal model for the European Plate. Geophysical Journal International, 185(1), 352-364.
- Neri, G., Marotta, A. M., Orecchio, B., Presti, D., Totaro, C., Barzaghi, R., & Borghi, A. (2012). How lithospheric subduction changes along the Calabrian Arc in southern Italy: geophysical evidences. International Journal of Earth Sciences, 101, 1949-1969.
- Nicolich, R. & G. Dal Piaz (1991). Isobate della Moho in Italia, in Structural Model of Italy, 6 fogli 1:500,000, Progetto Finalizzato ‘Geodinamica’ CNR, Rome.
- Nicolich R., Laigle M., Hirn A., Cernobori L. & Gallart J. (2000). Crustal structure of the Ionian margin of Sicily: Etna volcano in the frame of regional evolution. Tectonophysics, 329(1-4), 121-139.
- Nijholt, N., & Govers, R. (2015). The role of passive margins on the evolution of Subduction-Transform Edge Propagators (STEPs). Journal of Geophysical Research: Solid Earth, 120(10), 7203-7230.
- Palano, M., Ursino, A., Spampinato, S., Sparacino, F., Polonia, A., & Gasperini, L. (2020). Crustal deformation, active tectonics and seismic potential in the Sicily Channel (Central Mediterranean), along the Nubia–Eurasia plate boundary. Scientific reports, 10(1), 21238.PEPE, F., BERTOTTI, G., CELLA, F. and MARSELLA, E. (2000), Rifted margin formation in the South Tyrrhenian Sea: A high-resolution seismic profile across the north Sicily passive continental margin, Tectonics 19, 2, 241–257.
- Piana Agostinetti, N., & A. Amato (2009). Moho depth and vp/vs ratio in peninsular Italy from teleseismic receiver functions. J. Geophys. Res., 114, B06303, doi:10.1029/ 2008JB005899.
- Polonia, A., Torelli L., Mussoni P., Gasperini L., Artoni A. & Klaeschen D. (2011). The Calabrian Arc subduction complex in the Ionian Sea: Regional architecture, active deformation, and seismic hazard. Tectonics, 30, TC5018, doi:10.1029/2010TC002821.

- Pondrelli, S., Morelli, A., & Ekström, G. (2004). European-Mediterranean regional centroid-moment tensor catalog: solutions for years 2001 and 2002. Phys. Earth Plan. Int., 145, 1-4, 127-147
- Pontevivo, A., & G. Panza (2002). Group velocity tomography and regionalization in Italy and bordering areas, Phys. Earth Planet. Inter., 134, 1–15, doi:10.1016/S0031-9201 (02)00079-1.
- Pontevivo, A., & Panza, G. F. (2006). The lithosphere-asthenosphere system in the Calabrian Arc and surrounding seas–Southern Italy. Pure and Applied Geophysics, 163, 1617-1659.
- Rosenbaum, G., Lister, G. S., & Duboz, C. (2002). Reconstruction of the tectonic evolution of the western Mediterranean since the Oligocene. Journal of the Virtual Explorer, 8, 107–130.
- Rossi, S. & Sartori, R. (1981). A seismic reflection study of the external Calabrian Arc in the northern Ionian Sea (eastern Mediterranean). Marine Geophysical Researches, 4(4), 403-426.
- Roure, F., Howell, D. G., Müller, C., & Moretti, I. (1990). Late Cenozoic subduction complex of Sicily. Journal of Structural Geology, 12(2), 259-266.
- Sartori, R. (1990). The main results of ODP Leg 107 in the frame of Neogene to Recent geology of peri-Tyrrhenian areas. In Proceedings of the ocean drilling program, Scientific Results (Vol. 107, pp. 715-730).
- Sartori, R. (2003). The Tyrrhenian back-arc basin and subduction of the Ionian lithosphere. Episodes Journal of International Geoscience, 26(3), 217-221.
- Sartori, R., Torelli, L., Zitellini, N., Carrara, G., Magaldi, M., & Mussoni, P. (2004). Crustal features along a W–E Tyrrhenian transect from Sardinia to Campania margins (Central Mediterranean). Tectonophysics, 383(3-4), 171-192.
- Scarascia S., Lozej A and Cassinis R. (1994). Crustal structures of the Ligurian, Tyrrhenian and Ionian Seas and adjacent onshore areas interpreted from wide-angle seismic profiles. Boll. Di Geof. Teo. Ed Appl., XXXVI, 141-144.
- Scarfì, L., Barberi, G., Barreca, G., Cannavò, F., Koulakov, & I.,and Patanè, D. (2018). Slab narrowing in the Central Mediterranean: The Calabro-Ionian subduction zone as imaged by high resolution seismic tomography. Scientific reports, 8(1), 5178.
- Schellart, W. P., & Rawlinson, N. (2013). Global correlations between maximum magnitudes of subduction zone interface thrust earthquakes and physical parameters of subduction zones. Physics of the Earth and Planetary Interiors, 225, 41-67.

- Scognamiglio, L., Tinti, E., & Quintiliani, M. (2006). Time Domain Moment Tensor (TDMT) [Data set]. Istituto Nazionale di Geofisica e Vulcanologia (INGV). https://doi.org/10.13127/TDMT.
- Scrocca, D., E. Carminati, C. Doglioni, & D. Procaccianti (2012). Tyrrhenian Sea, inRegional Geology and Tectonics: Phanerozoic PassiveMargins, Cratonic Basins and Global Tectonic Maps, vol. 1C, edited by D. G. Roberts and A. W. Bally, pp. 473–485, Elsevier, Amsterdam
- Selli, R. & Rossi, S. (1975). 'The Main Geological Features of the Ionian Sea', Rapp. Comm. Int. Mer Medit. 23, 115–116
- Selvaggi, G., & Chiarabba, C. (1995). Seismicity and P wave velocity image of the Southern Tyrrhenian subduction zone, Geophys. J. Int., 121, 818–826
- Sgroi, T., Polonia, A., Barberi, G., Billi, A., & Gasperini, L. (2021). New seismological data from the Calabrian arc reveal arc-orthogonal extension across the subduction zone. *Scientific Reports*, *11*(1), 473.
- Silverman, B. W. (1986). Density estimation for statistics and data analysis. London: Chapman and Hall.
- Spada, M., Bianchi, I., Kissling, E., Agostinetti, N. P. & Wiemer, S. (2013). Combining controlled-source seismology and receiver function information to derive 3-D Moho topography for Italy. Geophysical Journal International, 194(2), 1050-1068.
- Stankiewicz, J. & de Wit, M. (2013). 3.5 billion years of reshaped Moho, southern Africa. Tectonophysics, 609, 675-689.
- Suhadolc, P., Panza, G. F., & Mueller, S. (1990). Physical properties of the lithosphere—asthenosphere system in Europe. Tectonophysics, 176(1-2), 123-135.
- Sulli, A. (2000). Structural framework and crustal characteristics of the Sardinia Channel Alpine transect in the central Mediterranean. Tectonophysics, 324(4), 321-336.
- Sulli A., Gasparo Morticelli M., Agate M., & Zizzo E. (2021). Active north-vergent thrusting in the northern Sicily continental margin in the frame of the quaternary evolution of the Sicilian collisional system. Tectonophysics, 802, 228717.
- Sun, Y., Niu, F., Chen, Y. & Liu, J. (2012). Crustal structure and deformation of the SE Tibetan plateau revealed by receiver function data, Earth planet. Sci. Lett., 349, 186–197.
- Syracuse, E. M., & G. A. Abers (2006). Global compilation of variations in slab depth beneath arc volcanoes and implications, Geochem. Geophys. Geosyst., 7, Q05017, doi:10.1029/2005GC001045

- Tassis, G. A., Grigoriadis, V. N., Tziavos, I. N., Tsokas, G. N., Papazachos, C. B., & Vasiljević, I. (2013). A new Bouguer gravity anomaly field for the Adriatic Sea and its application for the study of the crustal and upper mantle structure. Journal of Geodynamics, 66, 38-52.
- Tesauro, M., Kaban, M. K., & Cloetingh, S. A. (2008): EuCRUST-07: A new reference model for the European crust. Geophysical Research Letters, 35(5).
- Tirel, C., Gueydan, F., Tiberi, C., & Brun, J. P. (2004). Aegean crustal thickness inferred from gravity inversion. Geodynamical implications. Earth and Planetary Science Letters, 228(3-4), 267-280.
- Tugend J., Chamot-Rooke N., Arsenikos S., Blanpied C. & Frizon de Lamotte D. (2019): Geology of the Ionian Basin and margins: A key to the East Mediterranean geodynamics. Tectonics, 38(8), 2668-2702.
- Tugume, F., Nyblade, A., Julià, J. & van der Meijde, M. (2013). Precambrian crustal structure in Africa and Arabia: evidence lacking for secular variation. Tectonophysics, 609, 250-266.
- Van der Meer, D. G., Van Hinsbergen, D. J., & Spakman, W. (2018). Atlas of the underworld: Slab remnants in the mantle, their sinking history, and a new outlook on lower mantle viscosity. Tectonophysics, 723, 309-448.
- Van Der Meijde, M., Van Der Lee, S., & Giardini, D. (2003). Crustal structure beneath broad-band seismic stations in the Mediterranean region. Geophysical Journal International, 152(3), 729-739. https://doi.org/10.1046/j.1365-246X.2003.01871.x
- Vanacore, E. A., Taymaz, T., & Saygin, E. (2013). Moho structure of the Anatolian Plate from receiver function analysis. Geophysical Journal International, 193(1), 329-337.
- ViDEPI; 2009-2022: Progetto ViDEPI. Visibilità dei dati afferenti all'attività di esplorazione petrolifera in Italia Ministero dello sviluppo economico DGRME - Società Geologica Italiana – Assomineraria.
- Wang, C., Sandvol, E., Zhu, L., Lou, H., Yao, Z. & Luo, X. (2014). Lateral variation of crustal structure in the ordos block and surrounding regions, North China, and its tectonic implications, Earth planet. Sci. Lett., 387, 198–211.
- Wortel M. J. R. & Spakman, W. (2000). subduction and slab detachment in the Mediterranean-Carpathian region. Science, 290(5498), 1910-1917.
- Xu, L., Rondenay, S., & Van der Hilst, R.D. (2007). Structure of the crust beneath the southeastern Tibetan Plateau from teleseismic receiver functions, Phys. Earth planet. Inter., 165, 176–193

- Zhang, Z., Wang, Y., Chen, Y., Houseman, G.A., Tian, X., Wang, E., & Teng, J. (2009). Crustal structure across Longmenshan fault belt from passive source seismic profiling, Geophys. Res. Lett., 36, L17310, doi:10.1029/2009GL039580.
- Zhao, G., Liu, J., Chen, B., Kaban, M. K., & Zheng, X. (2020). Moho beneath Tibet based on a joint analysis of gravity and seismic data. Geochemistry, Geophysics, Geosystems, 21(2), e2019GC008849.
- Zhu, L. & Kanamori, H. (2000). Moho depth variation in southern California from teleseismic receiver functions. Journal of Geophysical Research: Solid Earth, 105(B2), 2969-2980.

CHAPTER 4
FROM SURFACE TO DEPTH: A COMPREHENSIVE ANALYSIS OF THE CENTRAL MEDITERRANEAN

4.1 Introduction

The Central Mediterranean region is an area shaped by the dynamic interplay between the African and Eurasian tectonic plates. This area is characterized by considerable variability in crustal thickness, which are indicative of its complex tectonic and geodynamic history. Despite significant advances in geological research, the underlying geological and geophysical frameworks of the Central Mediterranean remain inadequately understood, presenting challenges for a wide range of scientific inquiries.

Developing accurate three-dimensional models of the crust, Moho surface, and the seismogenic volume associated with the Ionian subduction zone is essential for enhancing our comprehension of the region's geodynamics. Such models serve not only to map deep structural features but also to assess potential seismic and tsunami hazards.

This thesis proposes a preliminary three-dimensional crustal model for the Central Mediterranean, constructed through the integration of well data, seismic refraction profiles, density model and P- and S- velocity models. This model is stratified into five distinct layers, clustered by P-wave velocities and geological ages.

Also, it was built the most detailed and complete Moho map available for the Central Mediterranean to date. This map was produced by synthesizing multidisciplinary data, including P- and S-wave velocity models, density profiles, and seismic reflection profiles. This integration enhances the definition of the crust-mantle boundary, addressing the previously unresolved issues surrounding the variability and resolution of existing Moho datasets.

Moreover, to deepen the understanding of the Ionian subduction structure, a refined model of the Ionian Crustal Seismogenic Volume was built, using earthquakes characterized by optimized hypocenter localization. This comparison with models based on non-optimized data emphasizes the significance of precise earthquake localization for accurate structural analysis.

In summary, this chapter aims to advance the knowledge of the geodynamic complexities of the Central Mediterranean, offering valuable insights that are crucial for effective seismic hazard assessment and enhancing our understanding of the region's intricate geological processes.

The content of this chapter is *in preparation.*

4.2 TECTONIC PUZZLE OF THE CENTRAL MEDITERRANEAN: MOHO TOPOGRAPHY, IONIAN SEISMOGENIC VOLUME IN SUBDUCTION AND PRELIMINARY 3D CRUSTAL MODELS

Tectonic Puzzle of the Central Mediterranean: Moho topography, Ionian seismogenic volume in subduction and preliminary 3D crustal Models

S. Bongiovanni[1], A. D'Alessandro[2], R. Martorana[1], A. Sulli[1]
[1]Università di Palermo, Dipartimento di Scienze della Terra e del Mare, Palermo, Italy
[2]Istituto Nazionale di Geofisica e Vulcanologia, Osservatorio Nazionale Terremoti, Rome, Italy

ABSTRACT

The Mediterranean region represents a complex geological puzzle formed by the interaction between two major tectonic plates, Africa and Eurasia. Developing robust 3D models of the crust, the Moho surface and the Ionian subducting seismogenic volume is crucial for advancing our understanding of the area's geodynamics, as well as for delineating the deep structures and assessing associated seismic and tsunami hazards.

In this study, we present a 3D crustal model of the Central Mediterranean, constructed using wells data, seismic refraction profiles, and velocity models. The model is composed of five layers, clustered according to P-wave velocities and geological age.

To accurately define the crust-mantle boundary, we provide the most complete and high-resolution Moho map of the central Mediterranean available to date, achieved through the integration of multidisciplinary data, including P- and S-wave velocity models, density profiles, and seismic refraction profiles.

Additionally, to better understand the geometry and characteristics of the Ionian subduction structure, we developed a model of the Ionian crustal seismogenic volume in subduction, using seismic events with optimized hypocenter localization. We compared this model with one based on non-optimized event data, highlighting the importance of an optimized localization of earthquakes for accurate structural modeling.

1. INTRODUCTION

The Central Mediterranean is a geodynamically complex area, situated at the convergence of the African and European tectonic plates. The region exhibits considerable variations in crustal thickness and lithospheric properties, reflecting the intricacies of its tectonic evolution. Despite extensive research, the geological and geophysical structures beneath the Central Mediterranean are still not fully understood, which presents a challenge for a variety of scientific disciplines.

Understanding the crustal structure of this region is critical for several key applications. These include upper-mantle tomography (e.g., Bozdag & Trampert, 2008; Ritsema et al., 2009), gravity modeling (Yegorova & Starostenko, 2002), and forward seismic wave propagation, which is essential for modeling the behavior of seismic waves as they travel through different geological layers (Capdeville & Marigo, 2008). Additionally, precise crustal models play an important role in the accurate location of seismic events, which is crucial for earthquake hazard assessment (Bisio et al., 2004).

A significant limitation of existing studies is that widely available European-scale crustal models (e.g. Tesauro et al., 2008; Molinari and Morelli, 2011; Artemieva and Thybo, 2013) fail to capture the complexity of the geological framework of the Central Mediterranean. Furthermore, significant discrepancies exist between different models largely due to the exclusion of small-scale geological features and the use of different data sources, some of which omit seismic information. One of the objectives of this study is to build a high-resolution three-dimensional crustal model of the Central Mediterranean. This model integrates data from multiple sources, including wells data, seismic reflection profiles and velocity and density models, providing a more accurate and detailed representation of the subsurface structure of the region. By combining these different datasets, the model aims to improve our understanding of the geodynamics of the Central Mediterranean and to improve the resolution of its subsurface features.

A fundamental instrument for constraining the bottom of the crustal model is the Moho surface model. One of the key unresolved issues regarding the Moho map of the Central Mediterranean is the lack of uniformity and resolution in the available datasets. The geodynamic complexity of the Central Mediterranean, characterized by rapid lateral variations in crustal thickness and tectonic activity, complicates efforts to accurately delineate the Moho.

Mediterranean Moho models included in European crustal models (Tesauro et al., 2008; Molinari and Morelli, 2011; Artemieva and Thybo, 2013), do not have the resolution to capture lateral variations caused by complex geodynamics. Though some Mediterranean Moho maps have been built (Nicolich and Dal Piaz, 1991; Lombardi et al., 2008), they remain incomplete, especially off-shore areas such as the Sicily Channel. In correspondence with the latter, Kherchouche et al. (2020) proposed a model with nearly constant Moho depth, which conflicts with known tectonic structures.

These issues highlight the need for multidisciplinary datasets to improve the accuracy and consistency of the Moho map in this geologically complicated area.

Bongiovanni et al. (2023, 2024) provided a detailed map of the western Sicily Channel using multidisciplinary data, but it covers only the western portion of the Sicily Channel.

More recently, Bongiovanni et al. (in sub.) proposed a Moho map covering the central Mediterranean (Sicily, Calabria and near offshore areas) using P-wave velocity models, density models and seismic refraction profiles. Since the methodological approach of using multidisciplinary data allowed the construction of a Moho map covering a large area with high detail, in this work we propose an extension of the Central Mediterranean Moho map by integrating S-wave velocity models and seismic reflection profiles reinterpreted with P-wave velocity models, seismic refraction profiles and density models.

Regarding subduction zones, it is of crucial importance to know in detail their exact locations and geometries as they host the most intense earthquakes. Global models such as those of Syracuse and Abers (2006) and Hayes et al. (2012) were proposed in the literature, but they lack detail, especially for the Ionian subduction zone.

Maesano et al. (2017) reconstructed the Ionian slab geometry up to a depth of about 300 km, but knowledge of the seismogenic volume in subduction remains incomplete. Hayes et al. (2018) mapped slab up to 480 km depth, but the resolution limits the observation of lateral and depth variations. DISS (2021) extended the model proposed by Maesano et al. (2017) to 440 km, but the deeper portion is largely simplified.

In a recent study, Bongiovanni et al. (in sub.) presented a model of the Crustal Seismogenic Volume (CSV) in subduction derived from the statistical analysis of seismic events using earthquakes occurring from 2005 to 2023 extrapolated from the ISIDe database (ISIDe Working Group, 2016). In this work, we introduce an updated CSV model by integrated data from the CLASS (Catalogo delle Localizzazioni ASSolute) catalog (Latorre et al., 2022), which contains earthquakes with optimized hypocentral localization, in addition to the ISIDe database (ISIDe Working Group, 2016). This approach enabled us to extend the temporal range of the earthquake dataset and produce a more constrained and refined model. Furthermore, we analyzed the characteristics of the top and bottom surfaces that constituite the CSV in subduction and compared them with the CSV model based on events with non-optimized hypocentral localization, highlighting differences and improvements.

2. GEOLOGICAL SETTING

The Central Mediterranean is a geodynamically complex region, shaped by the subduction processes of the African plate beneath the Eurasian plate over the past 30 Ma (Faccenna et al., 2001; Malinverno and Ryan, 1986). This interaction has resulted in the formation of distinct geological domains, each characterized by variations in lithospheric thickness and tectonic features.

In the center of the central Mediterranean lies Sicily. This is divided into several tectonic domains: the Sicilian-Maghrebian fold-and-thrust belt in central and western Sicily, the foreland domain in southeastern Sicily, and the Kabilo-Peloritanian-Calabrian domain in northeastern Sicily and Calabria (inset in Fig. 1). Volcanic activity is also a prominent feature, particularly in association with Mount Etna and the Aeolian Islands (Billi et al., 2006)

South of Sicily lies the Sicily Channel, an area characterized by complex tectonics, including both contractional and extensional structures. The contractional features include the Gela Thrust Front (GTF) (Fig. 1), while extensional structures are represented by the NW-SE oriented Pantelleria, Linosa, and Malta grabens (Finetti et al., 1984; Civile et al., 2010; Sulli et al., 2021) (Fig. 1). These grabens, formed due to crustal stretching, are associated with significant crustal thinning and local uplift of the Moho (Scarascia et al., 1994; Agius et al., 2022).

The Sicily Channel is also a site of volcanic activity, particularly in the northwestern sector between the southwestern coast of Sicily and Linosa Island. Recent studies have highlighted volcanic manifestations in this area, contributing to the region's geodynamic complexity (Palano et al., 2020; Maiorana et al., 2023). In this area lies the Capo Granitola-Sciacca Fault Zone (CGSFZ) (Fig. 1), which divides the offshore region of the Sicilian-Maghrebian Chain into two distinct sectors. These sectors experienced deformation at different times, exhibit contrasting structural orientations, and have undergone distinct tectonic evolutions (Argnani et al., 1986, 1987; Grasso, 2001).

The Sicily Channel is connected to the deep Ionian Sea through the Malta escarpment. The latter represents the dominant morphological feature offshore eastern Sicily.

The Ionian Sea is considered the last remnant of subducting oceanic crust in the Central Mediterranean (de Voogd et al., 1992; Faccenna et al., 2001, 2004; D'Agostino et al., 2008).

Seismic refraction data suggest that the crust beneath the Ionian Sea is either thinned oceanic or highly stretched continental crust (de Voogd et al., 1992). The Ionian subduction system is one of the narrowest in the world, with the subducting slab measuring approximately 200 km in width, extending to a depth of 500 km, and dipping northwestward at an angle of about 70° (Anderson and Jackson, 1987; Giardini and Velonà, 1991; Selvaggi and Chiarabba, 1995; Wortel and Spakman, 2000; Chiarabba and Palano, 2017; Scarfì et al., 2018).

Subduction in this region is further complicated by the presence of Subduction Transform Edge Propagator (STEP) zones, which develop at the edges of the subducting slab (Govers and Wortel, 2005; Nijholt and Govers, 2015). Two major STEP zones have been identified along the Ionian slab margins: the Tindari-Letojanni STEP (Fig. 1), a right-lateral shear zone associated with the Aeolian Islands, and the Palinuro STEP (Fig. 1), a left-lateral shear zone aligned with the Palinuro volcanic chain (Govers and Wortel, 2005; Cocchi et al., 2017; Scarfì et al., 2018; De Ritis et al., 2019).

The Calabrian Arc, an arc-shaped tectonic wedge, marks the boundary between African and European plates. Extending into the Ionian offshore, the Calabrian Arc consists of a large accretionary wedge, approximately 300 km wide and several hundred kilometers long (Cernobori et al., 1996; Polonia et al., 2011; Gallais et al., 2012; Corradino et al., 2020). This structure is known as the "External Calabrian Arc" (Selli and Rossi, 1975) (inset in Fig. 1).

Northwest of the Calabrian Arc there is the Southern Tyrrhenian Sea, that represents a retroarc basin that developed due to the rollback of the African subducting slab, which migrated southeastward over time (Sartori, 1990; Gueguen et al., 1998; Argnani and Savelli, 1999; Carminati et al., 2004). The Tyrrhenian Sea is primarily characterized by thinned continental crust (Lliboutry, 2000; Pepe et al., 2000), but also by the presence of oceanic crust in the Vavilov and Marsili basins, indicating a significant tectonic transition (Neri et al., 2012; Sartori et al., 2004; Pontevivo and Panza, 2006; Cella et al., 2008; Scrocca et al., 2012).

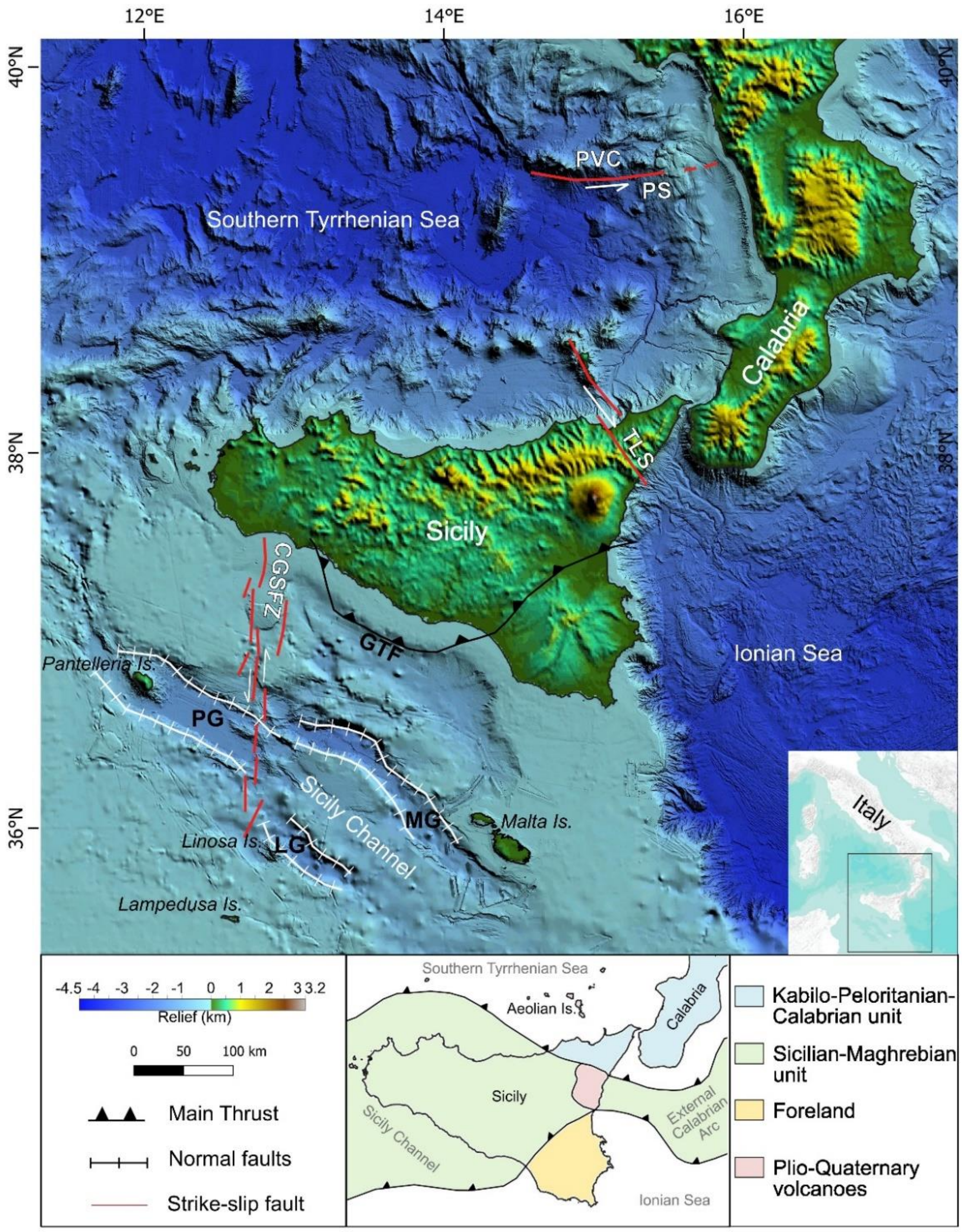

Figure 1: Geological setting of the Central Mediterranean area (modified by Bongiovanni et al., in sub.). VB: Vavilov Basin, MB: Marsili Basin; PVC: Palinuro volcano chain and PS: Palinuro STEP (Calderoni et al., 2020), TLS: Tindari-Letojanni STEP (Cocchi et al., 2017; De Ritis et al., 2019), GTF: Gela Thrust Front (Sulli et al., 2021); MG: Malta Graben, PG: Pantelleria Graben, LG: Linosa Graben, CGSFZ: Capo Granitola-Sciacca Fault Zone (Civile et al., 2018). The inset at the bottom right shows the tectonic sketch of the study area (modified from Sulli, 2000). Bathymetric data were downloaded from EMODnet (https://emodnet.ec.europa.eu/geoviewer/#).

3. DATA AND METHODS

3.1. SEISMIC REFLECTION PROFILES AND WELLS

We collected seismic reflection profiles from the ViDEPI database (https://www.videpi.com/videpi/videpi.asp) (location in Figure 2a) and digitized them using the 3D modeling software Move 2017 (Midland Valley Ltd.). Each profile was analyzed to trace the horizons of the geological layers, interpreted by multiple authors (Finetti, 2005; Catalano et al., 2013; Tugend et al., 2019; Sulli et al., 2021; Bongiovanni et al., 2023, 2024). These horizons, initially in two-way travel time (TWT), were subsequently converted to depth using the 3D Depth Conversion tool in the software. To achieve this, we created a database that included P-wave velocity values at the top of each horizon, and, where available, velocity gradients and density values, derived from various studies (Makris et al., 1986; Scarascia et al., 1994; Bello et al., 2000; Catalano et al., 2000; Chironi et al., 2000; Nicolich et al., 2000; Catalano et al., 2002; Cassinis et al., 2005; Tassis et al., 2013; Dellong et al., 2018; Dellong et al., 2020; Akimbekova et al., 2023).

We also imported 404 wells (Fig. 2a) extracted from the ViDEPI database (https://www.videpi.com/videpi/videpi.asp) into the 3D modeling software "Move 2017" (Midland Valley Ltd.). These wells are primarily located in Sicily, the Calabrian Arc, and the offshore area of southern Sicily near the coast. A dataset was constructed by assigning a horizon to the top of each layer representing a geological age.

3.2. P-AND S- WAVE VELOCITY MODELS AND DENSITY MODELS

In this study, we collected 16 P-wave velocity models (Fig. 2a) derived from different sources, including Deep Seismic Sounding (DSS) profiles, Wide-Angle Reflection and Refraction (WARR) profiles and seismic data from Ocean Bottom Seismometers (OBS) (Makris et al., 1986; De Voogd et al., 1992; Scarascia et al., 1994; Chironi et al., 2000; Nicolich et al., 2000; Cassinis et al., 2005; Dellong et al., 2018). In addition, we considered 7 S-wave velocity models (Fig. 2a) based on seismic surface waves (Agius et al., 2022) and 4 density model interpretations (Chironi et al., 2000; Dellong et al., 2018). These profiles were digitized using Move 2017 software (Midland Valley Ltd).

We traced constant-velocity horizons on both the P-wave and S-wave velocity models. For each horizon in the S-wave velocity models, a corresponding Vp value was assigned based on Vp/Vs ratios extracted from Calò et al. (2013) for the Sicily Channel and southern Tyrrhenian Sea, D'Alessandro et al. (2016) for the Ionian region, and Menichelli et al. (2022) for Sicily and the Calabrian Arc. The P-wave and S-wave velocity models were initially converted from depth to time (TWT) using the 3D Time Conversion Tool implemented in Move 2017 software, where rock properties such as velocity and velocity decay with depth were assigned to each geological layer. These velocity models were subsequently calibrated with seismic reflection profiles to ensure consistency, after which they were re-converted from time (TWT) to depth. The horizons were correlated with geological ages using data from various literature sources (Makris et al., 1986; Catalano et al., 2000; Finetti, 2005; Pepe et al., 2010; Gallais et al., 2012; Tugend et al., 2019; Akimbekova et al., 2023).

In parallel, we implemented density models (location in Fig. 2a) into the Move 2017 software and utilized them to map Moho horizons. These horizons were then calibrated against seismic reflection profiles to maintain internal consistency across the dataset.

3.3. EARTHQUAKES

We selected earthquakes with magnitudes M≥ 2 and depths ≥ 40 km within the area bounded by latitudes 37.9° to 39.7°N and longitudes 13.3° to 17.5°E. The seismic events were extracted from the ISIDe database (ISIDe Working Group, 2016) for the period from January 2005 to July 2024. To extend the temporal range, we included earthquakes from 1981 to 2018, sourced from the CLASS catalog (Catalog of Absolute Locations) (Latorre et al., 2022). These data are illustrated in Figure 2b, along with the focal mechanisms of major events reported in the Time Domain Moment Tensor (TDMT) catalog (Scognamilgio et al., 2006) and the European-Mediterranean Regional Centroid Moment Tensor (RCMT) catalog (Pondrelli et al., 2004). The focal mechanisms reveal two distinct patterns associated with the Ionian slab: a strike-slip regime in the northeastern sector and a normal faulting regime in the central zone.

The earthquake dataset was subdivided into depth intervals of 10 km with a 50% overlap between consecutive ranges. A statistical approach was applied to generate density plots for each depth range using a Kernel smoothed intensity function, implemented on a 0.01 x 0.01-pixel grid. This spatial function represents the density of events per unit area. Specifically, a Gaussian Kernel function was used to smooth patterns, which is particularly effective for regions with sparse data points (Davies et al., 2018). We then calculated the gradient density plot for each density plot.

Data organization was carried out using a custom MATLAB script, while the statistical processing was performed through the R statistical software, employing the "spatstat" (Baddeley and Turner, 2005) and "raster" (Hijmans, 2018) packages. From each gradient density plot, two isolines were extracted from the maximum values, corresponding to the top and bottom isolines of the seismogenic volume (CSV).

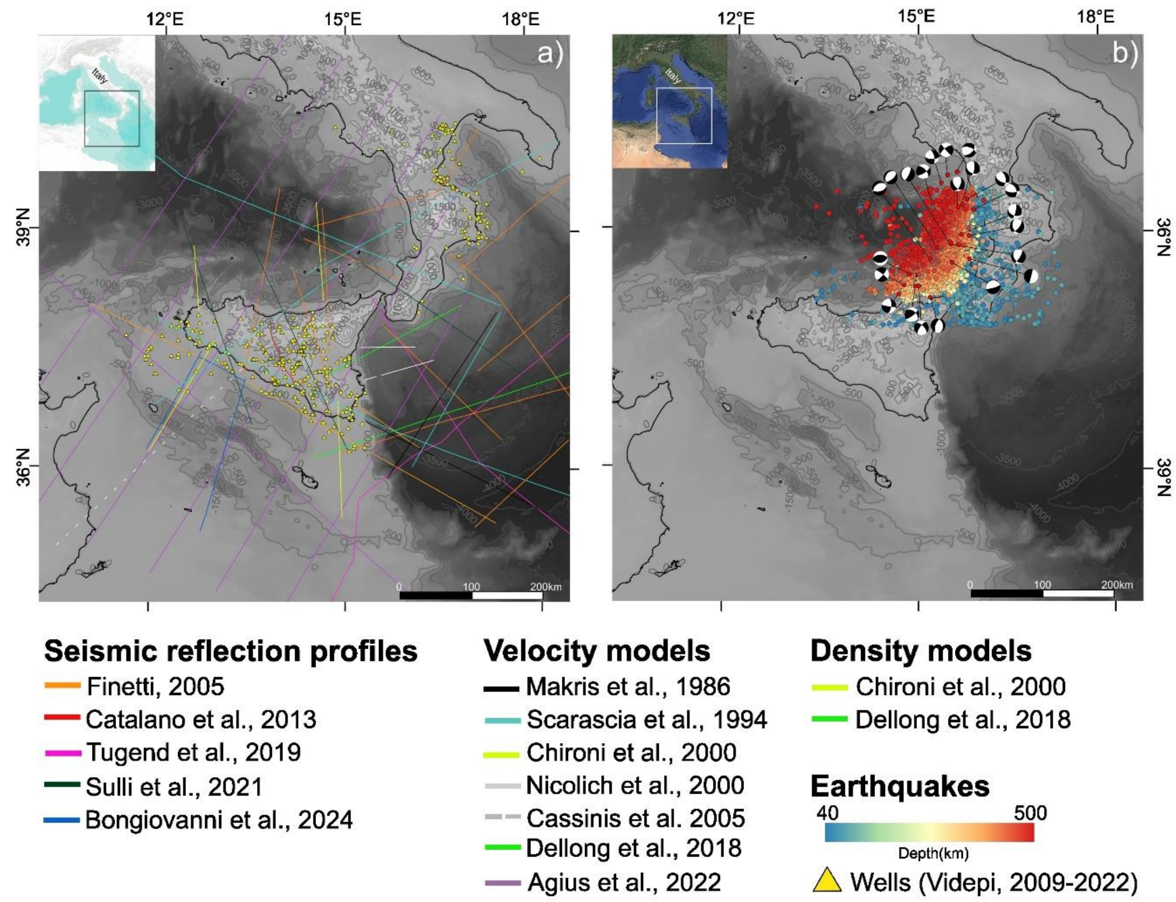

Figure 2: a), b) Map showing location of datasets used in this paper (see text for details).

3.4. 3D MODELS

In this paper, we build the Moho map of the Central Mediterranean, the CSV, and the 3D crustal model using Move 2017 software (Midland Valley Ltd).

To create the Moho surface, we interpolated the horizons previously plotted on seismic reflection profiles, which were converted from time (TWT) to depth, S-wave velocity models convert

into P-wave velocity models, P-wave velocity models, and density models. The Delaunay triangulation method was applied for this interpolation, as it provides more uniform geometry of triangles within a grid without altering the data points from the input dataset. The obtained surface was then simplified using a resampling mode with a 10 km x 10 km grid.

The isolines extrapolated from the maximum values of density gradient plots, were imported into the 3D modeling software "MOVE 2017" (Midland Valley Ltd.). We interpolated the top and bottom isolines of the CSV using the same Delaunay triangulation method. As with the Moho surface, the CSV surface was also simplified through resampling using a 10 km x 10 km grid.

To analyze the CSV in detail, we calculated the dip of the top and bottom surfaces as well as the CSV thickness. The dip of each Delaunay triangle forming the top and bottom surfaces of the CSV was calculated using the "Surface Geometry Analysis Tool" in MOVE 2017 (Midland Valley Ltd.). We then extracted these values and used them to construct Kernel density estimate curves to observe the predominant inclination of both surfaces. To accomplish this, we implemented a script in the statistical analysis software R, using a bandwidth determined by Silverman's (1986) rule and a Gaussian kernel.

We calculated the thickness of the CSV using the "thickness tool" implemented in "MOVE 2017" (Midland Valley Ltd.). The tool generated normal lines from the centroid of each Delaunay triangle that constituted the CSV top to its conjunction with those that constituted the CSV bottom.

Each triangle on the top surface was then assigned a thickness value corresponding to the length of the line connecting the top and bottom surfaces of the CSV.

To develop a preliminary, simplified 3D crustal model of the Central Mediterranean, we clustered the layers based on geological age and P-wave velocities, representing the following units: Lower Crust, Upper Crust, Oceanic Crust, Cretaceous-Jurassic-Triassic, and Pliocene-Miocene-Oligocene. Initially, we constructed the top surfaces of each layer using the same method applied for the CSV and Moho surfaces, incorporating horizons traced from seismic reflection profiles (converted from time to depth), P-wave velocity models, S-wave velocity models converted to P-wave velocities, and well data.

The volumes for each layer were generated using the "Tetravolume Tool" in the MOVE 2017 software (Midland Valley Ltd.). This tool calculates volumes by connecting the Delaunay triangles from the top and bottom surfaces of each layer to form tetrahedra. For our analysis, we used a tetrahedral edge length of 20 km.

Finally, to analyze the lateral variations of the layers in detail, we calculated the thickness of each layer using the "Thickness Tool" in MOVE 2017. This provided a thickness value for each triangle that constitutes the top and bottom surfaces of each layer in the volume.

4. RESULTS:

The Moho surface in the Central Mediterranean we propose in this study, reveals pronounced lateral heterogeneity throughout the region (Fig. 3).

We divided the Moho associated with the African plate (south of the blue line in the figure) from that of the European plate (north of the blue line in the figure). The African Moho reaches its greatest depths beneath Sicily, where it extends to 39 km, Tunisia, where it reaches 31 km, near the Malta Escarpment at 30 km, and along the External Calabrian Arc, in proximity to the Ionian subduction zone. In the Ionian Sea, moving away from the subduction zone, the Moho becomes shallower, reaching depths of 15 km, with more widely spaced isobaths indicating a more uniform structure. In contrast, near the Malta Escarpment, the isobaths are closely spaced, indicating a rapid deepening of the Moho surface from the Sicily Channel to the Ionian Sea. A similar pattern is observed southeast of the Sicily coast near the Gela Foredeep (GFT). The Moho surface in the Sicily Channel is highly heterogeneous. Moving away from the GFT and Malta Escarpment sectors, in the central region, the Moho reaches shallow depths beneath the Linosa, Malta, and Pantelleria Grabens, with the latter showing depths of about 15 km.

The European Moho also exhibits significant lateral variation. Very shallow depths are observed in northeastern Sicily and in the Tyrrhenian sectors, where the Moho reaches 10 km beneath the Vavilov and Marsili Basins. As the Calabrian Arc is approached, the Moho deepens, and there is a coexistence of the European and African Moho. The European Moho generally lies between 20 and 30 km, while the African Moho exceeds 35 km near the subduction zone

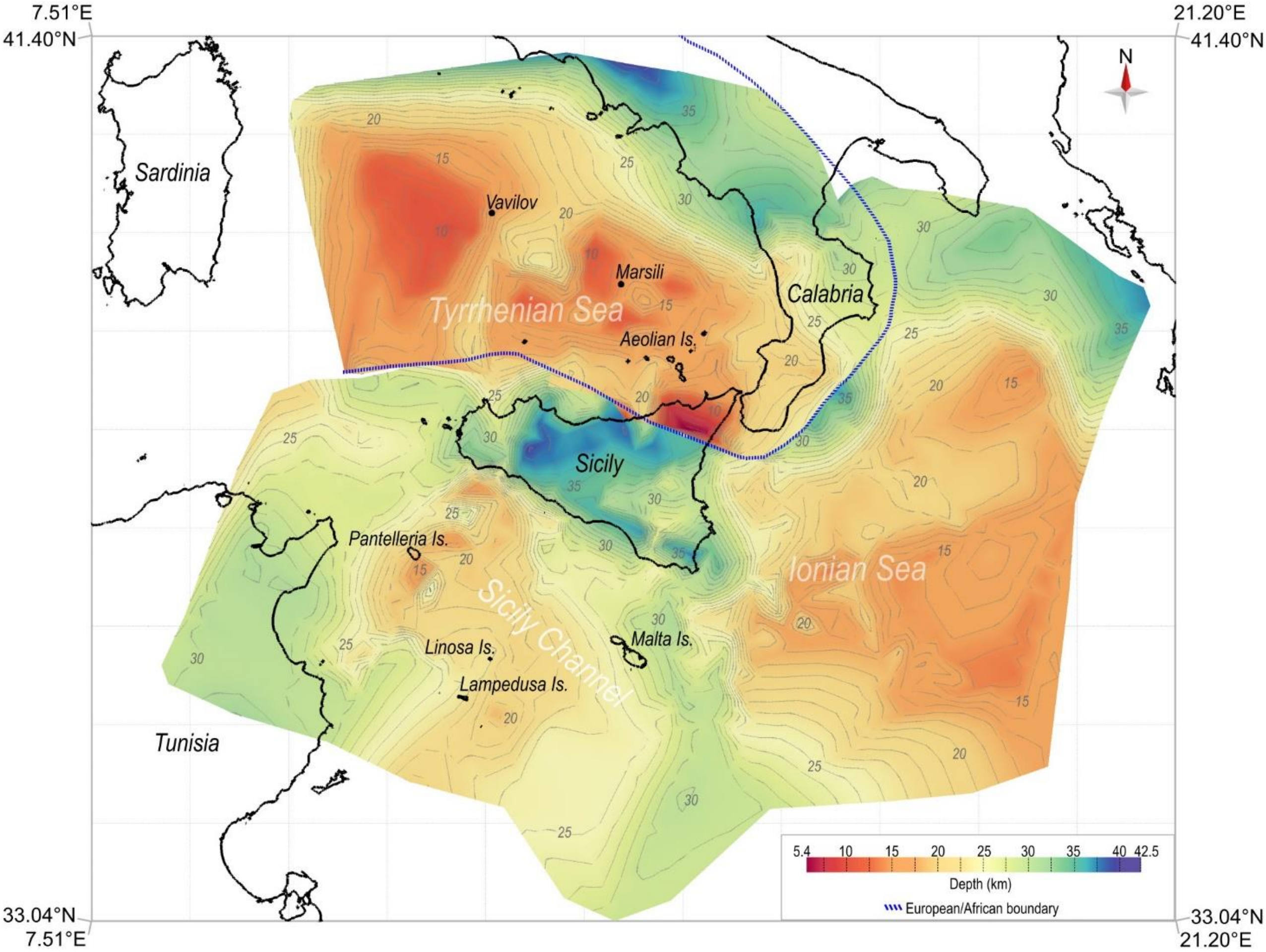

Figure 3: Moho map of the Central Mediterranean area

In this paper we built the Ionian CSV in subduction which extends up to 500km depth.

The surfaces delimiting the top (in gray in Fig. 4) and the bottom (in red in Fig. 4) of the CSV obtained in this study exhibit a variable trend along the depth profile. The top surface has a width of approximately 170 km at its shallowest part, which remains relatively constant for about 50 km in depth. From around 90 km to 170 km depth, the surface narrows, presenting an average width of about 80 km. Beyond this depth, the width increases again, reaching an average of 120 km at a depth of 350 km, before progressively narrowing further. The bottom surface of the CSV follows a similar pattern. The greatest width, approximately 190 km, is observed at the uppermost part. At a depth of around 130 km, it narrows, showing a width of approximately 88 km. From a depth of 200 km, the width increases again, reaching about 105 km, before progressively narrowing over the final 100 km of depth.

The CSV is highly inclined, as indicated by the dip values of the top and bottom surfaces (Fig. 5 a, b). The dip distribution of the top surface of the CSV is multimodal, with a prominent peak at approximately 54°. The dip values of the bottom surface display a trimodal distribution, with a prominent peak around 80°.

We also calculated the thickness of the CSV, shown in color scale on the top surface in Figure 5 c. A greater thickness is observed at the shallowest part of the CSV where the latter reaches thicknesses between 30 and 60 km. Corresponding to the decrease in width of both the top and bottom surfaces of the CSV, specifically between 120 km and 200 km in depth, there is also a noticeable reduction in thickness. The minimum thickness is observed at the deepest part of the CSV.

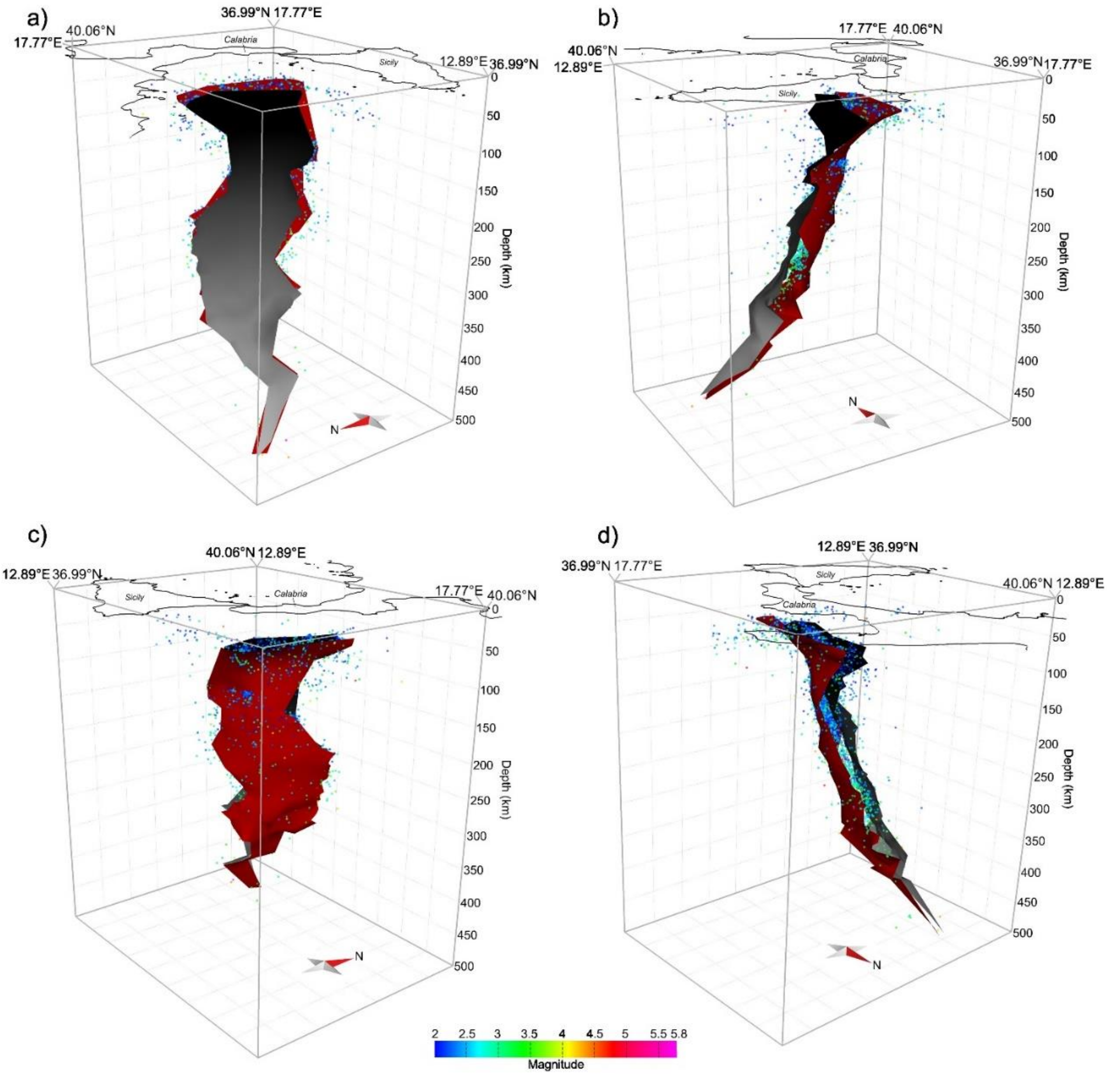

Figure 4: a), b), c), d) Different views of the top (in gray) and bottom (in red) surfaces of the CSV. Earthquakes are shown using a color scale based on magnitude

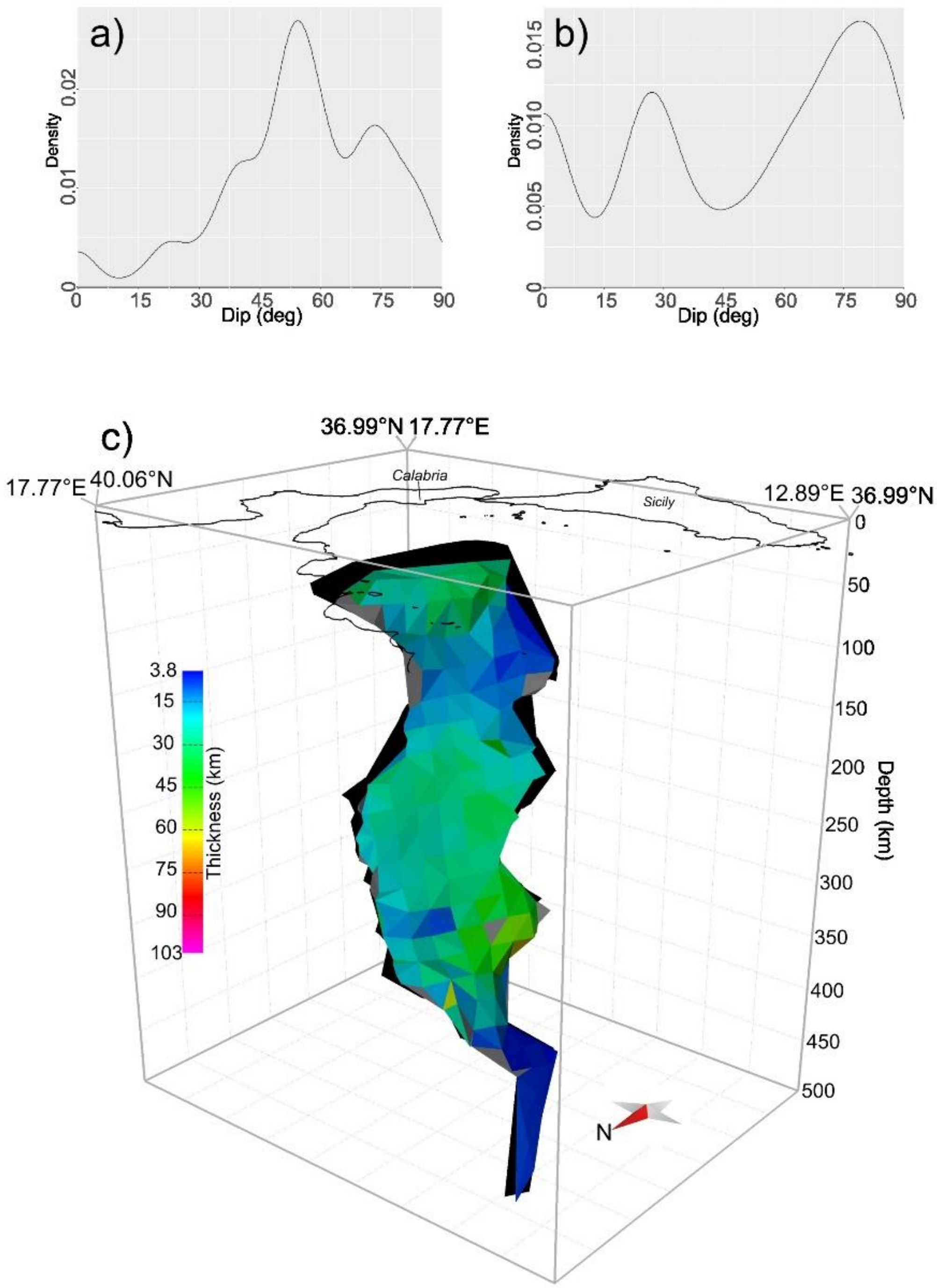

Figure 5: Distribution of dip values belonging to each Delaunay triangle that constitutes the top (a) and bottom (b) surface of the CSV; c) Bottom (in black) and top (color scale) surfaces of the CSV. The color scale represents the thickness of the CSV.

The preliminary, simplified 3D crustal model developed in this study is shown in Figure 6. The uppermost layer is the most complete, while the layers become progressively less extensive with increasing depth. To better visualize the lateral variations of each layer, we calculated the thickness of each one (Fig. 7 a). The layer corresponding to the Pliocene-Miocene-Oligocene exhibits thicknesses ranging from 0.2 km to 2 km in the Sicily Channel, from 2 km to 3 km in central Sicily, and from 4 km to 7 km in northeastern Sicily. In the Ionian Sea, thickness ranges between 3 km and 4.5 km, increasing significantly in the External Calabrian Arc.

The Cretaceous-Jurassic-Triassic layer (Fig. 7 b) displays reduced thicknesses in Calabria, northeastern Sicily, and the Ionian Sea, with values between 0.8 km and 2.5 km. Thickness increases near the Calabrian Arc, ranging from 5 km to 10 km, and in the Sicily Channel, where thicknesses vary from 8 km to 10 km, except along the south-central coast of Sicily, where they reach 12 km to 14 km.

The Upper Crust layer (Fig. 7 c) is fragmented and covers only a small part of the southern Tyrrhenian, a portion of the Ionian Sea, most of Sicily (excluding the northeastern sector), and parts of the Sicily Channel. In the Ionian Sea, this layer shows thickness values between 5 km and 10 km. In the southern Tyrrhenian Sea and Sicily Channel, thicknesses range from 5 km to 14 km.

In particular, the maximum values of thickness are observed at the location of the External Calabrian Arc. Sicily exhibits significant lateral variation, with a maximum thickness of up to 25 km in the north-central region.

Figure 7 d illustrates the thickness of a fragment of the Oceanic Crust in the Ionian Sea. In this area, values range from 4 km to 9 km.

The final layer represented in our 3D crustal model is the Lower Crust. This layer is also fragmented (Fig. 7 e) and exhibits thicknesses between 0.8 km and 12 km in the Ionian sector east of Calabria and the southern Tyrrhenian. In the Sicily Channel, the Lower Crust has thinner portions in the central area corresponding to Grabens (0.5 km to 2.8 km) and thicker sections to the east and west of the grabens, reaching up to 10 km. The greatest thickness in the Lower Crust is observed in the western and southeastern regions of Sicily, with values up to 20 km.

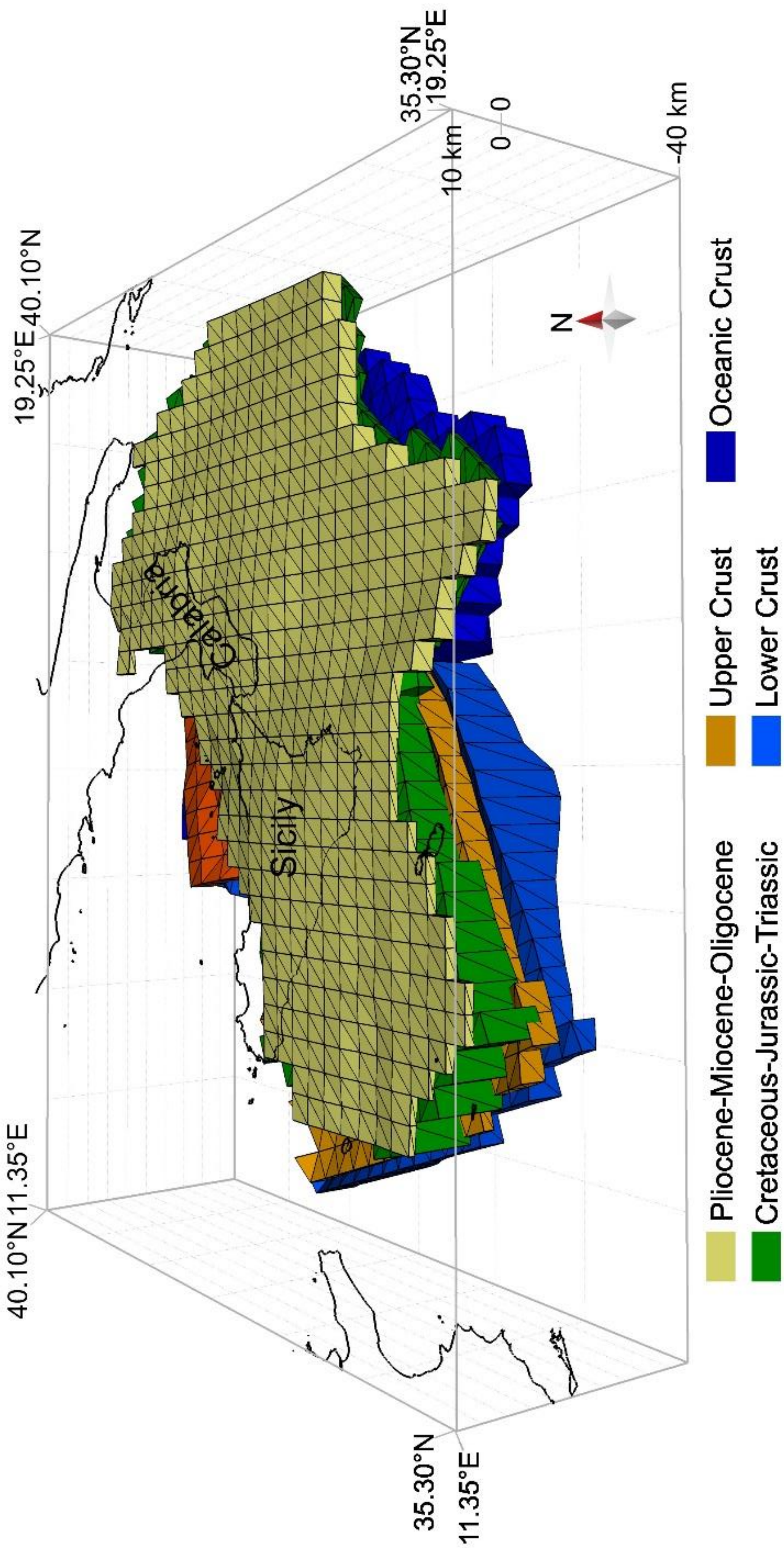

Figure 6: 3D crustal model of the Central Mediterranean (vertical exaggeration x4).

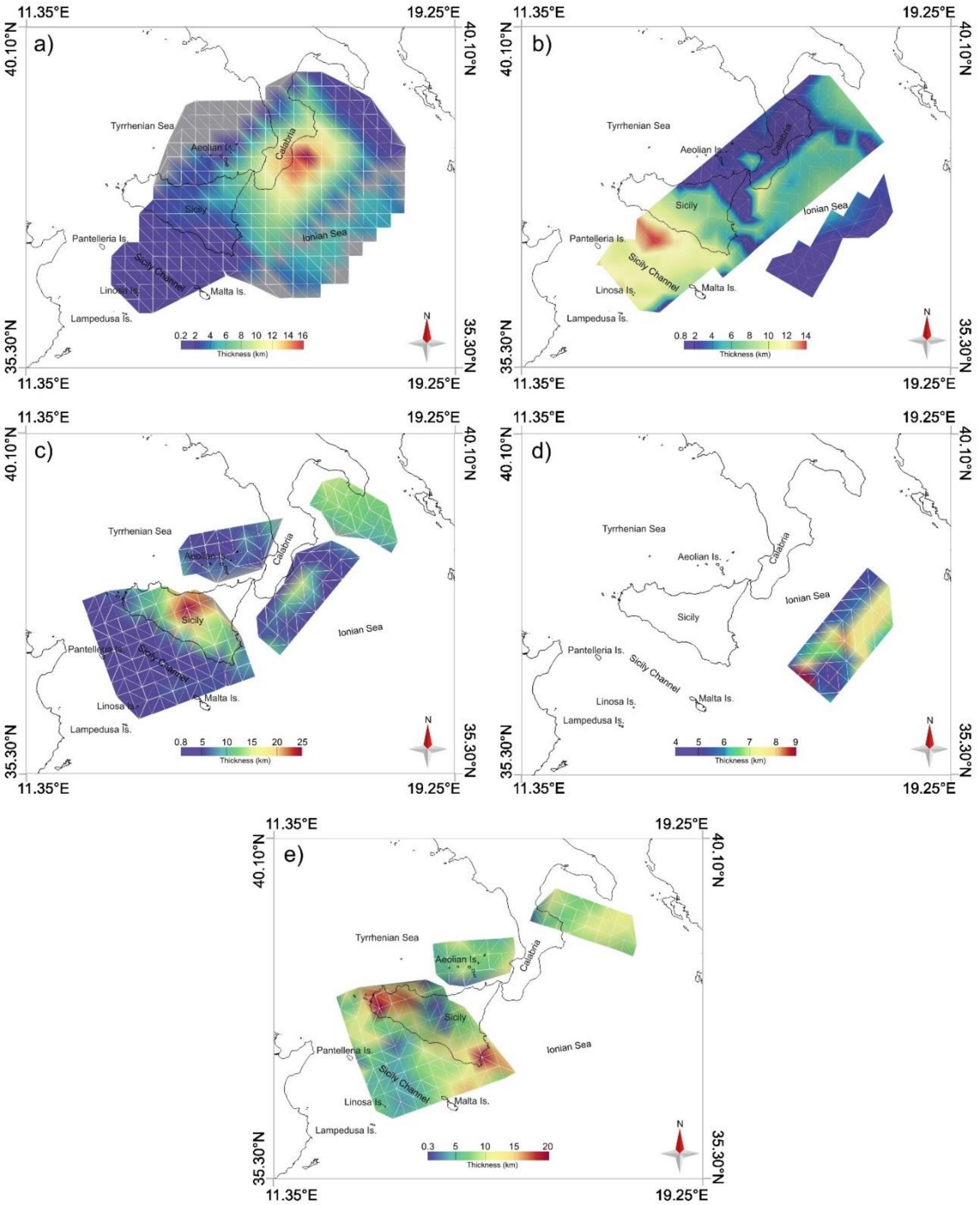

Figure 7: Thickness map of the layers that constitutes the crustal volume. a), b), c), d), e) represent respectively the thicknesses of the Pliocene-Miocene-Oligocene, Cretaceous-Jurassic-Triassic, Upper Crust, Oceanic Crust and Lower Crust layers. The triangles that constitute the surfaces are the Delaunay triangles with which these were constructed. The gray triangles represent areas with no value.

5. DISCUSSION

This study aims to provide a deeper understanding of the crustal structure in the Central Mediterranean and the Ionian subduction zone. The Moho map we propose represents the most comprehensive and detailed one available for the Central Mediterranean to date. By integrating multidisciplinary data, such as seismic reflection profiles, density models and P- and S-wave velocity models, we achieved greater coverage and resolution, particularly in critical areas like the Sicily Channel. Here, the Moho reflects the tectonic geometries of the Pantelleria, Linosa, and Malta Grabens and the morpho-bathymetric features like the Malta Escarpment. Unlike the more uniform Moho model proposed by Kherchouche et al. (2020), our Moho contours in the Sicily Channel align with the grabens, where the Moho depth is significantly shallower, ranging between 15 km and 20 km. Furthermore, an upwelling of the Moho along a NNE-SSW alignment is observed in correspondence with the CGSFZ. This would confirm the interpretation of this structure by Civile et al. (2018) who considers it a lithospheric leaf.

Compared to previous maps by Bongiovanni et al. (2024, in sub.), our Moho map of the Sicily Channel is more extensive and detailed, due to the inclusion of new data. We also achieved greater detail in the External Calabrian Arc, where the Moho contours clearly mark the geometry of this structure. In the southern Tyrrhenian Sea, our map extends over the Marsili and Vavilov basins, revealing very shallow Moho depths of up to 10 km, in line with the basin sizes reported by Marani and Trua (2002). In the north-eastern sector of Sicily, anomalous values of the Moho are found, showing very low depth values. In this sector, we consider the Moho as the lower limit of the crystalline basement of the European units involved in the deformation. As can be seen from Bianchi et al. (1987) and Roure et al. (1990), in this boundary this limit is very close to the surface.

In the Ionian Sea, and particularly in the sector between the east coast of Sicily and Calabria, the Moho isobaths show an arc shape that can be correlated with that of the velocity anomaly proposed by Sgroi et al. (2021).

Our model of the crustal seismogenic volume (CSV) extends down to 500 km in depth. A notable thinning of the CSV occurs between 120 km and 200 km depth, potentially caused by resistance to the subduction process.

We hypothesize that the presence of relict structures, such as oceanic ridges, may play a crucial role in this process. The enhanced rigidity of oceanic crust forming an oceanica ridge could provide mechanical resistance, potentially impeding subduction. Catalano et al. (2001) identified the existence of a aborted oceanic ridge in the Ionian Sea, located just a few kilometers from the boundary between the African and European plates. Another factor contributing to resistance against subduction might be the significant uplift rate observed in the Calabria Arc region, as evidenced by the M4 seismic line by Polonia et al. (2011).

The top surface of the CSV in our model appear much more complex than those proposed by Hayes et al. (2018) and the DISS database (2021), as shown in Figure 4. A map view of the CSV (Fig. 8) highlights its extension into the southern Tyrrhenian Sea, where it reaches between Marsili and Vavilov. Moreover, the CSV appears confined between the TLS and PS fault zones, structures considered as STEP faults (e.g., Neri et al., 2012, Gallais et al., 2013; Calderoni et al., 2020) according to the Subduction-Transform Edge Propagator model (Govers & Wortel, 2005). These faults may have developed as subduction rollback triggered segmentation of the subduction slab, producing lithospheric-scale sub-vertical tear faults. These types of faults are generally with strike-slip motion, such as the TLS and PS structures (Fig. 1).

We interpret these lateral tears as indicative of the early stages of slab detachment.

Sgroi et al. (2021) observed the presence of a lithospheric fault also in the Ionian Sea, continuing the TLS. It divides the subduction system into two lobes, a western and an eastern one, in which there are different detachment depths.

The CSV model presented in this paper (Fig. 9, black lines) is very comparable to the one proposed by Bongiovanni et al. (in sub.) (Fig. 9, red lines), but the inclusion of relocated seismic events allowed for greater detail in the geometry. The Ionian slab, which corresponds to the top of the CSV, shows even more pronounced lateral tears. In cross sections (Fig. 9), the top of the CSV is more discontinuous, particularly beyond 300 km depth, where our model shows a slightly less steep inclination compared to the earlier model.

Therefore, no substantial differences are observed between the two models, both of which are valid. The advantage of the model proposed by Bongiovanni et al. (in sub.) is its use of seismic catalogs available from the national seismic network. Instead, the model proposed in this paper aims to achieve a more precise and constrained model, which necessitates optimized location of the earthquake hypocenters, necessitating a relocation process and therefore longer processing times. In fact, the CLASS catalog (Latorre et al., 2022) available in the literature contains relocated seismic events but only within a time range extending up to 2018.

Additionally, we present a preliminary crustal model based on seismic reflection profiles, P- and S-wave velocity models, and well data. This model consists of 5 layers (Lower Crust, Upper Crust, Oceanic Crust, Cretaceous-Jurassic-Triassic, and Pliocene-Miocene-

Oligocene) (Fig. 6) clustered according to the ages and velocities of the P-waves travelling to them. To better understand the lateral variations of the layers, we created a thickness map for each of these (Fig. 7). In the External Calabrian Arc, where uplift rates are consistently, the model's layers are significantly thicker compared to surrounding areas. The upper crust is especially thin in the Sicily Channel and with a shallow Moho, consistent with the presence of thinned crust.

Overall, the thickness values in our crustal model align well with those of the EuCRUST-07 model by Tesauro et al. (2008), providing further validation of our findings.

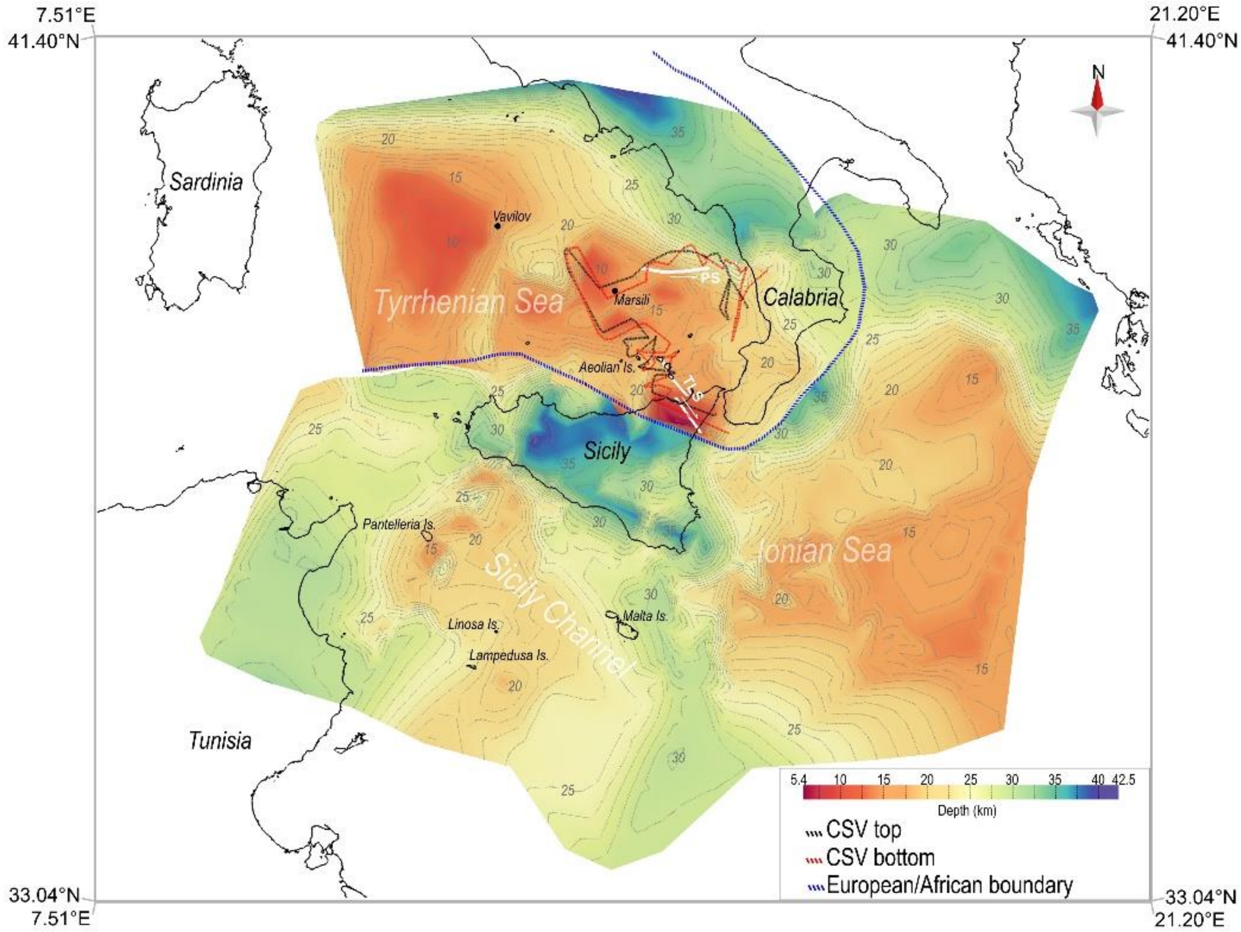

Figure 8: 3D Moho map of the Central Mediterranean area and map view of the top and bottom surfaces of the CSV. TLS: Tindari-Letojanni STEP (Cocchi et al., 2017; De Ritiis et al., 2019), PS: Palinuro STEP (Calderoni et al., 2020).

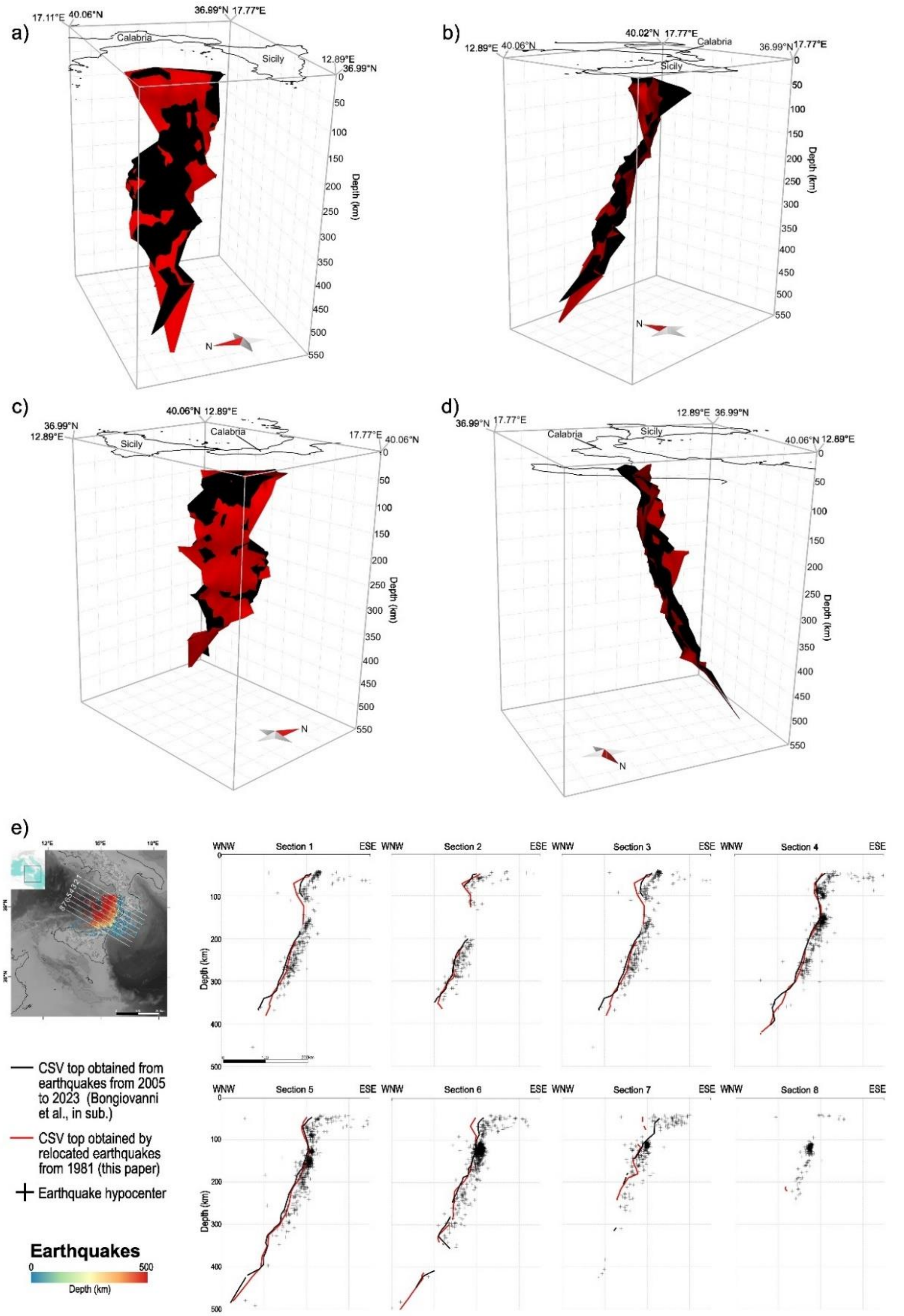

Figure 9: a),b),c),d) different views of the comparison between the CSV top constructed by Bongiovanni et al. (in sub.) (in red) using earthquakes from 2005 to 2023 and the CSV top constructed in this paper (in black) using relocated earthquakes from 1981 extrapolated from the CLASS catalog (Latorre et al., 2022), (e) cross section in which the two CSV tops are compared.

6. CONCLUSIONS

In this paper, we present a new, more extensive map of the Moho discontinuity in the Central Mediterranean area, an updated and better-constrained model of the Crustal Seismogenic Volume (CSV) in subduction, and a preliminary 3D crustal model of the region. These models aim to enhance the current understanding of the geological structures and geodynamic setting of the area, which remains incompletely understood.

A detailed Moho map is crucial for accurate geological and geodynamic modeling. By integrating multidisciplinary data, we developed the most comprehensive and detailed Moho map for the Mediterranean to date. Additionally, we built a more robustly constrained model of the CSV, derived from earthquakes with optimized localization. This has enabled us to produce a more precise geometric representation of the subducting CSV.

Lastly, we introduce a preliminary 3D crustal model of the Central Mediterranean, constrained at its base by the Moho surface. This model is an important tool for constructing velocity models that enhance the precision of seismic event localization. Our model shows significant alignment with the European crustal model by Tesauro et al. (2008) and is consistent with the tectonic and morphobathymetric structures in the area, despite some existing data gaps.

These models can be updated as new data becomes available, enabling future enhancements in their reliability and detail. The results have significant implications for seismic and tsunami hazard analysis and provide a resource for future geodynamic and tectonic studies in the Central Mediterranean.

References:

- Agius, M. R., Magrini, F., Diaferia, G., Kästle, E. D., Cammarano, F., Faccenna, C., Funiciello, F., & van der Meijde, M. (2022). Shear-Velocity Structure and Dynamics Beneath the Sicily Channel and Surrounding Regions of the Central Mediterranean Inferred From Seismic Surface Waves. Geochemistry, Geophysics, Geosystems, 23(10), e2022GC010394.
- Akimbekova, A., Carboni, F., Mancinelli, P., Barreca, G., Scarfì, L., Pauselli, C., Monaco, C., & Barchi, M. R. (2023). Gravity modelling of the Tyrrhenian-Calabrian-Ionian subduction system. Frontiers in Earth Science, 11.
- Anderson, H., & J. Jackson (1987). Active tectonics of the Adriatic Region, Geophys. J. R. Astronom. Soc., 91, 937–983.
- Argnani, A., & Savelli, C. (1999). Cenozoic volcanism and tectonics in the southernTyrrhenian sea: Space-time distribution and geodynamicsignificance. Journal of Geodynamics, 27(4-5), 409-432.
- Argnani, A., Cornini, S., Torelli, L., & Zitellini, N. (1986). Neogene-quaternary foredeep system in the Strait of Sicily. Memorie Società Geologica Italiana 36, 123–130.
- Baddeley A. & Turner R. (2005). Spatsat: an r package for analyzing spatial point patterns. J. Stat Softw 12, i06
- Bello, M., & Merlini, S. (2000). Structual model of central eastern Sicily. In EAGE Conference on Geology and Petroleum Geology of the Mediterranean and Circum-Mediterranean Basins (pp. cp-109). European Association of Geoscientists & Engineers.
- Bianchi, F., Carbone, S., Grasso, M., Invernizzi, G., Lentini, F., & Longaretti, G. (1987). Sicilia orientale. Profilo geologico Nebrodi-Iblei. Memorie della Società Geologica Italiana, 38, 429-458.
- Billi, A., Barberi, G., Faccenna, C., Neri, G., Pepe, F., & Sulli, A. (2006). Tectonics and seismicity of the Tindari Fault System, southern Italy: Crustal deformations at the transition between ongoing contractional and extensional domains located above the edge of a subducting slab. Tectonics, 25(2).
- Bisio, L., Di Giovambattista, R., Milano, G., & Chiarabba, C. (2004). Three-dimensional earthquake locations and upper crustal structure of the Sannio-Matese region (southern Italy). Tectonophysics, 385(1-4), 121-136.
- Bongiovanni, S., D'Alessandro, A., Martorana, R., & Sulli., A. A new three-dimensional Moho model of the central Mediterranean area and a reconstruction of the Ionian Crustal Seismogenic Volume in subduction. In submission to Tectonophysics

- Bongiovanni, S., Maiorana, M., D'Alessandro, A., Martorana, R., & Sulli., A. (2024): a new Moho map of the central-western Sicily Channel: correlation with volcanoes, tectonic structures and seismogenic volumes. Submitted to Scientific Reports

- Bongiovanni, S., Maiorana, M., D'Alessandro, A., Martorana, R., & Sulli, A. (2023). Multidisciplinary approach to the study of a crustal tectonic discontinuity: an example from the Central Mediterranean offshore (Sicily channel). In EGU General Assembly Conference Abstracts (pp. EGU-11843)

- Bozdağ, E., & Trampert, J. (2008). On crustal corrections in surface wave tomography. Geophysical Journal International, 172(3), 1066-1082. -Capdeville Y. Marigo J., 2008. Shallow layer correction for Spectral Element like methods, Geophys. J. Int., 172(3), 1135–1150.

- Calderoni, G., Gervasi, A., La Rocca, M., & Ventura, G. (2020). Strike-Slip Earthquakes at the Northern Edge of the Calabrian Arc Subduction Zone. Seismological Society of America, 92(2A), 1023-1035.

- Calò, M., Parisi, L., & Luzio, D. (2013). Lithospheric P-and S-wave velocity models of the Sicilian area using WAM tomography: procedure and assessments. Geophysical Journal International, 195(1), 625-649.

- Carminati, E., Doglioni, C., Argnani, A., Carrara, G., Dabovski, C., Dumurdzhanov, N., Dumurdzhanov, N., Gaetani, M., Georgiev, G., Mauffret, M., Sartori, R., Scionti, V., Scrocca, D, Seranne, M., Torelli, Luigi, & Zagorchev, I., (2004). TRANSMED TRANSECT III, towards a geological cross-section through Western and Central Mediterranean. In The TRANSMED ATLAS, The Mediterranean Region from Crust to Mantle (pp. 1-43). Springer, Berlin Heidelberg.

- Cassinis R., Scarascia S. and Lozej A. (2005). Review of Seismic Wide-Angle Reflection—Refraction (WARR) Results in the Italian Region (1956-1987). CROP PROJECT: Deep Seismic Exploration of the Central Mediterranean and Italy , pp. 31–55, Elsevier.

- Catalano R., Valenti V., Albanese C., Accaino F., Sulli A., Tinivella U., Gasparo Morticelli M., Zanolla C. & Giustiniani M. (2013). Sicily's fold–thrust belt and slab roll-back: the SI. RI. PRO. seismic crustal transect. Journal of the Geological Society, 170(3), 451-464.

- Catalano, R., Franchino, A., Merlini, S., & Sulli, A. (2000). Central western Sicily structural setting interpreted from seismic reflection profiles. Mem. Soc. Geol. It, 55, 5-16.

- Catalano, R., Merlini, S., & Sulli, A. (2002). The structure of western Sicily, central Mediterranean. Petroleum Geoscience, 8(1), 7-18.

- Cella, F., M. Fedi, G. Florio, V. Paoletti, & A. Rapolla (2008). A review of the gravity and magnetic studies in the Tyrrhenian basin and itsvolcanic districts,Ann. Geophys.,51(1), doi:10.4401/ag-3035

- Cernobori, L., A. Hirn, J. H.McBride, R. Nicolich, L. Petronio, M. Romanelli, & Streamers/Profiles Working Groups (1996). Crustal image of the Ionian basin and its Calabrian margins, Tectonophysics, 264, 175–189, doi:10.1016/S0040-1951(96)00125-4.

- Chiarabba, C., & Palano, M. (2017). Progressive migration of slab break-off along the southern Tyrrhenian plate boundary: Constraints for the present day kinematics. Journal of Geodynamics, 105, 51-61.

- Chironi C., De Luca L., Guerra I., Luzio D., Moretti A., Vitale M. & Sealand Group. (2000). Crustal structures of the Southern Tyrrhenian Sea and the Sicily Channel on the basis of the M25, M26, M28, M39 WARR profiles. Boll. Soc. Geol. It., 119(1), 189-204.

- Civile, D., Lodolo, E., Accaino, F., Geletti, R., Schiattarella, M., Giustiniani, M., Fedorik, J., Zecchin, M., & Zampa, L. (2018). Capo granitola-sciacca fault zone (Sicilian Channel, Central Mediterranean): structure vs magmatism. *Marine and Petroleum Geology*, *96*, 627-644.

- Civile, D., Lodolo, E., Accettella, D., Geletti, R., Ben-Avraham, Z., Deponte, M., Facchin, L., Ramella, R., & Romeo, R. (2010). The Pantelleria graben (Sicily Channel, Central Mediterranean): an example of intraplate ‘passive’rift. Tectonophysics, 490(3-4), 173-183.

- Cocchi, L., S. Passaro, F. C. Tontini, & G. Ventura (2017). Volcanism in slab tear faults is larger than in island-arcs and back-arcs, Nat. Commun. 8, no. 1, 1451, doi: 10.1038/s41467-017-01626-w.

- Corradino, M., Pepe, F., Bertotti, G., Picotti, V., Monaco, C., & Nicolich, R. (2020). 3-D architecture and Plio-Quaternary evolution of the Paola Basin: Insights into the forearc of the Tyrrhenian-Ionian subduction system. Tectonics, 39(2), e2019TC005898.

- D’Agostino, N., A. Avallone, D. Cheloni, E. D’Anastasio, S. Mantenuto, & G. Selvaggi (2008). Active tectonics of the Adriatic region from GPS and earthquake slip vectors, J. Geophys. Res., 113, B12413, doi:10.1029/2008JB005860.

- D’Alessandro, A., Mangano, G., D’Anna, G., & Scudero, S. (2016). Evidence for serpentinization of the Ionian upper mantle from simultaneous inversion of P-and S-wave arrival times. Journal of Geodynamics, 102, 115-120.

- Davies, T. M., Marshall, J. C., & Hazelton, M. L. (2018). Tutorial on kernel estimation of continuous spatial and spatiotemporal relative risk. Statistics in medicine, 37(7), 1191-1221.

- De Ritis, R., F. Pepe, B. Orecchio, D. Casalbore, A. Bosman, M. Chiappini, F. Chiocci, M. Corradino, R. Nicholich, E. Martorelli, C., Monaco, Presti, D., & Totaro, C. (2019). Magmatism along lateral slab edges: Insights from the Diamante–Enotrio–Ovidio volcanic-intrusive complex (southern Tyrrhenian Sea), Tectonics 38, 2581–2605, doi: 10.1029/2019TC005533.

- de Voogd, B., C. Truffert, N. Chamot-Rooke, P. Huchon, S. Lallemant, & X. Le Pichon (1992). Two-ship deep seismic soundings in the basins of the eastern Mediterranean Sea (Pasiphae cruise), Geophys. J. Int., 109, 536–552, doi:10.1111/j.1365-246X.1992.tb00116.x.

- Dellong, D., Klingelhoefer, F., Dannowski, A., Kopp, H., Murphy, S., Graindorge, D., Margheriti, L., Moretti, M., Barreca, G., Scarfì, L., Polonia, A., & Gutscher, M. A. (2020). Geometry of the deep Calabrian subduction (Central Mediterranean Sea) from wide-angle seismic data and 3-D gravity modeling. Geochemistry, Geophysics, Geosystems, 21(3).

- Dellong, D., Klingelhoefer, F., Kopp, H., Graindorge, D., Margheriti, L., Moretti M., Murphy, S. & Gutscher, M. A. (2018). Crustal structure of the Ionian basin and eastern Sicily margin: Results from a wide-angle seismic survey. J. Geophys.. Res.: Solid Earth, 123(3), 2090-2114, DOI: 10.1002/2017JB015312.

- DISS Working Group (2021). Database of Individual Seismogenic Sources (DISS), Version 3.3.0: A compilation of potential sources for earthquakes larger than M 5.5 in Italy and surrounding areas. Istituto Nazionale di Geofisica e Vulcanologia (INGV). https://doi.org/10.13127/diss3.3.0

- Faccenna, C., C. Piromallo, A. Crespo-Blanc, L. Jolivet, & F. Rossetti (2004). Lateral slab deformation and the origin of the western Mediterranean arcs, Tectonics, 23, TC1012, doi:10.1029/2002TC001488.

- Faccenna, C., T. W. Becker, F. P. Lucente, L. Jolivet, & F. Rossetti (2001). History of subduction and back-arc extension in the central Mediterranean, Geophys. J. Int., 145, 809–820, doi:10.1046/j.0956- 540x.2001.01435.x.

- Finetti I. R. (1984). Geophysical study of the Sicily Channel Rift Zone. Boll. Geofis. Teor. Appl., 26 , pp. 3-28

- Finetti, I. R. (Ed.). (2005). CROP project: deep seismic exploration of the central Mediterranean and Italy. Elsevier.

- Gallais F., Gutscher M. A., Klaeschen D. & Graindorge D. (2012). Two-stage growth of the Calabrian accretionary wedge in the Ionian Sea (Central Mediterranean): Constraints from depth-migrated multichannel seismic data. Marine Geology, 326-328, 28-45, http://dx.doi.org/10.1016/j.margeo.2012.08.006.

- Gallais, F., Graindorge, D., Gutscher, M. A., & Klaeschen, D. (2013). Propagation of a lithospheric tear fault (STEP) through the western boundary of the Calabrian accretionary wedge offshore eastern Sicily (Southern Italy). Tectonophysics, 602, 141-152.
- Giardini, D., & M. Velonà (1991). Deep seismicity of the Tyrrhenian Sea, Terra Nova, 3, 57–64.
- Govers, R., & Wortel, M. J. R. (2005). Lithosphere tearing at STEP faults: Response to edges of subduction zones. Earth and Planetary Science Letters, 236(1-2), 505-523.
- Grasso, M., 2001. The Apenninic-Maghrebian orogen in southern Italy, Sicily and adjacent
- Gueguen, E., Doglioni, C., & Fernandez, M. (1998). On the post-25 Ma geodynamic evolution of the western Mediterranean. Tectonophysics, 298(1-3), 259-269.
- Hayes, G. P., Moore, G. L., Portner, D. E., Hearne, M., Flamme, H., Furtney, M., & Smoczyk, G. M. (2018). Slab2, a comprehensive subduction zone geometry model. Science, 362(6410), 58-61.
- Hayes, G. P., Wald, D. J., & Johnson, R. L. (2012). Slab1. 0: A three-dimensional model of global subduction zone geometries. Journal of Geophysical Research: Solid Earth, 117(B1).
- Hijmans R.J. (2018). Raster: geographic data analysis and modeling, r package version 2.8-4
- ISIDe Working Group (2016). ISIDe, Italian Seismological Instrumental and Parametric Database, version 1.0. DOI:10.13127/ISIDe
- Kherchouche, R., Ouyed, M., Aoudia, A., Mellouk, B. & Saadi, A. (2020). Structure of the crust and uppermost mantle beneath the Sicily Channel from ambient noise and earthquake tomography. Annals of Geophysics, 63(6), SE666-SE666.
- Latorre D., Di Stefano R., Castello B., Michele M. & Chiaraluce L. (2022). Catalogo delle Localizzazioni ASSolute (CLASS): locations (Version 1). Istituto Nazionale di Geofisica e Vulcanologia (INGV) https://doi.org/10.13127/class.1.0.
- Lliboutry, L. (2000). Quantitative geophysics and geology. Springer Science & Business Media.
- Lombardi, D., J. Braunmiller, E. Kissling & D. Giardini (2008). Moho depth and poissons ratio in the western central Alps from receiver functions, Geophys. J. Int., 173, 249–264, doi:10.1111/j.1365-246X.2007.03706.x

- Maesano, F. E., Tiberti, M. M., & Basili, R. (2017). The Calabrian Arc: three-dimensional modelling of the subduction interface. Scientific reports, 7(1), 8887.
- Maiorana, M., Artoni, A., Le Breton, E., Sulli, A., Chizzini, N., & Torelli, L. (2023). Is the Sicily Channel a simple Rifting Zone? New evidence from seismic analysis with geodynamic implications. Tectonophysics, 864, 230019.
-Makris, J., Nicolich, R., & Weigel, W. (1986). A seismic study in the Western Ionian Sea. In Annales geophysicae. Series B. Terrestrial and planetary physics (Vol. 4, No. 6, pp. 665-678).
- Malinverno, A., & Ryan, W.B.F. (1986). Extension in the Tyrrhenian Sea and shortening in the Apennines as result of arc migration driven by sinking of the lithosphere. Tectonics 5, 227–245.
- Marani, M. P., & Trua, T. (2002). Thermal constriction and slab tearing at the origin of a superinflated spreading ridge: Marsili volcano (Tyrrhenian Sea). Journal of Geophysical Research: Solid Earth, 107(B9), EPM-3.
- Menichelli, I., De Gori, P., Lucente, F. P., Improta, L., Valoroso, L., Baccheschi, P., Bagh, S., Montuori, C., & Chiarabba, C. (2022). Minimum 1D VP and VP/VS models and hypocentral determinations in the central Mediterranean area. Seismological Society of America, 93(5), 2670-2685.
- Neri, G., Marotta, A. M., Orecchio, B., Presti, D., Totaro, C., Barzaghi, R., & Borghi, A. (2012). How lithospheric subduction changes along the Calabrian Arc in southern Italy: geophysical evidences. International Journal of Earth Sciences, 101, 1949-1969.
- Nicolich R., Laigle M., Hirn A., Cernobori L. and Gallart J. (2000). Crustal structure of the Ionian margin of Sicily: Etna volcano in the frame of regional evolution. Tectonophysics, 329(1-4), 121-139.
- Nicolich, R. & G. Dal Piaz (1991). Isobate della Moho in Italia, in Structural Model of Italy, 6 fogli 1:500,000, Progetto Finalizzato 'Geodinamica' CNR, Rome.
- Palano, M., Ursino, A., Spampinato, S., Sparacino, F., Polonia, A., & Gasperini, L. (2020). Crustal deformation, active tectonics and seismic potential in the Sicily Channel (Central Mediterranean), along the Nubia–Eurasia plate boundary. Scientific reports, 10(1), 21238.
- Pepe, F., Bertotti, G., Cella, F. and Marsella, E. (2000). Rifted margin formation in the South Tyrrhenian Sea: A high-resolution seismic profile across the north Sicily passive continental margin, Tectonics 19, 2, 241–257.

- Pepe, F., Sulli, A., Bertotti, G., & Cella, F. (2010). Architecture and Neogene to Recent evolution of the western Calabrian continental margin: An upper plate perspective to the Ionian subduction system, central Mediterranean. Tectonics, 29(3).

- Polonia, A., Torelli L., Mussoni P., Gasperini L., Artoni A. & Klaeschen D. (2011). The Calabrian Arc subduction complex in the Ionian Sea: Regional architecture, active deformation, and seismic hazard. Tectonics, 30, TC5018, doi:10.1029/2010TC002821.

- Pondrelli, S., Morelli, A., & Ekström, G. (2004). European-Mediterranean regional centroid-moment tensor catalog: solutions for years 2001 and 2002. Phys. Earth Plan. Int., 145, 1-4, 127-147

- Pontevivo, A., & Panza, G. F. (2006). The lithosphere-asthenosphere system in the Calabrian Arc and surrounding seas–Southern Italy. Pure and Applied Geophysics, 163, 1617-1659.

- Ritsema, J., Van Heijst, H. J., Woodhouse, J. H., & Deuss, A. (2009). Long-period body wave traveltimes through the crust: implication for crustal corrections and seismic tomography. Geophysical Journal International, 179(2), 1255-1261.

- Roure, F., Howell, D. G., Müller, C., & Moretti, I. (1990). Late Cenozoic subduction complex of Sicily. Journal of Structural Geology, 12(2), 259-266.

- Sartori, R. (1990). The main results of ODP Leg 107 in the frame of Neogene to Recent geology of peri-Tyrrhenian areas. In Proceedings of the ocean drilling program, Scientific Results (Vol. 107, pp. 715-730).

- Sartori, R., Torelli, L., Zitellini, N., Carrara, G., Magaldi, M., & Mussoni, P. (2004). Crustal features along a W–E Tyrrhenian transect from Sardinia to Campania margins (Central Mediterranean). Tectonophysics, 383(3-4), 171-192.

- Scarascia S., Lozej A &Cassinis R. (1994). Crustal structures of the Ligurian, Tyrrhenian and Ionian Seas and adjacent onshore areas interpreted from wide-angle seismic profiles. Boll. Di Geof. Teo. Ed Appl., XXXVI, 141-144.

- Scarfì, L., Barberi, G., Barreca, G., Cannavò, F., Koulakov, I., & Patanè, D. (2018). Slab narrowing in the Central Mediterranean: The Calabro-Ionian subduction zone as imaged by high resolution seismic tomography. Scientific reports, 8(1), 5178.

- Scognamiglio, L., Tinti, E., & Quintiliani, M. (2006). Time Domain Moment Tensor (TDMT) [Data set]. Istituto Nazionale di Geofisica e Vulcanologia (INGV). https://doi.org/10.13127/TDMT.

- Scrocca, D., E. Carminati, C. Doglioni, & D. Procaccianti (2012). Tyrrhenian Sea, inRegional Geology and Tectonics: Phanerozoic PassiveMargins, Cratonic Basins and

Global Tectonic Maps, vol. 1C, edited by D. G. Roberts and A. W. Bally, pp. 473–485, Elsevier, Amsterdam

- Selli, R. & Rossi, S. (1975). 'The Main Geological Features of the Ionian Sea', Rapp. Comm. Int. Mer Medit. 23, 115–116

- Selvaggi, G., and C. Chiarabba (1995). Seismicity and P wave velocity image of the Southern Tyrrhenian subduction zone, Geophys. J. Int., 121, 818–826.

- Sgroi, T., Polonia, A., Barberi, G., Billi, A., & Gasperini, L. (2021). New seismological data from the Calabrian arc reveal arc-orthogonal extension across the subduction zone. *Scientific Reports*, *11*(1), 473.

-Silverman, B. W. (1986). Density estimation for statistics and data analysis. London: Chapman and Hall.

- Sulli A., Gasparo Morticelli M., Agate M., & Zizzo E. (2021). Active north-vergent thrusting in the northern Sicily continental margin in the frame of the quaternary evolution of the Sicilian collisional system. Tectonophysics, 802, 228717.

- Syracuse, E. M., & G. A. Abers (2006). Global compilation of variations in slab depth beneath arc volcanoes and implications, Geochem. Geophys. Geosyst., 7, Q05017, doi:10.1029/2005GC001045

- Tassis, G. A., Grigoriadis, V. N., Tziavos, I. N., Tsokas, G. N., Papazachos, C. B., & Vasiljević, I. (2013). A new Bouguer gravity anomaly field for the Adriatic Sea and its application for the study of the crustal and upper mantle structure. Journal of Geodynamics, 66, 38-52.

- Tesauro, M., Kaban, M. K., & Cloetingh, S. A. (2008). EuCRUST-07: A new reference model for the European crust. Geophysical Research Letters, 35(5).

-Tugend J., Chamot-Rooke N., Arsenikos S., Blanpied C. and Frizon de Lamotte D. (2019). Geology of the Ionian Basin and margins: A key to the East Mediterranean geodynamics. Tectonics, 38(8), 2668-2702.

- Wortel M. J. R. & Spakman, W. (2000). subduction and slab detachment in the Mediterranean-Carpathian region. Science, 290(5498), 1910-1917.

- Yegorova, T. P., & Starostenko, V. I. (2002). Lithosphere structure of European sedimentary basins from regional three-dimensional gravity modelling. Tectonophysics, 346(1-2), 5-21.

areas. In: Vai, G.B., Martini, I.P. (Eds.), Anatomy of an Orogen: the Apennines and Adjacent Mediterranean Basins. Kluwer Academic Publishers, Norwell, Massachusetts, pp. 255–286.

CHAPTER 5
VELOCITY MODELS AND RELOCATION OF EARTHQUAKES IN THE CENTRAL MEDITERRANEAN

5.1 INTRODUCTION

As discussed in Chapters 2, 3, and 4, the Central Mediterranean region exhibits a complex geodynamic landscape shaped by the interaction of the European and African plates. This seismically active area presents significant challenges for accurate earthquake localization.
Precise localization of earthquakes is essential for understanding seismicity, assessing potential hazards, and deepening our knowledge of tectonic processes. In the field of geophysics, the accurate determination of earthquake hypocenters is heavily dependent on the velocity models utilized in localization algorithms. Robust velocity models offer critical insights into the geological structures that influence the propagation of seismic waves. The relationship between seismic wave velocities and geological characteristics is crucial; variations in material properties, such as density and elasticity, lead to alterations in P- and S-wave velocities. Such variability can significantly impact the calculated arrival times of seismic waves, thereby affecting the accuracy of hypocenter determinations (Kissling et al., 1994).
The need for earthquake relocation is closely tied to minimizing the root-mean-square travel time residual (RMS). This region's unique challenges arise from its heterogeneous crust and diverse tectonic features. Previous studies, such as those by D’Alessandro et al. (2016), have emphasized the necessity of optimized velocity models to better understand seismic behavior in this geodynamically active zone.
In this thesis, earthquakes in the central Mediterranean recorded by the national seismic network from 2005 to 2018 have been relocated using layer thickness and their associated P-wave velocity models derived from the models developed in this thesis and described in Chapters 2, 3 e 4.
The importance of this work lies not only in enhancing our understanding of the seismic landscape of the Central Mediterranean but also in providing data for future research initiatives. Improved earthquake localization enables a more thorough analysis of seismic patterns and source mechanisms. Moreover, the insights gained from this study can contribute to the development of more advanced three-dimensional (3D) tomographic models, illuminating the underlying geodynamics of this complex region.

5.2 DATA AND METHODS

Seismic events that occurred in the Central Mediterranean from 2005 to 2018 were relocated, based on records from the national seismic network. To achieve this, the software HYPOINVERSE-2000 was employed, along with velocity models extrapolated from those described in Chapters 2, 3, and 4.

HYPOINVERSE-2000 is a Fortran Program used to determine the locations of earthquakes. It is a command-line software that use an ASCII file containing references to other ASCII files, among which the 1D-velocity models to be used for localization of earthquakes.

The software requires dividing the area into circular subregions. For each model, the nodes are indicated as the centers of the circles (red points in Fig. 1), within which a constant model is used. An inner circle (Fig.1, in yellow) is designated where only that specific model is applied, while an outer circle (Fig. 1, in green) uses weighted averages of the travel times. In the areas outside of these circles are assigned the so-colled default model, that is a simplified 1D-velocity model generally used for the entire area of interest. The Central Mediterranean area was divided into 62 circular sectors (Fig. 1), assigning one of the 22 velocity models (Fig. 1).

Initially, the location algorithm was ran using only the default model and observed the average RMS (Root-Mean-Square travel time residual) value obtained. Subsequently, relocation was performed using both the default model and the 22 velocity models, and the results were compared.

Finally, the localization algorithm was repeated using the default model in conjunction with each of the 22 proposed models to determine which models resulted in an improvement in the localization of the earthquake hypocenters and which did not.

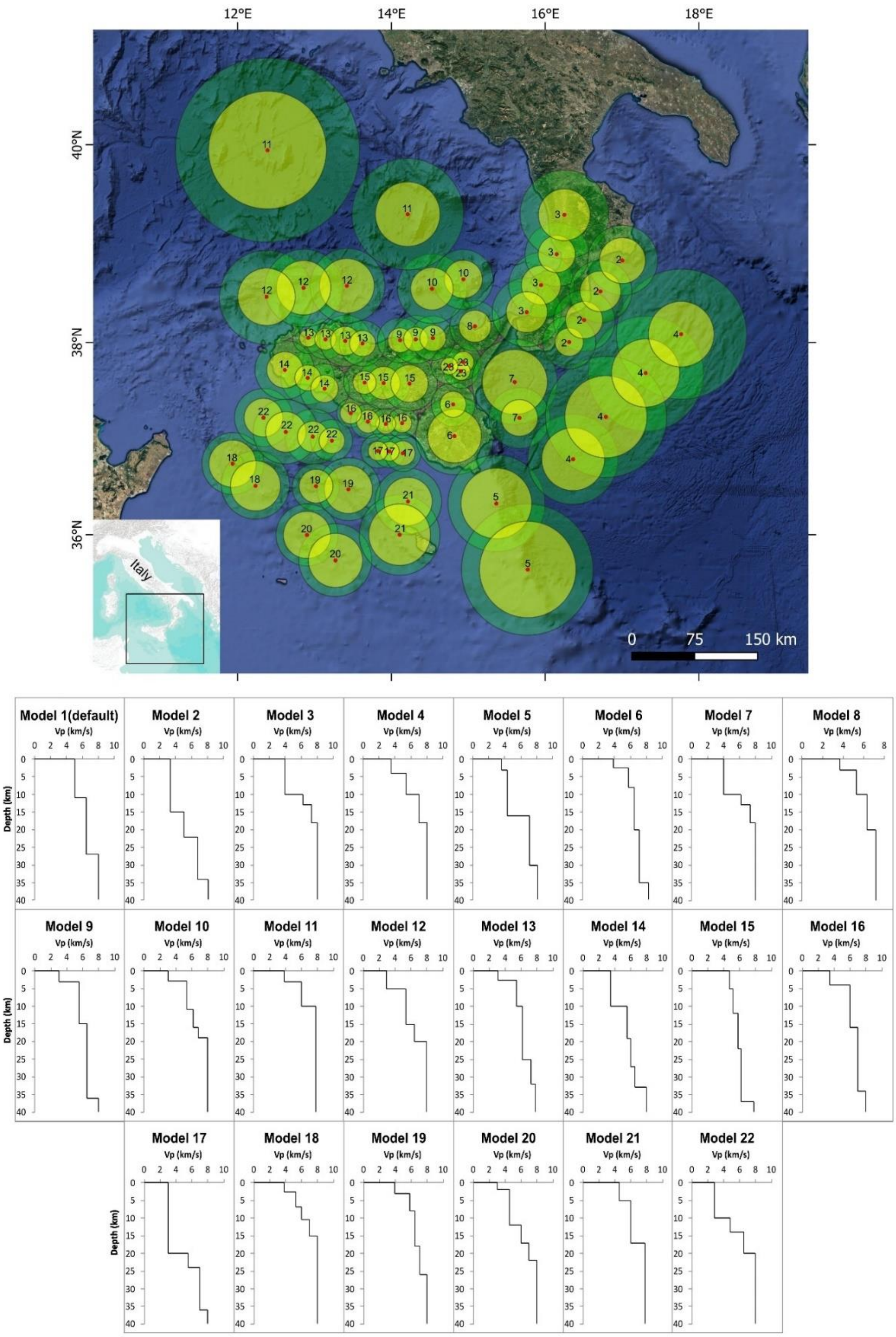

Figure 1: Velocity models used for earthquake relocation. At the top, the nodes (red points), inner circles (yellow), and outer circles (green) correspond to the sectors where the velocity models obtained by us were assigned. Each number inside the circles represents a different velocity model. The velocity models are shown at the bottom.

5.3 RESULTS

The 1D-velocity models proposed in this thesis (Fig. 1) were tested by implementing them in the HYPOINVERSE-2000 software and localizing earthquakes that occurred in the Central Mediterranean area from 2005 to 2018. Initially, the localization of the earthquakes was performed using the default model. Subsequentlt, the earthquakes were relocated using the 22 1D-velocity models proposed (Fig. 1). To assess the improvement in hypocentral localization resulting from the use of our models, the RMS values were compared. Approximately 65% of the relocated earthquakes showed improvement, with an average RMS reduction of about 10%. The seismic events that exhibited better localization are highlighted in green in Figure 2. To identify which of the 1D-velocity models led to an improvement in earthquake localization, they were tested individually. The models that improved localization comprise half of those utilized, specifically models 3, 8, 9, 10, 13, 14, 17, 18, 20, and 21 (Fig. 1).

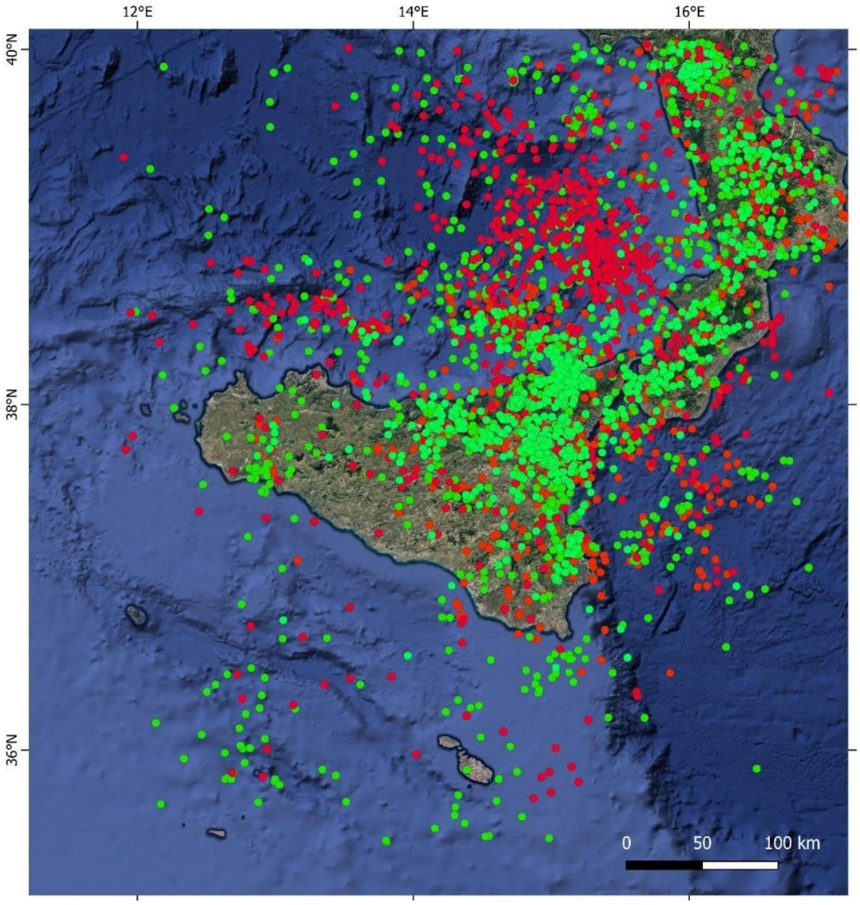

Figure 2: Map of earthquake epicenters relocated in this study: green points indicate events with a decrease in RMS of about 10%; red points indicate events for which the RMS has not improved.

5.4 DISCUSSION AND CONCLUSIONS

22 1D-velocity models derived from the results obtained in Chapters 2, 3, and 4 were tested. Half of these models led to an improvement in the localization of approximately 65% of the earthquakes, with an average RMS improvement of 10%. The models that did not result in enhanced localization include models 2, 4, 5, 6, 7, 11, 12, 15, 16, and 19. These models are shown in Figure 1. The areas where these models are located are characterized by significant geological and geodynamic complexity, as discussed in previous chapters. For instance, the External Calabrian Arc (offshore Calabria) is an area of strong uplift (Polonia et al., 2011) near the subduction of the African plate beneath the European plate. In the southern Tyrrhenian Sea, we observe a highly thinned crust and the coexistence of two plates. Moreover, like many offshore areas, it suffers from poor data coverage. Fortunately, through the reprocessing and reinterpretation of reflection seismic profiles in the western sector of the Sicily Channel (see Chapter 2 for details), a velocity model was obtained that resulted in improved earthquake localization in an offshore area with limited data, particularly regarding seismic stations. However, due to the significant lateral variation in the crustal and lithospheric structure of the Sicily Channel, some velocity models do not yield improved relocations.

The lack of improved earthquake localization in some areas may also be attributed to the limitations of the software used. HYPOINVERSE-2000 employs 1D-velocity models within a defined radius, which, despite being adjustable, restricts the ability to capture lateral velocity variations accurately. Additionally, it does not support velocity inversions with increasing depth.

In conclusion, the use of robust velocity models is crucial for better location of seismic events. To achieve this, a substantial amount of well-distributed data within the study area is necessary. To overcome the challenge of poor data coverage, a multidisciplinary approach was employed to derive crustal and lithospheric models, from which the 1D-velocity models were extrapolated. However, a denser data grid, particularly in offshore areas, would be beneficial, for example by installing Ocean Bottom Seismometers (OBSs).

Furthermore, the future objective is to obtain 3D velocity models based on the 3D crustal and lithospheric models and to utilize relocation software that incorporates these models. The implementation of 3D velocity models will enable the capture of the significant lateral variations present in the Central Mediterranean, facilitating more accurate localization, improved characterization of earthquake mechanisms, and serving as initial reference models for accurate 3D tomography.

CHAPTER 6

CONCLUSION AND FINAL REMARKS

This PhD thesis aims to unravel the complex geodynamic puzzle of the Central Mediterranean. A multidisciplinary approach was employed, using data from different methodologies, including seismic reflection profiles, P- and S-wave velocity models, density models, well data, and earthquakes. This approach enabled a denser data distribution and effectively filled gaps present in the existing literature.

The most extensive and detailed Moho map for the Central Mediterranean has been modeled. Previous Moho maps are either incomplete or based on mono-disciplinary methodologies that fail to capture the complexities of the area and the lateral variations of geological and lithospheric structures.

The Moho map obtained in this thesis shows strong lateral variation (Chap. 4, Fig. 3). The African Moho shows the greatest depths (between 30 km and 40 km) at Sicily, Tunisia, the Gela fordeep, and the Malta escarpment. In the Ionian Sea and in the Sicily Channel, the African Moho is shallower with values up to 15 km at the Pantelleria Graben. The European Moho is deeper in the onshore areas except in northeastern Sicily where the Moho is very close to the surface and is considered to be the lower limit of the crystalline basement of the European units involved in deformation. The offshore sector of the European Moho hosts the Tyrrhenian Sea where Moho depth reaches 10 km at the Marsili and Vavilov basins.

A detailed Moho map serves as a crucial tool for constraining the crustal structures of the region at the bottom and for the construction of velocity models, which are essential for improving the accuracy of earthquake localization.

A preliminary model of the crustal volume of the Central Mediterranean has been developed, along with maps of the thicknesses of each layer that composes this volume to understand the lateral variations of each layer. Acquiring information about the crustal structure of this region is essential for several important applications. These include upper-mantle tomography and the development of velocity models to optimize the location of hypocenters.

Additionally, from the statistical analysis of the earthquakes, two Lithospheric Seismogenic Volumes (LSVs) (Chap. 2 Fig. 5) were constructed in the central-western Sicily Channel and one Crustal Seismogenic Volume (CSV) (Chap. 4, Fig. 6) in subduction in the Ionian sector.

The two LSVs have NS and EW trends and are concordant, respectively, with the structure of the CGSFZ, interpreted by Civile et al. (2018) as a lithospheric fault, and with the normal faults delimiting the Grabens of Pantelleria, Linosa, and Malta (Chap. 2 Fig. 7). In addition, the NS-trending LSV has a superficial gap below the island of Pantelleria and a great depth gap below the island of Linosa (Chap. 2 Fig. 5). This provides important information regarding the depth of the magma chambers of the two sectors.

The Ionian CSV in subduction extends about 500 km in depth, and the top and bottom surfaces that constitute it exhibit an articulated geometry. The thickness varies with depth with a maximum in the shallowest part (between 30 km and 60 km thick) and a minimum in the deepest part (up to about 5 km thick) (Chap. 4, Fig. 5).

In addition, the surface-projected CSV appears to be confined between the TLS and PS fault zones (Chap. 4, Fig. 8).

Understanding the geometry of these structures is crucial for assessing the dimensions of seismogenic sources, subduction mechanisms, and the associated seismic and tsunami hazards.

From the models obtained in this PhD thesis, 21 1D-velocity models were extracted and tested to optimize the location of seismic events recorded by the national seismic network between 2005 and 2018.

The results of this thesis provide valuable insights into the geodynamic framework of the area, outlining both the surface and deep structures associated with seismic and tsunami hazards.

The models presented in this study can be easily updated with new data. Ongoing refinement of these models will enhance their detail and reliability, providing essential resources for future geodynamic and tectonic studies.

The results of this thesis highlight the need for ongoing interdisciplinary research to unravel the intricate geodynamic of the Central Mediterranean. Future efforts should focus on enhancing data coverage in the Central Mediterranean region through the integration of new data such as seismic reflection profile, velocity models, density models. The installation of Ocean Bottom Seismometers (OBSs) in offshore areas would also be beneficial, along with the development of advanced three-dimensional velocity models to better capture the lateral variations of the complex structures in the Central Mediterranean.

References

- - Agius, M. R., Magrini, F., Diaferia, G., Kästle, E. D., Cammarano, F., Faccenna, C., Funiciello, F., & van der Meijde, M. (2022). Shear-Velocity Structure and Dynamics Beneath the Sicily Channel and Surrounding Regions of the Central Mediterranean Inferred From Seismic Surface Waves. Geochemistry, Geophysics, Geosystems, 23(10), e2022GC010394.
- Anderson, H., & J. Jackson (1987). Active tectonics of the Adriatic Region, Geophys. J. R. Astronom. Soc., 91, 937–983.
- Argnani, A., & Savelli, C. (1999). Cenozoic volcanism and tectonics in the southernTyrrhenian sea: Space-time distribution and geodynamicsignificance. Journal of Geodynamics, 27(4-5), 409-432.
- Artemieva, I. M., & Thybo, H. (2013). EUNAseis: A seismic model for Moho and crustal structure in Europe, Greenland, and the North Atlantic region. Tectonophysics, 609, 97-153.
- Billi, A., Barberi, G., Faccenna, C., Neri, G., Pepe, F., & Sulli, A. (2006). Tectonics and seismicity of the Tindari Fault System, southern Italy: Crustal deformations at the transition between ongoing contractional and extensional domains located above the edge of a subducting slab. Tectonics, 25(2).
- Carminati, E., Cavazza, W., Roure, F., Spakman, W., Stampfli, G. M., & Ziegler, P. A. (2004). TRANSMED Transect III: Massif Central-Provence-Gulf of Lion-Provençal Basin-Sardinia-Tyrrhenian Basin-Southern Apennines-Apulia-Adriatic Sea-Albanides-Balkans- Moesian Platform. In W. Cavazza, F. Roure, W. Spakman, G. M. Stampfli, & P. A. Ziegler (Eds.), The TRANSMED Atlas: The Mediterranean Region from crust to mantle. Heidelberg: Springer-Verlag.
- Catalano, R., C. Doglioni, and S. Merlini; 2001: On the Mesozoic Ionian basin, Geophys. J. Int., 144, 49–64, doi:10.1046/j.0956-540X.2000.01287.x.Hayes, G. P., Wald, D. J., & Johnson, R. L. (2012). Slab1. 0: A three-dimensional model of global subduction zone geometries. Journal of Geophysical Research: Solid Earth, 117(B1).
- Catalano, R., C. Doglioni, & S. Merlini (2001). On the Mesozoic Ionian basin, Geophys. J. Int., 144, 49–64, doi:10.1046/j.0956-540X.2000.01287.x.
- Cella, F., M. Fedi, G. Florio, V. Paoletti, & A. Rapolla (2008). A review of the gravity and magnetic studies in the Tyrrhenian basin and itsvolcanic districts,Ann. Geophys.,51(1), doi:10.4401/ag-3035.

- Cernobori, L., Hirn, A., H.McBride, J., Nicolich, R., Petronio, L., Romanelli, M., & Streamers/Profiles Working Groups (1996). Crustal image of the Ionian basin and its Calabrian margins, Tectonophysics, 264, 175–189, doi:10.1016/S0040-1951(96)00125-4.
- Chiarabba, C., & Palano, M. (2017). Progressive migration of slab break-off along the southern Tyrrhenian plate boundary: Constraints for the present day kinematics. Journal of Geodynamics, 105, 51-61.
- Civile, D., Lodolo, E., Accaino, F., Geletti, R., Schiattarella, M., Giustiniani, M., Fedorik, J., Zecchin, M., & Zampa, L. (2018). Capo granitola-sciacca fault zone (Sicilian Channel, Central Mediterranean): structure vs magmatism. *Marine and Petroleum Geology*, *96*, 627-644.
- Civile, D., Lodolo, E., Accettella, D., Geletti, R., Ben-Avraham, Z., Deponte, M., Facchin, L., Ramella, R., & Romeo, R. (2010). The Pantelleria graben (Sicily Channel, Central Mediterranean): an example of intraplate 'passive'rift. Tectonophysics, 490(3-4), 173-183.
- Cocchi, L., S. Passaro, F. C. Tontini, & G. Ventura (2017). Volcanism in slab tear faults is larger than in island-arcs and back-arcs, Nat. Commun. 8, no. 1, 1451, doi: 10.1038/s41467-017-01626-w.
- Corradino, M., Pepe, F., Bertotti, G., Picotti, V., Monaco, C., & Nicolich, R. (2020). 3-D architecture and Plio-Quaternary evolution of the Paola Basin: Insights into the forearc of the Tyrrhenian-Ionian subduction system. Tectonics, 39(2), e2019TC005898.
- D'Agostino, N., A. Avallone, D. Cheloni, E. D'Anastasio, S. Mantenuto, & G. Selvaggi (2008). Active tectonics of the Adriatic region from GPS and earthquake slip vectors, J. Geophys. Res., 113, B12413, doi:10.1029/2008JB005860.
- D'Alessandro, A., Mangano, G., D'Anna, G., & Scudero, S. (2016). Evidence for serpentinization of the Ionian upper mantle from simultaneous inversion of P-and S-wave arrival times. Journal of Geodynamics, 102, 115-120.
- De Ritis, R., F. Pepe, B. Orecchio, D. Casalbore, A. Bosman, M. Chiappini, F. Chiocci, M. Corradino, R. Nicholich, E. Martorelli, C., Monaco, Presti, D., & Totaro, C. (2019). Magmatism along lateral slab edges: Insights from the Diamante–Enotrio–Ovidio volcanic-intrusive complex (southern Tyrrhenian Sea), Tectonics 38, 2581–2605, doi: 10.1029/2019TC005533.

- de Voogd, B., C. Truffert, N. Chamot-Rooke, P. Huchon, S. Lallemant, & X. Le Pichon (1992). Two-ship deep seismic soundings in the basins of the eastern Mediterranean Sea (Pasiphae cruise), Geophys. J. Int., 109, 536–552, doi:10.1111/j.1365-246X.1992.tb00116.x.
- Di Stefano, R., Bianchi, I., Ciaccio, M. G., Carrara, G. & Kissling, E. (2011). Three-dimensional Moho topography in Italy: New constraints from receiver functions and controlled source seismology. Geochemistry, Geophysics, Geosystems, 12(9).
- Faccenna, C., Davy, P., Brun, J. P., Funiciello, R., Giardini, D., Mattei, M., & Nalpas, T. (1996). The dynamics of back-arc extension: an experimental approach to the opening of the Tyrrhenian Sea. Geophysical Journal International, 126(3), 781-795.
- Faccenna, C., T. W. Becker, F. P. Lucente, L. Jolivet, & F. Rossetti (2001). History of subduction and back-arc extension in the central Mediterranean, Geophys. J. Int., 145, 809–820, doi:10.1046/j.0956- 540x.2001.01435.x.
- Faccenna, C., C. Piromallo, A. Crespo-Blanc, L. Jolivet, & F. Rossetti (2004). Lateral slab deformation and the origin of the western Mediterranean arcs, Tectonics, 23, TC1012, doi:10.1029/2002TC001488.
- Finetti I. R. (1984). Geophysical study of the Sicily Channel Rift Zone. Boll. Geofis. Teor. Appl., 26, pp. 3-28.
- Gallais F., Gutscher M. A., Klaeschen D., & Graindorge D. (2012). Two-stage growth of the Calabrian accretionary wedge in the Ionian Sea (Central Mediterranean): Constraints from depth-migrated multichannel seismic data. Marine Geology, 326-328, 28-45, http://dx.doi.org/10.1016/j.margeo.2012.08.006.
- Giardini, D., & M. Velonà (1991). Deep seismicity of the Tyrrhenian Sea, Terra Nova, 3, 57–64.
- Govers, R., & Wortel, M. J. R. (2005). Lithosphere tearing at STEP faults: Response to edges of subduction zones. Earth and Planetary Science Letters, 236(1-2), 505-523.
- Gueguen, E., Doglioni, C., & Fernandez, M. (1998). On the post-25 Ma geodynamic evolution of the western Mediterranean. Tectonophysics, 298(1-3), 259-269.
- Handy, M. R., Schmid, S. M., Bousquet, R., Kissling, E., & Bernoulli, D. (2010). Reconciling plate-tectonic reconstructions of Alpine Tethys with the geological-geophysical record of spreading and subduction in the Alps. Earth-Science Reviews, 102(3-4), 121–158.

- Hayes, G. P., Moore, G. L., Portner, D. E., Hearne, M., Flamme, H., Furtney, M., & Smoczyk, G. M. (2018). Slab2, a comprehensive subduction zone geometry model. Science, 362(6410), 58-61.
- Hayes, G. P., Wald, D. J., & Johnson, R. L. (2012). Slab1. 0: A three-dimensional model of global subduction zone geometries. Journal of Geophysical Research: Solid Earth, 117(B1).
- ISIDe Working Group (2016). ISIDe, Italian Seismological Instrumental and Parametric Database, version 1.0. DOI:10.13127/ISIDe
- Jolivet, L., C. Gorini, J. Smit, & S. Leroy (2015). Continental breakup and the dynamics of rifting in back-arc basins: The Gulf of Lion margin,Tectonics,34, 662–679, doi:10.1002/2014TC003570
- Kherchouche, R., Ouyed, M., Aoudia, A., Mellouk, B. & Saadi, A. (2020). Structure of the crust and uppermost mantle beneath the Sicily Channel from ambient noise and earthquake tomography. Annals of Geophysics, 63(6), SE666-SE666.
- Kissling, E., Ellsworth, W. L., Eberhart-Phillips, D., Kradolfer, U.: Initial reference models in local earthquake tomography. J. Geophys. Res. 99, 19635–19646 (1994).
- Latorre D., Di Stefano R., Castello B., Michele M. & Chiaraluce L. (2022). Catalogo delle Localizzazioni ASSolute (CLASS): locations (Version 1). Istituto Nazionale di Geofisica e Vulcanologia (INGV) https://doi.org/10.13127/class.1.0.
- Lliboutry, L. (2000). Quantitative geophysics and geology. Springer Science & Business Media.
- Lombardi, D., J. Braunmiller, E. Kissling & D. Giardini (2008). Moho depth and poissons ratio in the western central Alps from receiver functions, Geophys. J. Int., 173, 249–264, doi:10.1111/j.1365-246X.2007.03706.x
- Maesano, F. E., Tiberti, M. M., & Basili, R. (2017). The Calabrian Arc: three-dimensional modelling of the subduction interface. Scientific reports, 7(1), 8887.
- Maiorana, M., Artoni, A., Le Breton, E., Sulli, A., Chizzini, N., & Torelli, L. (2023). Is the Sicily Channel a simple Rifting Zone? New evidence from seismic analysis with geodynamic implications. Tectonophysics, 864, 230019.
- Malinverno, A., & Ryan, W.B.F. (1986). Extension in the Tyrrhenian Sea and shortening in the Apennines as result of arc migration driven by sinking of the lithosphere. Tectonics 5, 227–245.

- Marani, M. P., & Trua, T. (2002). Thermal constriction and slab tearing at the origin of a superinflated spreading ridge: Marsili volcano (Tyrrhenian Sea). Journal of Geophysical Research: Solid Earth, 107(B9), EPM-3.
- Molinari, I., & Morelli, A. (2011). EPcrust: a reference crustal model for the European Plate. Geophysical Journal International, 185(1), 352-364.
- Neri, G., Marotta, A. M., Orecchio, B., Presti, D., Totaro, C., Barzaghi, R., & Borghi, A. (2012). How lithospheric subduction changes along the Calabrian Arc in southern Italy: geophysical evidences. International Journal of Earth Sciences, 101, 1949-1969.
- Nijholt, N., & Govers, R. (2015). The role of passive margins on the evolution of Subduction-Transform Edge Propagators (STEPs). Journal of Geophysical Research: Solid Earth, 120(10), 7203-7230.
- Palano, M., Ursino, A., Spampinato, S., Sparacino, F., Polonia, A., & Gasperini, L. (2020). Crustal deformation, active tectonics and seismic potential in the Sicily Channel (Central Mediterranean), along the Nubia–Eurasia plate boundary. Scientific reports, 10(1), 21238.
- Pepe, F., Bertotti, G., Cella, F. and Marsella, E. (2000). Rifted margin formation in the South Tyrrhenian Sea: A high-resolution seismic profile across the north Sicily passive continental margin, Tectonics 19, 2, 241–257.
- Piana Agostinetti, N., & Amato, A. (2009). Moho depth and vp/vs ratio in peninsular Italy from teleseismic receiver functions. J. Geophys. Res., 114, B06303, doi:10.1029/ 2008JB005899.
- Polonia, A., Torelli L., Mussoni P., Gasperini L., Artoni A. & Klaeschen D. (2011). The Calabrian Arc subduction complex in the Ionian Sea: Regional architecture, active deformation, and seismic hazard. Tectonics, 30, TC5018, doi:10.1029/2010TC002821.
- Pontevivo, A., & G. Panza (2002). Group velocity tomography and regionalization in Italy and bordering areas, Phys. Earth Planet. Inter., 134, 1–15, doi:10.1016/S0031-9201 (02)00079-1.
- Pontevivo, A., & Panza, G. F. (2006). The lithosphere-asthenosphere system in the Calabrian Arc and surrounding seas–Southern Italy. Pure and Applied Geophysics, 163, 1617-1659.

- Rosenbaum, G., Lister, G. S., & Duboz, C. (2002). Reconstruction of the tectonic evolution of the western Mediterranean since the Oligocene. Journal of the Virtual Explorer, 8, 107–130.
- Sartori, R. (1990). The main results of ODP Leg 107 in the frame of Neogene to Recent geology of peri-Tyrrhenian areas. In Proceedings of the ocean drilling program, Scientific Results (Vol. 107, pp. 715-730).
- Sartori, R., Torelli, L., Zitellini, N., Carrara, G., Magaldi, M., & Mussoni, P. (2004). Crustal features along a W–E Tyrrhenian transect from Sardinia to Campania margins (Central Mediterranean). Tectonophysics, 383(3-4), 171-192.
- Scarascia S., Lozej A &Cassinis R. (1994). Crustal structures of the Ligurian, Tyrrhenian and Ionian Seas and adjacent onshore areas interpreted from wide-angle seismic profiles. Boll. Di Geof. Teo. Ed Appl., XXXVI, 141-144.
- Scarfì, L., Barberi, G., Barreca, G., Cannavò, F., Koulakov, & I.,and Patanè, D. (2018). Slab narrowing in the Central Mediterranean: The Calabro-Ionian subduction zone as imaged by high resolution seismic tomography. Scientific reports, 8(1), 5178.
- Scrocca, D., E. Carminati, C. Doglioni, & D. Procaccianti (2012). Tyrrhenian Sea, inRegional Geology and Tectonics: Phanerozoic PassiveMargins, Cratonic Basins and Global Tectonic Maps, vol. 1C, edited by D. G. Roberts and A. W. Bally, pp. 473–485, Elsevier, Amsterdam.
- Selli, R. & Rossi, S. (1975). 'The Main Geological Features of the Ionian Sea', Rapp. Comm. Int. Mer Medit. 23, 115–116.
- Selvaggi, G., & Chiarabba, C. (1995). Seismicity and P wave velocity image of the Southern Tyrrhenian subduction zone, Geophys. J. Int., 121, 818–826.
- Sulli A., Gasparo Morticelli M., Agate M., & Zizzo E. (2021). Active north-vergent thrusting in the northern Sicily continental margin in the frame of the quaternary evolution of the Sicilian collisional system. Tectonophysics, 802, 228717.
- Syracuse, E. M., & G. A. Abers (2006). Global compilation of variations in slab depth beneath arc volcanoes and implications, Geochem. Geophys. Geosyst., 7, Q05017, doi:10.1029/2005GC001045.
- Tesauro, M., Kaban, M. K., & Cloetingh, S. A. (2008). EuCRUST-07: A new reference model for the European crust. Geophysical Research Letters, 35(5).
- Van Der Meijde, M., Van Der Lee, S., & Giardini, D. (2003). Crustal structure beneath broad-band seismic stations in the Mediterranean region. Geophysical

Journal International, 152(3), 729-739. https://doi.org/10.1046/j.1365-246X.2003.01871.x.

- Wortel M. J. R. & Spakman, W. (2000). subduction and slab detachment in the Mediterranean-Carpathian region. Science, 290(5498), 1910-1917.